MONTHLY NOTICES

OF THE

ROYAL ASTRONOMICAL SOCIETY

Vol. 100 No. 6

MEETING OF 1940 APRIL 12

Professor H. C. Plummer, President, in the Chair.

The election by the Council of the following Fellow was duly confirmed :—

G. H. Archenhold, D.Phil., Solar Physics Observatory, Cambridge.

The following candidates were proposed for election as Fellows of the Society, the names of the proposers from personal knowledge being appended :—

Ronald Gordon Giovanelli, M.Sc., Rural School, Carlingford, N.S.W., Australia, and National Physical Laboratory, Teddington, Middlesex (proposed by R. v. d. R. Woolley) ;

Richard Francis Turney Granger, Manor Court, Bramcote, Notts. (proposed by H. W. Cox) ;

Charles Haller, F.R.S.A., F.R.M.S., The White House Cottage, Wimbledon Common, London, S.W. 19 (proposed by R. C. Morrell) ; and

Gerald James Whitrow, M.A., D.Phil., Christ Church, Oxford, and 37 Cedars Road, Clapham, London, S.W. 4 (proposed by E. A. Milne).

Seventy-five presents were announced as having been received since the last meeting, including :—

Four volumes on the "History of the Royal Swedish Academy of Sciences" (presented by the Academy on the occasion of its bi-centenary).

ON THE SUITABILITY OF EROS FOR THE ACCURATE DETERMINATION OF THE SOLAR PARALLAX

H. Spencer Jones, F.R.S., Astronomer Royal, Chairman, Sub-Committee on Solar Parallax, International Astronomical Union

1. Extensive observations of Eros were obtained at the favourable opposition in 1931. Many observatories participated in these observations, which were planned by the Solar Parallax Commission of the International Astronomical Union for the purpose of deriving more accurate values of the solar parallax and of the mass of the Moon. The discussion of the observations is now in progress at the Royal Observatory, Greenwich, and the results of most of the series of observations have been received, in many cases in manuscript in advance of publication.

2. The results of the observations made at the Bergedorf Observatory have recently been published.* The discussion of these observations by Dr. Vick led him to conclude that Eros is a complex system, consisting of at least three bodies, and that the centroid of brightness has periodic motions about the centroid of mass, giving rise to an orbital path of varying shape. In consequence, the planet Eros, in spite of its close approach to the Earth at favourable oppositions, is not a suitable body for the derivation of an improved value of the solar parallax.

3. If these conclusions are confirmed, the extensive programme of observations made at the opposition of 1931 and the heavy labour of their reduction, as well as the considerable, though less extensive, programme at the opposition of 1901, have been made in vain. It becomes of importance, therefore, to examine whether the conclusions reached in the discussion of the Bergedorf observations can be confirmed by the much more extensive series of observations made at other observatories.

4. It is desirable first to summarise the Bergedorf results in order to make clear the magnitude of the effect that is to be looked for.

Observations were made at Bergedorf with four instruments : the A.G. astrograph (scale 1 mm. = 100″·20) ; the normal refractor of the Lippert astrograph (scale 1 mm. = 59″·45) ; the 60-cm. refractor (scale 1 mm. = 22″·63) ; the 1-m. reflector (scale 1 mm. = 70″·20). Discussion of the probable errors showed that in portions of the series, particularly in some of the observations with the reflector and the R.A. observations with the long-focus refractor, the probable errors of the Eros positions were much greater than was anticipated. An explanation was sought in the hypothesis that the centroids of brightness and of mass do not coincide. If observations

* *Astronomische Abhandlungen der Hamburger Sternwarte in Bergedorf*, Bd. V, No. 3, 1939.

extended over a full period of the motion of the centroid of brightness about the centroid of mass, the effect of the motion would be largely eliminated from the mean of the series; it was remarked that the mean nightly differences Observed *minus* Tabular for the different instruments were in best agreement when the series of observations covered the longest time.

With the A.G. astrograph two exposures of Eros, each of 60^s duration, were given, with a time-interval of 9^m between the mid-times of the two exposures. The displacements between the two images, after correction for the motion of Eros in the interval and for differential parallax, showed ranges in each co-ordinate exceeding 1″. These were interpreted as orbital motions. Further discussion led to the conclusion that there was a combination of two periods, one of 12·5311 minutes and one of 79·6845 minutes. The total amplitude of the variation of longer period was between 0″·3 and 0″·4, and though the observations were somewhat scanty, a three-looped orbit, similar to the periodic orbits of type *g*, investigated by E. Strömgren was suggested. Doubt was expressed whether the shape of the orbit remained the same over a period of time.

5. Displacements of the centroid of brightness of Eros with respect to the centroid of mass amounting to several tenths of a second of arc can be readily checked from the extensive material now available from the programme of observations at the opposition of 1931. It may be remarked, however, that if there were displacements of the centroid of light of such magnitude, they could scarcely have escaped notice in the discussion of the observations made at the opposition of 1901. Hinks examined whether there was any variation with periods of $2^h\ 38^m$ or $5^h\ 16^m$, associated with the total period of variation in brightness of Eros or with the half-period, the odd and even minima being unequal. No effect was detected in declination, but a small effect, with semi-amplitude of between 0″·03 and 0″·04, was suspected in right ascension. Vick remarks that Hinks grouped the observations in each period of light variation into 8 groups, each extending over about 40 minutes of time, and that such grouping would largely conceal periods as short as $12\frac{1}{2}$ and 79 minutes.

6. To investigate the reality of a period as short as $12\frac{1}{2}$ minutes, the separate reduction of the individual exposures on Eros is necessary. In many series of observations in the 1931 work the several measures on one plate were combined and, in order to reduce computation, a single reduction for the plate was made. For the series made at the Dearborn Observatory, however, with the $17\frac{1}{2}$-inch refractor (scale 1 mm. = 29″·3), each image has been separately reduced. The observations of January 17, 20 and 21 were selected for investigations, because on these nights a large number of images of Eros are available, and because these dates come in the interval of time covered by the Bergedorf observations. The observations extend from January 17·1736–17·5132, 20·2034–20·4389 and 21·1771–21·4472, the exposures on Eros being made at two-minute intervals, with some gaps.

The observations were reduced with a provisional value of the solar

parallax of 8″·795, as it appears certain that the observations at the 1931 opposition will give a value smaller than 8″·80 and probably within a few thousandths of a second of 8″·795. With Vick's elements for the short-period variation,

$$T = 1931 \text{ Jan. } 1{\cdot}161885 \text{ U.T.},$$
$$p = 0^{d}{\cdot}00870217 = 12{\cdot}5311 \text{ minutes},$$

the observations were grouped into 12 groups, with phase-angles 0°–30°, 30°–60°, etc., the residuals Observed *minus* Tabular position of Eros being collected for $\Delta\alpha \cos\delta$ and $\Delta\delta$.

The mean differences for each phase-group, after subtracting the mean of all the groups, for January 17 and for January 20–21, and the number of observations in each group, are given in the following table. In combining the nights January 20 and 21 allowance was made for the change in the (O – T) values between the two nights.

Suspected Period, 12·5311 *Minutes*

Phase-angle	January 17			January 20–21		
	$\Delta\alpha \cos\delta$	$\Delta\delta$	Number	$\Delta\alpha \cos\delta$	$\Delta\delta$	Number
° °	″	″		″	″	
0– 30	·00	−·06	10	+·07	−·09	10
30– 60	+·07	+·01	9	−·05	·00	17
60– 90	−·03	−·11	8	+·06	−·02	13
90–120	−·10	−·01	12	+·07	+·07	13
120–150	+·03	−·01	9	−·15	+·06	14
150–180	+·20	+·03	11	−·11	+·11	12
180–210	−·04	+·01	8	+·03	−·06	8
210–240	−·13	+·07	10	−·16	−·04	14
240–270	−·04	+·12	11	−·03	+·04	8
270–300	+·18	+·12	10	+·19	−·12	12
300–330	−·07	−·08	10	+·16	−·12	7
330–360	−·06	−·13	10	+·05	+·07	19

There is no evidence of any periodicity in these mean values, and a variation with an amplitude of the order of several tenths of a second of arc is clearly out of the question.

The harmonic analysis of the figures in the above table gives the following results, when the inequalities in weights of the different phase-groups are disregarded :—

R.A.	Jan. 17	$+{\cdot}005 \sin\theta - {\cdot}011 \cos\theta$
	20–21	$-{\cdot}033 \sin\theta + {\cdot}090 \cos\theta$
Dec.	Jan. 17	$-{\cdot}053 \sin\theta - {\cdot}056 \cos\theta$
	20–21	$+{\cdot}048 \sin\theta - {\cdot}038 \cos\theta$

where θ is the phase-angle. The differences between the results for the two days indicate that there is no true periodicity.

If the scatter in the observed values is attributed to purely random

variations, the probable error in the position of Eros, derived from a single exposure, is found to be as follows :—

	R.A.	Dec.
	″	″
Jan. 17	± 0·21	± 0·19
20	± ·18	± ·26
21	± ·28	± ·25

The probable errors for a single exposure derived from the means of groups, according to phase-angle, given in the above table are: in R.A. ± 0″·23 and ± 0″·27 for January 17 and 20–21 respectively, and in Dec. ± 0″·17 and ± 0″·18.

The conclusion is that there is no evidence of any periodicity with a period of 12·5311 minutes. The 3 nights of the Dearborn observations contain 265 separate exposures. The Bergedorf material contains 48 separate exposures on Eros on 5 nights.

7. For the investigation of the reality of the suspected period of 79·6845 minutes, 3 nights were selected for which there was abundant material and which were near in time to the Bergedorf observations. The nights selected, and the material used, were as follows :—

Jan. 27.—Cape 13-in., 9 plates (3 only were measured in Dec.); Cape 24-in., 7 plates; Cordoba 13-in., 6 plates; Greenwich 13-in., 4 plates; Greenwich 26-in., 8 plates; Radcliffe 24-in., 7 plates; Algiers 13-in., 2 plates; Melbourne 13-in., 10 plates; Van Vleck 20-in., 15 plates; Dearborn 18½-in., 4 plates.

Jan. 30.—Cape 13-in., 11 plates (3 only measured in Dec.); Cape 24-in., 7 plates; Yale (Johannesburg) 26-in., 3 plates; Melbourne 13-in., 6 plates; Johannesburg 10-in., 5 plates; Van Vleck 20-in., 16 plates; Dearborn 18½-in., 10 plates.

Feb. 5.—Cape 13-in., 12 plates (3 only measured in Dec.); Cape 24-in., 10 plates; Cordoba 13-in., 6 plates; Melbourne 13-in., 12 plates; Johannesburg 10-in., 1 plate; Algiers 13-in., 2 plates; Yale (Johannesburg), 26-in., 3 plates; Van Vleck 20-in., 16 plates; Dearborn 18½-in., 10 plates.

These 3 nights give a total of 202 plates. The existence of the 79^m variation was inferred at Bergedorf from 26 plates obtained with 3 instruments on 5 nights (131 separate exposures on Eros).

The observations were reduced with a provisional value of the solar parallax of 8″·795. The elements of the variation derived at Bergedorf,

$$T = 1931 \text{ Jan. } 1{\cdot}188694 \text{ U.T.},$$
$$p = 0^d{\cdot}05533645 = 79{\cdot}6845 \text{ minutes},$$

were used and the phase-angle for each observation was found. The mean values for the entire series of each day were subtracted from the observations on that day, and the residuals were collected according to phase-angle in groups of 30°. The mean values for the 12 phase-groups are given in the following table :—

Suspected Period, 79·6845 Minutes

Phase-angle	January 27, 30, February 5			
	$\Delta\alpha \cos\delta$	No.	$\Delta\delta$	No.
° °	″		″	
0– 30	+·03	15	−·06	14
30– 60	+·05	11	+·07	10
60– 90	−·07	18	+·03	17
90–120	+·03	16	−·04	13
120–150	−·05	14	−·03	14
150–180	·00	18	+·03	14
180–210	+·04	16	−·04	15
210–240	+·02	15	−·01	11
240–270	+·03	21	+·05	21
270–300	−·03	22	−·02	18
300–330	+·02	13	+·04	13
330–360	−·07	23	−·02	19

There is no evidence in these residuals of any periodicity ; a periodicity with total amplitude of 0″·3 or 0″·4 can definitely be excluded.

For the purpose of this discussion equal weight has been given to a single plate from each observatory. By one plate is meant a group of Eros images, usually by the interrupted exposure method, with one series of comparison star images. Two such groups, photographed for convenience on the same plate, have been treated as two plates.

If the discordances between the results for the single plates are regarded as purely random, the probable errors for a single plate on each night are found to be as follows :—

	R.A.	Dec.
	″	″
Jan. 27	± 0·10	± 0·09
30	± ·10	± ·12
Feb. 5	± ·12	± ·09

These probable errors are in themselves sufficiently small to show that the existence of any periodicity with a total amplitude of the order of 0″·3 or 0″·4 is extremely improbable.

It is therefore concluded that there is no periodic variation in the centroid of brightness of Eros with a period of 79·6845 minutes. No further proof of the unreality of this period has accordingly been sought.

8. The explanation of the large probable errors of some of the Bergedorf observations must therefore be looked for in some other direction. The method by which the observations were taken is probably responsible.

In order to secure approximate equality in brightness between Eros and the reference stars, and to avoid the loss of accuracy entailed in the measurement of trailed images, a method of interrupted exposures had been recommended for the photographic observations of Eros. As an example, using a star for guiding, an exposure of one minute might be given. At the end of this exposure the shutter might be closed for two minutes and a second exposure of one minute given. Because of the rapid motion of Eros, two separated and sensibly round star-like images of Eros would be obtained

for comparison with the single image of each reference star. The number and length of the exposures on Eros and of the interruptions were to be chosen so as to secure properly separated star-like images of Eros, and approximate equality between each image of Eros and the average reference star image. The advantage of this method is that the mean of the small group of Eros images should correspond closely to the built-up reference star images, guiding errors and effects due to atmospheric irregularities being largely compensated. The results obtained by this method have proved that this is the case.

This method of observation was not used at Bergedorf, but the following methods were used. With the A.G. astrograph, an exposure of 10^m was given on the comparison stars, and two exposures of 1^m on Eros, at the beginning and end of the 10^m exposure ; all plates with this instrument were taken in this way. With the Lippert astrograph, some plates were given 4^m exposure on the comparison stars, Eros being exposed for 1^m in the middle. Other plates were obtained with exposures of the same length on Eros and stars. All plates with the 60-cm. refractor were given 3^m exposure on the stars, with 55^s on Eros in the middle. With the 1-m. reflector, equal exposures were given on stars and planet with two exceptions. On November 16 and 18, 11 and 15 exposures, respectively, were obtained on Eros, with a single total exposure on the stars. These two plates were intended to give information about the variation in brightness of Eros and not primarily for the derivation of its position. The plate of November 16, with 11 exposures of 30^s each on Eros, spread over a time-interval of $2\frac{1}{2}$ hours, was measured, however, for position.

The investigation of probable errors of the observations with the reflector gave satisfactorily small probable errors except for the observations on October 2 (when a large probable error in R.A. was found, but, being based on four images only, is obviously unreliable) and on November 16. The large probable errors of the Eros positions on the latter date, $\pm$ 0″·64 in R.A. and $\pm$ 0″·84 in Dec., as compared with the probable errors from a long series of observations on January 27, viz. $\pm$ 0″·17 in each co-ordinate, illustrates the errors that can be introduced when the exposures on Eros and the comparison stars are not identical ; the position derived from the *mean* of the group on this night is nevertheless in close agreement with the position from the Lippert astrograph observations on the same night, which were obtained with the same exposures on planet and stars. The mean of the Eros images therefore corresponded closely with the star images, in spite of the long time-interval over which the observations were spread.

With the 60-cm. refractor, the probable errors were high in both co-ordinates ($\pm$ 0″·42 in R.A., $\pm$ 0″·19 in Dec., as compared with $\pm$ 0″·14 in R.A., $\pm$ 0″·10 in Dec., for the stars) for a long-focus instrument. The reason is that the exposures on planet and stars were not identical.

With the Lippert astrograph, the probable errors were investigated separately for the period 1930 October to December and 1931 January. In the former period, the guiding was on a star, in the latter on Eros. The probable errors of the Eros positions are greater for the January observations,

when for some (but not all) plates the exposures on Eros and stars were unequal, than for the earlier period, during which the same exposures were given on Eros and stars.

The probable errors with the A.G. astrograph were satisfactorily small, and, though this was the shortest focus instrument of the four employed on the Eros observations, were as small as the smallest values with any of the other instruments. It appears that the mean of the two Eros images, at the beginning and end of the exposure on the stars, is in close agreement with the star images.

It seems certain that where the probable errors of the Bergedorf positions of Eros are unduly large, this must be attributed to an unsatisfactory method of observation.

9. Though the short-period variations in the position of the centre of brightness of Eros, suspected at Bergedorf, are not confirmed, an investigation of the possibility of some variation in the observed position of the planet with the period of the total light variation, $5^h\ 16^m$, or with the period between consecutive minima of brightness, $2^h\ 38^m$, is desirable. No conclusive evidence of such variation having been obtained by Hinks in the discussion of the 1901 observations, it may be expected that any such effect will be small. The satisfactorily small probable errors derived above for the average of all observatories on three different nights confirms the expectation that no large effect is to be looked for. Inasmuch, however, as a considerable amount of material is now available, some closer investigation seemed desirable.

The observations of v. d. Bos and Finsen at the Union Observatory, Johannesburg, make such an investigation imperative, if confidence is to be placed in the value of the solar parallax deduced from the observations at the opposition of 1931. It may be recalled that these observers, using the $26\frac{1}{2}$-inch visual refractor of the Union Observatory, found that Eros appeared to be of a figure-of-eight shape, resembling a nearly separated double star with a distance of $0''\cdot18$, and that the direction of elongation made a complete revolution in $5^h\ 17^m$, *i.e.* in the complete period of the variation of brightness.* It appears probable that the variation in brightness is attributable to unequal surface brightness of the planet's disk. The symmetrical appearance of the figure-of-eight shape suggests that any variation in position of the centroid of brightness with respect to the centroid of figure during the period of light-variation must be small.

The amplitude of the variation in brightness of Eros changes with change in the position of the Earth with respect to the pole of the axis of rotation of Eros. From a discussion of numerous observations of the variation of brightness at the opposition of 1931, Zessewitsch † found that the variation in the amplitude could be closely represented by the empirical formula $1^m\cdot50 - 0^m\cdot0275\ |\ \delta\ |$, where δ denotes the declination of Eros in degrees. The amplitude was accordingly greatest when Eros was on the equator, which occurred on 1931 January 27.

* *Ast. Nach.*, **241**, No. 5780, 297, 1931.
† *Ast. Nach.*, **246**, No. 5904, 441, 1932.

10. If the magnitude of the effect under investigation depends upon the amplitude of the variation in brightness, observations obtained when the planet was not far from the equator should presumably be most suitable for detecting the effect. Preliminary investigation showed that the effect, if it existed, was small, and that a considerable amount of material would need to be used in order to determine it with accuracy. This makes it necessary to combine observations spread over a number of nights, introducing the complications of a changing error of the ephemeris of Eros and of inhomogeneity in the system of star-places. In order to minimise the uncertainties introduced by these factors, the observations near the stationary point of Eros can be used. For an interval of about two weeks, it is found that there was no appreciable variation in the error of the ephemeris and, because of the slow apparent motion of Eros, the same comparison stars could be used for several nights.

Three good series of observations, extending fairly continuously over this interval, are available, viz. the two Cape series, obtained with the astrographic and 24-inch refractors, and the Cordoba series, obtained with the astrographic refractor. The observations in the interval March 9·7 to 24·3 were used; during this time the error of the ephemeris in each coordinate can be regarded as constant. For each of the three series the means in R.A. and Dec. were subtracted from the individual values and the residuals were grouped according to phase-angle, using the elements given by Zessewitsch *,

$$T = \text{J.D. } 2426282{\cdot}186 + 0^{d}{\cdot}2195942\, E.$$

The results for each series and for the three series combined are given in the following table :—

$5^{h}\ 16^{m}$ *Period* (*March* 9–24)
(Unit $0''{\cdot}01$)

Phase-angle	$\Delta\alpha \cos\delta$				$\Delta\delta$			
	Cape 13-in.	Cape 24-in.	Cordoba	Combined	Cape 13-in.	Cape 24-in.	Cordoba	Combined
° °								
0– 30	− 4₇	−1₈	+ 4₁₀	+0·425	−7₇	−1₈	− 7₁₀	−5·225
30– 60	− 1₁₀	+2₁₁	0₅	+0·326	−3₁₀	−1₁₁	+ 2₅	−1·426
60– 90	+ 4₅	+1₁₂	+ 8₆	+3·523	+7₅	0₁₂	− 6₆	−0·323
90–120	+ 1₅	−3₁₄	−25₂	−3·921	+1₅	+1₁₄	+ 8₂	+1·621
120–150	− 2₁₁	−1₁₃	− 1₇	−1·731	+1₁₁	+1₁₃	+ 3₇	+1·331
150–180	−11₇	+3₉	− 2₁₂	−2·728	−1₇	−4₉	+ 2₁₂	−0·728
180–210	+ 3₈	+1₁₀	− 1₅	+1·323	0₈	−4₁₀	0₅	−1·723
210–240	− 1₁₀	+1₁₅	− 1₄	+0·229	0₁₀	0₁₅	+ 2₄	+0·329
240–270	− 1₈	−4₉	+ 5₃	−1·520	+2₈	+4₉	+ 1₃	+2·620
270–300	+ 2₉	0₁₅	− 1₆	+0·330	+4₉	+4₁₅	+13₆	+5·530
300–330	+ 4₁₀	−1₁₀	− 1₆	+0·726	0₁₀	+4₁₀	− 1₆	+1·326
330–360	+ 6₈	+3₇	+ 2₁₁	+3·326	−2₈	−6₇	− 4₁₁	−4·026

* *Ast. Nach.*, **246**, No. 5904, 441, 1932.

The number of plates on which each value is based is given in the subscript figures.

The probable errors for a single plate in each of the three series, obtained by supposing that during the whole of this period the differences from plate to plate can be regarded as purely random, are as follows :—

	R.A.	Dec.	No.
	″	″	
Cape 13-in.	± 0·068	± 0·056	98
,, 24-in.	± ·057	± ·067	133
Cordoba 13-in.	± ·079	± ·078	77

The smallness of these probable errors is due, in part, to the motion of Eros being very slow near the stationary point and, in part, to the slowness of the motion making it possible to use the same comparison stars for several nights, so that the effects of inaccuracies of the star-places are reduced to a minimum.

The average number of plates in each phase-group in the combination of the three series being 25, the probable errors of the values in the 5th and 9th column of the above table lie between 0″·01 and 0″·02.

It is apparent from the figures in columns 5 and 9 that at this time any displacement of the centroid of brightness of Eros with respect to the centroid of mass in the period of the light-variation could not have exceeded a few hundredths of a second of arc. This is in agreement with the conclusion reached by Hinks from the discussion of the 1901 observations. The results in R.A. do not show any regularity, but there is a suspicion of an effect in declination in the half-period, $2^h\ 38^m$, the values near 0° and 180° being negative, and near 90° and 270° being positive. Combining corresponding groups at 180° apart in phase-angle, with equal weight, the variations in a period of $2^h\ 38^m$, in groups covering 60° in phase-angle, are as follows :—

Phase-angle	0°–60°	60°–120°	120°–180°	180°–240°	240°–300°	300°–360°
R.A.	+0·6	+0·2	+0·7	−1·3	−0·4	+0·2
Dec.	−3·5	−0·5	+1·1	+3·6	+1·3	−2·4

No effect is shown in R.A., but the results in Dec. show what appears, in relation to the probable errors, to be a small but real effect. When this suspected variation in the half-period is allowed for, there is some evidence of a variation of smaller amplitude with the period of $5^h\ 16^m$. The reality of the variation with the full period is doubtful, and is suggested more by a sequence in signs of consecutive values than by the magnitude of individual values, which are not much in excess of their probable errors.

The discussion of the most accurate portion of the observations at the opposition of 1931, *i.e.* those made near the stationary point, indicates that there is no variation in position in R.A. with periods of $2^h\ 38^m$ or $5^h\ 16^m$, but that there is a small variation in position in Dec. with period

$2^h\ 38^m$ and, possibly though less certainly, a smaller variation with period $5^h\ 16^m$.

11. In order to confirm these conclusions from a larger amount of material, the investigation was extended to cover the interval from February 20 to March 31. The changes in the error of the ephemeris during this time were sufficiently small for corrections on this account to introduce very little uncertainty. The investigation was restricted to the same three series that were used near the stationary point, and the total material was more than doubled.

The results from this extended investigation are given in the following table, which is arranged in a similar manner to the previous table :—

$5^h\ 16^m$ *Period* (*February* 20–*March* 31)

(Unit $0''.01$)

Phase-angle	$\Delta\alpha \cos\delta$				$\Delta\delta$			
	Cape 13-in.	Cape 24-in.	Cordoba	Combined	Cape 13-in.	Cape 24-in.	Cordoba	Combined
° °								
0– 30	-1.7_{17}	-1.2_{19}	-2.5_{23}	-1.9_{59}	-2.7_{17}	-4.9_{19}	-3.8_{23}	-3.8_{59}
30– 60	-1.6_{19}	-1.9_{21}	-1.5_{12}	-1.7_{52}	0.0_{19}	-1.6_{21}	$+2.1_{12}$	-0.2_{52}
60– 90	$+2.0_{15}$	-0.1_{26}	$+1.2_{15}$	$+0.8_{56}$	$+4.5_{15}$	$+3.0_{26}$	$+0.4_{15}$	$+2.7_{56}$
90–120	$+3.1_{23}$	$+2.1_{27}$	-11.5_{5}	$+1.3_{55}$	-0.3_{23}	$+2.4_{27}$	-2.9_{5}	$+0.8_{55}$
120–150	-2.9_{25}	$+1.6_{29}$	$+1.6_{16}$	0.0_{70}	$+0.9_{25}$	0.0_{29}	$+1.8_{16}$	$+0.7_{70}$
150–180	-1.7_{20}	$+1.2_{25}$	$+0.9_{21}$	$+0.3_{66}$	-2.5_{20}	-0.6_{25}	-2.3_{21}	-1.7_{66}
180–210	$+1.9_{19}$	$+1.7_{19}$	$+7.8_{19}$	$+3.8_{57}$	-2.3_{19}	-2.8_{19}	$+0.3_{19}$	-1.6_{57}
210–240	$+4.2_{21}$	0.0_{28}	-3.1_{10}	$+0.9_{59}$	$+0.9_{21}$	-0.2_{28}	$+7.8_{10}$	$+1.6_{59}$
240–270	-3.8_{21}	-2.5_{19}	$+4.6_{15}$	-1.1_{55}	-0.1_{21}	$+2.8_{19}$	-7.1_{15}	-1.0_{55}
270–300	-1.9_{25}	$+1.1_{23}$	$+5.4_{11}$	$+0.7_{59}$	$+3.0_{25}$	$+4.8_{23}$	$+9.2_{11}$	$+4.8_{59}$
300–330	$+0.7_{20}$	-0.5_{26}	-2.7_{21}	-0.8_{67}	$+0.4_{20}$	$+1.6_{26}$	-1.4_{21}	$+0.3_{67}$
330–360	$+1.9_{19}$	-0.9_{24}	$+0.1_{22}$	$+0.3_{65}$	-1.4_{19}	-4.0_{24}	-4.5_{22}	-3.4_{65}

None of the three series individually, nor the combined mean, shows any evidence of a variation in R.A. with either the full period of the light-variation or the half-period. In declination there is some evidence from each series of a variation with a period of $2^h\ 38^m$, the values near 0° and 180° being negative, and near 90° and 270° being positive. The means of the values separated by 180° gives for the variation in declination in the half-period the following results :—

Declination : $2^h\ 38^m$ *Period*

Phase-angle	0°–60°	60°–120°	120°–180°	180°–240°	240°–300°	300°–360°	No. of Plates
Cape 13-in.	−2.5	+0.5	+2.2	+1.4	+0.7	−2.0	244
,, 24-in.	−3.8	−0.9	+2.9	+3.6	+0.8	−2.3	286
Cordoba	−1.8	+4.9	−3.3	+3.2	+0.2	−3.4	190
Combined	−2.7	+0.7	+0.9	+2.8	+0.5	−2.6	720

The general agreement between these three series confirms the reality of the variation in the period of $2^h\ 38^m$, the extreme range of the variation being about 0″·06. There is no evidence of variation with period $5^h\ 16^m$. The amplitude of the variation in brightness of Eros at this time, inferred from the empirical relation given by Zessewitsch, was about $0^m{\cdot}78$.

12. In order to investigate whether this variation was larger in amount when the amplitude in the variation of brightness of Eros was greater, a few days near the end of January were selected close to the time when the planet crossed the equator and when the total amplitude of variation was $1^m{\cdot}5$. The rapid motion of the planet at this time is a complicating factor; different comparison stars had to be used from night to night and inhomogeneities in the system of star-places increase the probable errors. The error of the ephemeris was also changing rather rapidly (about 0″·05 a day in declination); corrections to take account of this were read off from a smooth curve, though there is evidence that the errors at this time are rather irregular—presumably the reflection of the irregularities in the system of star-places. To obtain sufficient material within a short period of time the results from several telescopes had to be combined, which again increases the probable error, for there is evidence of small systematic differences in declination between different instruments.

The period selected was January 27 to February 5, and the results from the following telescopes were utilised: Cape 13-in., Cape 24-in., Cordoba 13-in., Melbourne 13-in., Greenwich 13-in., Greenwich 26-in., Dearborn $18\frac{1}{2}$-in., Van Vleck 20-in., Radcliffe 24-in., Yale (Johannesburg) 26-in., Algiers 13-in.

The same weight was given to one plate of each series, though some series have higher accuracy than others.

The results were as follows:—

$5^h\ 16^m$ *Period* (*January 27–February 5*)

Phase-angle	$\Delta\alpha \cos\delta$ (Unit 0″·01)	No.	$\Delta\delta$ (Unit 0″·01)	No.
° °				
0– 30	−6·3	23	−6·0	18
30– 60	−4·6	29	+2·3	25
60– 90	+4·9	29	+6·5	23
90–120	+6·9	34	+1·5	31
120–150	+2·7	40	−1·5	37
150–180	−2·7	36	−1·2	33
180–210	+2·2	38	+0·3	31
210–240	+2·2	43	+1·5	40
240–270	−4·0	32	+3·6	26
270–300	−1·8	36	−2·3	31
300–330	−3·0	42	−4·7	28
330–360	+3·9	31	+0·2	26

The average probable error for a single plate for the whole series is ± 0″·106 in R.A. and ± 0″·105 in Dec. The probable error of a phase-group mean is somewhere about 2, in the units of columns 2 and 4.

As before there is no certain evidence of periodicity, except that in the declinations there is a suggestion of a variation with the half-period. Collecting into phase-groups of 60° for this variation, we find :

$2^h\ 38^m$ *Period* (*January 27–February 5*)

(Unit 0″·01)

Phase-angle	0°–60°	60°–120°	120°–180°	180°–240°	240°–300°	300°–360°
R.A.	−2·0	−0·7	+0·4	+2·5	−0·1	+0·6
Dec.	−2·8	+1·9	+5·0	−0·4	−3·1	−0·4

There is no evidence of a variation in R.A. with period of $2^h\ 38^m$. The results in declination, in consequence of the increased probable error, are not so smooth as previously, but appear to confirm on the whole the reality of the variation. As Eros crossed the equator on January 27, the amplitude of its variation in brightness was nearly twice as great during the time January 27 to February 5 as it was in the period near the stationary point, previously discussed. The results for the earlier period are not confirmatory of the supposition that the greater amplitude in the variation of brightness may have been accompanied by a greater variation in the position of the centroid of brightness with respect to the centroid of mass.

13. It is concluded, therefore, that the variation in the brightness of Eros does not produce any detectable displacement in right ascension of the centroid of brightness with respect to the centroid of mass ; there is a small, but apparently adequately confirmed, displacement in declination with a period of $2^h\ 38^m$ (time-interval between consecutive minima), the total amplitude of which is of the order of 0″·05, but there is no displacement in declination with the period of $5^h\ 16^m$ (total period of variation in brightness).

This conclusion is not in agreement in detail with the investigation of Hinks * from the 1901 observations. No displacements with period of $5^h\ 16^m$ were detected by Hinks ; a small displacement with period $2^h\ 38^m$, and total amplitude of between 0″·06 and 0″·08, was suspected in right ascension, but no effect was found in declination. The amount of material on which these conclusions were reached was considerably less than the amount used in the present discussion.

The solar parallax may be derived either from the observations in right ascension, by comparing observations at differing hour-angles at the same observatory, or from the observations in declination by comparing observations at nearly the same time at two observatories, one in the northern hemisphere and one in the southern. An apparent displacement of Eros, with total range of the order of 0″·05 and period $2^h\ 38^m$, would not be negligible in R.A., for the accurate determination of the correction to the assumed value of the solar parallax depends upon the accurate determination of small differences in R.A. between evening and morning observations.

* *M.N.*, 64, 701, 1904 (see p. 722, § 22).

But a displacement of this nature has not been found to exist. The parallax factor in declination does not vary greatly through a night, and the determination of the solar parallax from the comparison between results obtained at northern and southern observatories depends upon the difference between the means of all the observations on the same night at the two places. The effects of small periodic displacements with period $2^h\ 38^m$ are eliminated to a large extent in taking the mean of the night, and any residual effect can be regarded as an accidental error.

There accordingly appears to be no reason why Eros should not be regarded as an entirely suitable object for the accurate determination of the solar parallax.

Summary

1. An extensive programme of observations of Eros, for the improved determination of the solar parallax and of the mass of the Moon, was made near the favourable opposition of 1931. The results are now under discussion.

2. In a recent publication, short-period variations in the position of the centroid of brightness of Eros with respect to the centroid of mass, with periods of approximately 12·5 and 79·5 minutes, are asserted to occur. It is suggested that Eros is a multiple system with at least three components. The total amplitude of the suspected variations (several tenths of a second of arc) leads to the conclusion that Eros is not a suitable object for the accurate determination of the solar parallax.

3. The reality of these short-period variations is investigated, using more extensive and more accurate material. It is found that such variations do not exist.

4. Eros is known to be variable in brightness, with a total period of $5^h\ 16^m$. Consecutive minima are unequal and spaced at equal intervals of $2^h\ 38^m$. Under high magnification v. d. Bos and Finsen found that Eros had the appearance of a figure-of-eight. Apparent variations in position of the centroid of brightness, with periods of $5^h\ 16^m$ or $2^h\ 38^m$, are therefore investigated.

5. No detectable variation with period of $5^h\ 16^m$ is found, nor can a variation with period of $2^h\ 38^m$ be detected in the right ascensions. There appears to be a small variation in declination, of total range about $0''{\cdot}05$, with period $2^h\ 38^m$.

6. The range of this small variation does not seem to become greater with the increase in the amplitude of the variation in brightness of Eros.

7. This variation will not have any systematic effect on the determination of the solar parallax from the comparison between the observations in declination at a northern and southern observatory.

8. It is concluded that Eros is a suitable object for the accurate determination of the solar parallax.

RELATIVE DIMENSIONS OF SHELLS AROUND NOVA HERCULIS 1934

W. S. Tai

The Materials.—The spectrograms used in this investigation are listed in Table I. The first thirteen spectrograms are used for the study of the hydrogen absorption components, the three G spectrograms for the study of the D lines, and the Cambridge spectrograms for the study of the *Ti*II and *Fe*II lines.

In Table I, the apparent visual magnitudes are taken from Beer's paper *, and the colour temperatures from E. G. Williams's paper.† Spectral range means the range of the spectrum which is of sufficiently good definition and is sufficiently free from blending for photometric work. Calibration data for the Mount Wilson spectrograms were kindly supplied by Dr. W. S. Adams, and those for the Greenwich spectrogram by Mr. E. Martin.

TABLE I

Nova Herculis Spectrograms

Plate No.	Taken at	Date (U.T.)	m_v	T_e	Spectral Range
121	Greenwich	1934 Dec. 18·7	2·5		$H\alpha$ to $H18$
C 6599	Mt. Wilson	16·1	2·8		$H\beta$ to Hζ
V 692	...	20·1	2·2		$H\beta$ to $H\zeta$
V 699	...	21·1	2·0		$H\beta$ to K
V 703	...	22·0	1·6		$H\beta$ to $H18$
V 728	...	1935 Jan. 6·6	2·4	9,300°	$H\beta$ to $H10$
V 738	...	16·6	2·7	9,000°	$H\beta$ to $H\zeta$
V 767	...	Feb. 2·5	3·6	11,000°	$H\beta$ to $H10$
V 792	...	28·5	3·2	12,500°	$\lambda\lambda$ 4950–3680
V 800	...	Mar. 13·5	3·8	15,000°	$\lambda\lambda$ 4950–3680
V 813	...	16·4	4·3	16,000°	$H\beta$ to $H12$
V 827	...	18·5	4·5	16,500°	$H\beta$ to $H18$
V 833	...	23·5	4·7	15,500°	$H\beta$ to $H14$
G 1147	...	1934 Dec. 22·1	1·5	11,000°	$H\alpha$ to λ 5300
G 1187	...	31·1	2·4	9,600°	$H\alpha$ to λ 5300
G 1205	...	1935 Jan. 21·1	2·5	8,700°	$H\alpha$ to λ 5300
T 261	Cambridge	5·2	2·5	9,400°	$\lambda\lambda$ 4600–3900
T 268	...	7·2	2·5	9,300°	$\lambda\lambda$ 4900–4200
T 295	...	15·3	2·5	9,000°	$\lambda\lambda$ 4600–3900
T 319	...	26·8	2·5	9,500°	$\lambda\lambda$ 5000–4100

The Central Absorption of the Hydrogen Components.—On the December spectrograms only one absorption component (Abs. I) is present. The designation of the absorption components given by McLaughlin ‡ will be

* *M.N.*, **95**, 538, 1935.
† *M.N.*, **99**, 105, 1939.
‡ *Pub. Obs. Univ. Mich.*, **6**, No. 12, 1937.

employed in this paper. On the January and February spectrograms, two absorption components are present : Abs. II, which is comparatively sharp ; and a more displaced broad component which is a blend of Abs. III and Abs. IV. The broad component is observed on the microphotometer tracings to have two absorption maxima. Since these two maxima have practically the same depth, their intensities are not recorded separately. In March, the hydrogen lines developed a more complicated structure. On the first three of the March spectrograms, at least four components are definitely present, namely, II (− 370 km./sec.), VII (− 570), III (− 750) and IV (− 850). Besides, Professor Stratton measured two faint components at − 450 and − 670 km./sec. approximately on these spectrograms for the lines $H\zeta$, $H\eta$ and $H\theta$. Since they are very faint and neither of them is observed in all the three H lines measured and on all the three spectrograms, they are neglected in this work. On the last March spectrogram available (V 833, March 23·5), the faint component at − 450 has become nearly as strong as Abs. II, and is displaced more to the violet (about − 480). This is probably the short-lived component which McLaughlin called Abs. IX. VII, IV, and the faint component at − 670 (− 650 on this spectrogram) are still present ; whereas III has become very faint and is therefore neglected. A new and much displaced component (about − 1000) appears, and is probably that which McLaughlin called Abs. V.

The central absorption of the various hydrogen components are measured and given in Tables II, III and IV. Central Absorption (A_c), or Percentage Depth, is defined by the formula $A_c = 100(1 - r_c)$, where r_c is the central intensity of the absorption component. A_c is expressed in percentage of the intensity of the background in the immediate neighbourhood of the absorption component. By "background in the immediate neighbourhood" is meant not only the continuous spectrum due to the radiation from the central star, but also the line emission. This choice of unit will be discussed again later on in this paper. In the tables a dash means that no absorption component of the specified velocity was detected. When the measured value of A_c is enclosed in parenthesis, that absorption component is blended with the H line of *Ca*II. A colon placed after any tabulated value means that the value is of smaller weight than those values without colon. A_c is also given for the K line of *Ca*II to enable one to judge what proportion of the observed values of the blend $H\epsilon$ + H may be due to *Ca*II.

Other quantities given in the tables are :

n. Principal quantum number.

E_c. Central emission, or emission at the undisplaced position, expressed in percentage of the intensity of the continuous spectrum at the same position. The quantity E_c is given just to show how far the measured intensity of the absorption lines might be affected by their blending with the emission. No attempt has been made to reduce this quantity to a common unit, for such a step would be unnecessary in this case. In the tables a dash means that no emission is detected for that line ; it amounts to the same thing as putting 100 for E_c. When the measured value of E_c is enclosed in parenthesis, that emission is blended with the H emission of *Ca*II.

TABLE II

Intensity of Hydrogen Lines (Abs. I) in December

Plate No.		C 6599			Greenwich No. 121		V 692			V 699			V 703	
Date		Dec. 16·1			Dec. 18·7		Dec. 20·1			Dec. 21·1			Dec. 22·0	
Tabulated Quantity		E_c	A_c	W	E_c	A_c	E_c	A_c	W	E_c	A_c	W	E_c	A_c
	n													
$H\beta$	4	300:	63	3·19			200	69	2·38	135	62	2·46	—	45
$H\gamma$	5	240:	65	2·53			140:	88:	2·55	—	72	2·92	—	60
$H\delta$	6	170	58	2·22	145:	45	120	79	2·18	—	68	2·05	—	59
$H\epsilon$	7	(175)	(61)		(130)	(44)	(130)	(69)		(140)	(57)		—	(58)
$H\zeta$	8	150	46	1·32	—	43	—	74	1·56				—	61
$H\eta$	9				—	39							—	65
$H\theta$	10				—	36							—	53:
$H\iota$	11				—	42							—	52:
$H\kappa$	12				—	37							—	55:
$H\lambda$	13				—	39							—	60:
$H\mu$	14				—	32							—	58:
$H\nu$	15				—	38							—	64 bl?
$H\xi$	16				—	35:							—	52:
$H\sigma$	17				—	33:							—	54:
$H\pi$	18				—	27:							—	52:
*Ca*II (*K*)		130	50		130:	39	130	67		140	61			

TABLE III

Intensity of Hydrogen Lines in January and February

Plate No.		V 728			V 738			V 767			V 792		
Date		Jan. 6·6			Jan. 16·6			Feb. 2·5			Feb. 28·5		
Tabulated Quantity		E_c	A_c II	A_c III–IV	E_c	A_c II	A_c III–IV	E_c	A_c II	A_c III–IV	E_c	A_c II	A_c III–IV
	n												
$H\beta$	4	300	30:	40:	420	50	80	740:	40:	72	330	59:	71
$H\gamma$	5	190	60:	65:	140:	30:	78:	?	?	83:	145:	50:	68
$H\delta$	6	190	60:	64	185	39	85	220	70	87	140:	51:	70
$H\epsilon$	7	(190)	(89)	(75)	(210)	(84)	(87)	(270)	?*	(85)	(160)	(70)	(81)
$H\zeta$	8	120:	40:	50:	190:	44:	54	150:	58	76	145:	48:	68
$H\eta$	9	130:	32:	37:				180:	35:	53:	155:	52:	60
$H\theta$	10	130:	35:	35:				150:	41:	56:	—	44:	63
*Ca*II (*K*)		170	93	80	200	80	77	270			150	73:	81

* Blend with violet emission maximum.

TABLE IV

Intensity of Hydrogen Lines in March

Plate No. / Date		V 800 March 13·5					V 813 March 16·4				
Tabulated Quantity / Displacement		E_c	A_c II −370	VII −570	III −750	IV −850	E_c	A_c II −370	VII −570	III −750	IV −850
	n										
$H\beta$	4	320	60	58	67		530	88	80	81	
$H\gamma$	5	200	70	71	86		250	82	71	79	80
$H\delta$	6	185:	75	74	83	82	310	82	72	76	75
$H\epsilon$	7	180:	52	(71)	63	64	190	70	(77)	68	69
$H\zeta$	8	130:	55	56	56	48:	145	70	64	52	54
$H\eta$	9	115:	50	58	56	51	135	61	57	46	49
$H\theta$	10	120	43	46	48	28	120:	63:	55:	41:	42:
$H\iota$	11	120	33	30	29	24	115:	51:	43:	26:	26:
$H\kappa$	12	110	29	30	27	18	—	49:	52:	31:	26:
$H\lambda$	13	105:	23	20	15	10					

Plate No. / Date		V 827 March 18·5					V 833 March 23·5					
Tabulated Quantity / Displacement		E_c	A_c II −370	VII −570	III −750	IV −850	E_c	A_c II −370	IX −480	VII −570	IV −850	V −1000
	n											
$H\beta$	4	260	66:	66	65:		250	77		77:	58	25:
$H\gamma$	5	170	77	79	80:	76	210	85		78	67	32
$H\delta$	6	205	72	71	68	65	180	87	84	77	63	28
$H\epsilon$	7	(155)	62	(68)	61	58	140	80	(83)	(83)	58	32
$H\zeta$	8	140	60	58	50	47	120	66	63	56	42	22
$H\eta$	9	125	56	52	35	37	115	62:	56:	50	40	20
$H\theta$	10	120:	57	55	30	28	—	56:	51:	46	31	21:
$H\iota$	11	110	46	43	21	19	—	50:	49:	30	15	?
$H\kappa$	12	—	45	46	28	17	—	54:	55:	40	25	?
$H\lambda$	13	—	44	37	9	12	—	43:	40:	27	17:	
$H\mu$	14	—	42	32	—	—	—	44	33:	31:	14:	
$H\nu$	15	—	35:	32:	—	—						
$H\xi$	16	—	33:	25:	—	—						
Ho	17	—	26:	18:	—	—						
$H\pi$	18	—	24:	15:	—	—						

W. Equivalent Width. The unit is the energy contained in one angstrom unit of the background in the immediate neighbourhood of the absorption component. It is given only for the first three Mount Wilson

spectrograms, because for others it is difficult to measure W owing to blending or other reasons.

In fig. 1, central absorption is plotted against principal quantum number

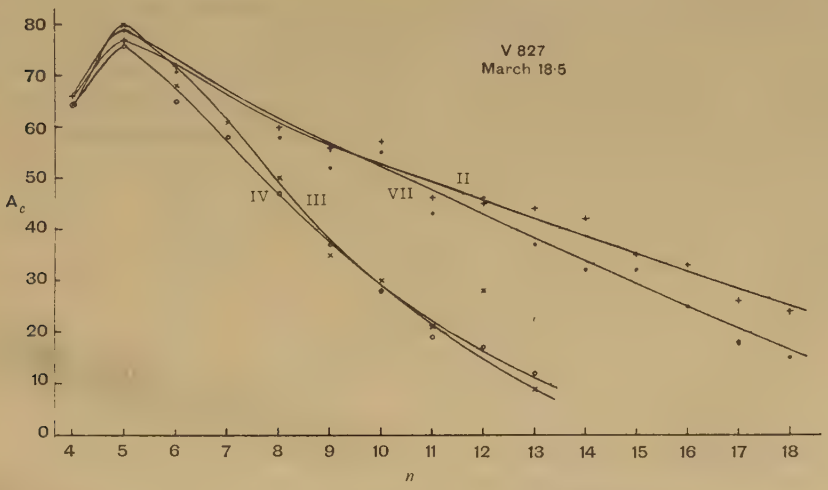

FIG. 1.—*Relative Depths of Balmer Absorption Lines.*

for one March spectrogram. In fig. 2 the same quantities are plotted for Abs. II in March.

Calculation of Electron Pressures.—It is a well-known fact that the number of absorption lines of the Balmer series present on a stellar spectrum is not

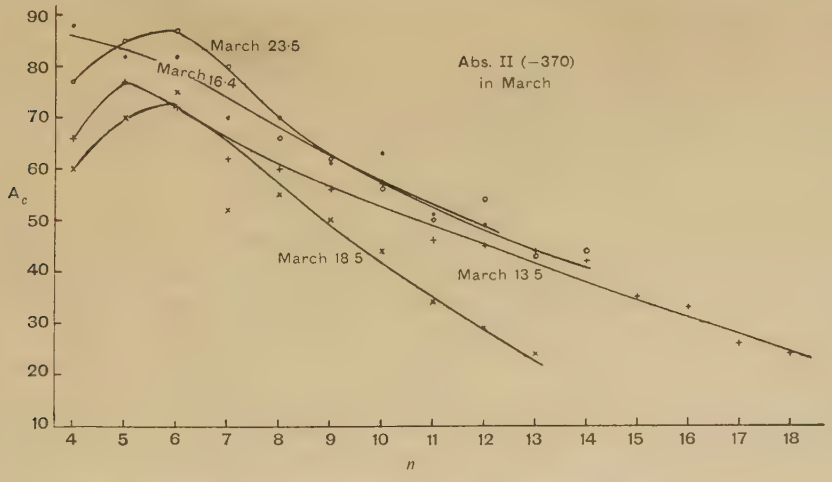

FIG. 2.—*Relative Depths of Balmer Absorption Lines.*

the same for stars of the same spectral type. Several factors determine the number of lines present, of which the most important is the electron pressure in the layers which produce the absorption lines. The bigger the ionic concentration, the greater the electric field, and the more the lines are broadened by Stark effect. When the higher members of a series are

sufficiently broadened, they merge into the continuous spectrum, and the series terminates.

Recently Inglis and Teller * derived a formula connecting the ionic concentration N with the maximum quantum number n_m, which is the effective quantum number of the line with which the series terminates. The formula, $N = 0{\cdot}027 a_0^{-3} n_m^{-7{\cdot}5}$ †, can be applied to any one-electron spectra. Inglis and Teller show that for $T < 10^5/n_m{}^\circ K$, $N = 2N_e$, where N_e is the electron concentration. Mohler ‡ verified the formula experimentally for

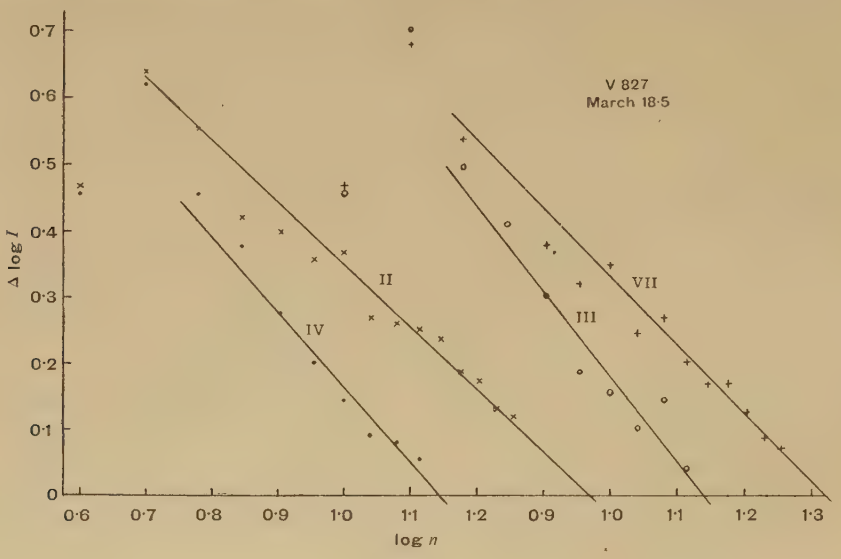

FIG. 3.—*Determination of n_m.*

the emission spectrum of cæsium. By introducing the relation $P_e = kTN_e$, where P_e is the electron pressure, Mohler obtained the working formula

$$\log P_e = 1{\cdot}19 + \log T - 7{\cdot}5 \log n_m,$$

in which the constant term has been slightly modified in order to fit the experimental results. Mohler applied the formula to hydrogen absorption lines in stellar spectra, using the observational data of Merrill and Wilson §, and found reasonable values of P_e for 5 early type stars (of which two are supergiants) and a white dwarf. The same method is now applied to Nova Herculis. Fig. 3 illustrates the method of determining n_m. Ordinate represents $\Delta \log I$, which is logarithm of the ratio of the intensity of the continuous background to that at line centre, and is numerically equal to $-\log r_c$. Abscissa represents $\log n$. After plotting the observed points, a straight line is drawn through them, and the intercept at $\Delta \log I = 0$ gives the value of n_m. In drawing the straight line, more weight is given to the higher members of the series, because the formula used involves the concept

* *Ap. J.*, **90**, 439, 1939. † *Ap. J.*, **90**, 429, 1939.
‡ a_0 is the radius of the first Bohr orbit, $= 0{\cdot}53 \cdot 10^{-8}$ cm.
§ *Ap. J.*, **80**, 19, 1934.

of electron orbit and can only be applied to the higher members. Furthermore, the lower members have much stronger emission, so the absorption components of these members are affected more by blending with emission than those of the higher members. For these two reasons, not much attention is paid to $H\beta$, γ, δ and ϵ. In a few cases, however, it is found that $H\epsilon$ (when it is not blended with *Ca*II), $H\delta$ and even $H\gamma$ fall in line with the higher members. On the diagram, some of the lines are shifted along the $\log n$ direction, so that the points would not get too crowded. The drawing of a straight line through the plotted points does not have any theoretical basis, but the observational data Mohler used show that the points do lie on a straight line. This is also what we have found for Nova Herculis (after the lower members of the series are neglected). In practically no case do the plotted points appear to curve upwards or downwards. The scatter on the diagrams must be due to blending and other observational errors.

From the $\Delta \log I - \log n$ diagram there seems to be an actual difference in the gradient of the straight lines. This difference can also be noticed in fig. 7 of Merrill and Wilson's paper (A_c *vs* n) *, or fig. 1 of Mohler's paper ($\Delta \log I$ *vs* $\log n$). The gradient indicates how fast the higher members of a series diminish in intensity; it is probably some function of the physical variables. Mohler's formula only tells us when the series terminates, but does not give the relative intensity of the lines. For the spectrogram *V* 703 and the Greenwich spectrogram (both taken near the light maximum) the intensity gradient of the Balmer lines is extremely small from $H\gamma$ to *H* 18. This is taken to indicate that we have not yet come to the descending branch of the central absorption curve (A_c *vs* n). For β Orionis (*c*B8), the central absorption is practically constant from $H\gamma$ to *H* 17, then suddenly the curve bends downwards, until the central absorption vanishes at $n = 23{\cdot}5$. (See Merrill and Wilson's paper; Pannekoek's theoretical calculations † for *H* emission lines near the Balmer limit also shows the same phenomenon.) The same is true for α Cygni. This bending of the central absorption curve after *H* 17 would most probably be observed for the nova near light maximum if the spectrum beyond *H* 18 suitable for photometric work could be secured. McLaughlin's measurement of Abs. I ‡ verified this.

For the spectrogram *V* 792 (Feb. 28·5), the intensity decreases very slowly from $H\beta$ to *H* 10. *H* 10 is plainly visible on the spectrum, whereas *H* 11 is almost invisible either on the spectrum or on the tracing, so are *H* 12, *H* 13, etc. This may be partly due to blending with the numerous metallic lines in that region of the spectrum on that date. On the other hand, the H lines might actually diminish in intensity very rapidly after *H* 10. This abrupt termination of the Balmer series (also observed in some stellar spectra) cannot be explained in terms of the broadening of line by Stark effect and consequent gradual merging into the continuous spectrum. Some other explanation is needed.

The values of T_c given in Table I were combined by E. G. Williams

* The difference is especially pronounced when we compare the Balmer with the Paschen lines.

† *M.N.*, **98**, 694, 1938. ‡ *Loc. cit.*, p. 115.

from several sources *, and represent the temperature of the continuous radiation of the central star if the star is radiating like a black body. Some observers † reported that to the red of λ 4000, the intensity curve of the Nova's continuous spectrum fits the Planck curve within 10 per cent., whereas below λ 4000 there is a great excess of radiation. The gradual appearance of high excitation lines, however, indicates that the colour temperatures we have adopted for the first three months of 1935 can reasonably represent the effective temperatures of the absorbing shells which are nearest to the central star.

The following two assumptions are made with regard to temperature :—

1. Assume that atoms cease to be spectroscopically active when they get too far away from the central star, and that the shells are continuously replenished from below. Then the effective radii of the shells are not very different from one another, and the shells have nearly the same temperature at any one time. Under this assumption we take the tabulated values of T_c on each date to be the effective temperatures of all the shells on that date. The electron pressures of the different shells calculated by Mohler's formula from these temperatures and the values of n_m obtained from the intensity gradient of the Balmer absorption lines are listed in Table V.

TABLE V

Electron Pressures of the Absorbing Shells

Plate No.	Date	T_c	Component	n_m	P_e*
V 728	Jan. 6·6	9,300°	II	15·3 :	1·9 :
			III–IV	14·8 :	2·4 :
V 792	Feb. 2·5	11,000°	II	13·0 :	7·6 :
			III–IV	13·2 :	6·8 :
V 800	Mar. 13·5	15,000°	II	16·3	1·8
			VII	15·1	3·4
			III	14·5	4·6
			IV	13·0	6·7
V 813	Mar. 16·4	16,000°	II	20·0	0·43
			VII	22·6	0·18
			III	14·5	4·9
			IV	14·2	5·7
V 827	Mar. 18·5	16,500°	II	23·5	0·14
			VII	20·9	0·32
			III	13·7	7·6
			IV	13·7	7·6
V 833	Mar. 23·5	15,500°	II	24·6	0·09
			IX	24·1	0·10
			VII	19·5	0·51
			IV	16·1	2·1
			V	17·8?	1·0?

* In unit of 10^{-4} atm.

* Petrie, *Ap. J.*, **81**, 483, 1935 ; Beileke and Hachenberg, *Zs. f. Ap.*, **10**, 366, 1935 ; Greaves and Martin, *M.N.*, **96**, 425, 1936 ; Oehler, *Zs. f. Ap.*, **12**, 281, 1936.

† Beileke and Hachenberg, *loc. cit.* ; Williams and Green, *M.N.*, **96**, 434, 1936.

2. In the case of shells II and IV, assume a constant temperature of 7000°. This temperature is deduced from the spectral type (*F* 5) of Abs. II and IV at the beginning of their existence. If the shells grow bigger and bigger or if they are detached and get further and further away from the central star, their effective temperatures would decrease unless the temperature of the exciting radiation increased. The fact that the temperature of the continuous radiation did increase may render the effective temperatures of the absorbing shells more or less constant. Electron pressures calculated under this assumption are given in Table VI. Shell III probably behaved in the same manner as IV. VII, IX and V all emerged at later dates, and might therefore have higher effective temperatures. Consequently their P_e are not calculated on this assumption.

TABLE VI

Electron Pressures of Shells II and IV

(Assume a constant temperature of 7000°)

Date	II		IV	
	n_m	P_e*	n_m	P_e*
Jan. 6·6	15·3 :	1·4 :	14·8 :	1·8 :
Feb. 2·5	13·0 :	4·7 :	13·2 :	4·2 :
Mar. 13·5	16·3	0·88	13·0	4·7
16·4	20·0	0·19	14·2	2·5
18·5	23·5	0·06	13·7	3·3
23·5	24·6	0·04	16·1	0·77

* In unit of 10^{-4} atm.

The P_e calculated for January 6·6 and February 2·5 are each based on only four lines, and are not to be regarded as of much weight. They are, nevertheless, useful for comparison with the March data.* From Tables V and VI there seems to be no great change in the electron pressures of shells III and IV from the early part of January to the middle of March, the value of P_e remaining in the vicinity of $5 \cdot 10^{-4}$ atm. until March 18·5. Between March 18·5 and March 23·5, III disappeared from the scene, whereas IV narrowed down into a sharp absorption line, with its P_e diminished about 4-fold. Subsequently, this sharp Abs. IV component decreased in intensity gradually, and completely disappeared before April 4, when only emission lines remained. The P_e of shell II began to decrease in the middle of March, and on March 23·5 its value was only 1/20th of that ten days before. Like Abs. IV and all other absorption lines, Abs. II also disappeared completely before April 4. The P_e of shell VII diminished about 10-fold between March 13·5 and March 16·4, and then remained quite constant until March 23·5. The data

* P_e is not calculated for January 16·6 and February 28·5. Judged by the relative intensity of the lower members of the Balmer series, P_e must be lower for these two dates than for January 6·6 and February 2·5. This will not be surprising when we remember that m_v of the nova is going up and down during these two months.

for IX and V are scanty; they are obtained from only one spectrogram. It seems likely that IX is similar to II in P_e, whereas the P_e of V is probably of the same order as that of IV.

The assumption of a constant and lower temperature only decreases a little the P_e of II and IV in March; but the order of magnitude remains about the same, and the P_e ratio for the two shells is practically unaltered. P_e is proportional to $Tn_m^{-7\cdot5}$, so it is comparatively insensitive to change in temperature. The observed results have not enabled us to decide which temperature scale is more correct.

The Blending of Absorption and Emission.—The presence of strong emission bands in the spectra of novæ makes it very difficult to measure the intensity of the absorption lines; on the other hand, this blending of emission and absorption may give us useful information and may help to reveal the physical nature of the shells. As pointed out by Williams *, if we regard the blending of emission and absorption as mere superposition, that is to say, if the atoms which produce the absorption line do not also absorb from the line emission at the same wave-length, then the measured central absorption often exceeds 100 per cent. of the continuous spectrum. This is also found to be the case for the spectrograms used in this investigation. For the December spectrograms this difficulty is not met, because there is only one component then and there is practically no extra emission at the wave-length of the absorption line. For all the rest—January, February and March spectrograms—the central absorption would exceed 100 per cent. of the continuous spectrum for most of the hydrogen components from $H\beta$ to $H\zeta$, if we regard the blending as mere superposition. Now if we take the background in the immediate neighbourhood of the line, continuous spectrum plus line emission, and express the line absorption in percentage of this background, we get much more reasonable values of A_c. Take an example: For $H\gamma$ on the spectrogram V 800 (March 13·5) we get the following values of A_c:—

		Abs. II	Abs. IV
Case 1.	Mere superposition . .	210	240
Case 2.	Line emission also absorbed .	70	86

An extreme case is found in $H\beta$ on the spectrogram V 813 (March 16·4). On this date, the line emission was very strong, and we get:

	Abs. II	Abs. IV
Case 1	540	430
Case 2	88	81

Another indication that Case 2 is nearer the truth is to be found in the shape of the central absorption curve (A_c *vs* n). Most of these curves (see figs. 1 and 2) slope upwards from $H\beta$, reach the maximum point at $H\gamma$ or $H\delta$, and then slope downwards. For the spectrogram V 703 on which no line emission is present, the curve is also like others. On fig. 7 of Merrill and Wilson's paper, we see the same kind of curves for early type stellar spectra with only

* *Observatory*, 59, 331, 1936.

absorption lines. If we take Case 1, then for the nova on most dates, the central absorption curve would start with a very high value of A_c for $H\beta$ and slope steeply downwards to the higher members.

These facts from the hydrogen lines indicate that the H atoms in the shell which produces Abs. II also absorb from the radiation emitted by the H atoms in the shell which produces Em. IV, and therefore Abs. II has a much bigger effective radius than Em. IV. In March there is also line emission to the violet of Abs. IV. The fact that Case 2 is also much nearer the truth for Abs. IV in March shows that these violet emissions probably originate from an inner gas shell of very high velocity.

The D lines are also suitable for studying the blending of absorption and emission, because the two lines are quite close together. Three Mount Wilson G spectrograms were selected for the photometry of the D lines. The first spectrogram, G 1147, was taken on December 22·1 when only Abs. I is present and Em. I is so faint that it can be neglected. A_c and W are obtained for both lines (see Table VII), and the ratios D_2/D_1 for both

TABLE VII

Intensity of the D Lines

G 1147 Dec. 22·1			G 1187 Dec. 31·1					G 1205 Jan. 21·1		
	A_c	W		A_c		W			A_c	
				Case 1	Case 2	Case 1	Case 2		Case 1	Case 2
D_1I	24	0·48 A.	D_1II	73	49	1·90	1·32	D_1II	81	43
D_2I	30	0·75	D_2II	66	60	1·89	1·69	D_2II	102	62
D_2/D_1	1·25	1·55	D_2/D_1	0·90	1·22	1·0	1·28	D_2/D_1	1·26	1·44
								D_2IV	84	72
				$E_c = 170$					$E_c = 210$	

A_c and W are calculated. These ratios will be used as criteria for choosing between Case 1 and Case 2 for the other two spectrograms. On the second spectrogram, G 1187, December 31·1, Abs. I is completely gone, whereas Abs. II and Em. II are present. D_1 absorption is blended with D_2 emission. By assuming a symmetrical emission contour with the axis of symmetry at the mean of the undisplaced positions of D_1 and D_2, A_c and W are measured for both lines by both methods (Case 1 and Case 2). From Table VII we see that Case 1 gives an impossible ratio D_2/D_1 for A_c and an unlikely one for W, whereas Case 2 gives much more reasonable ratios. This shows that for *NaI* Abs. II also absorbed from Em. II, so that the former had a much bigger effective radius than the latter. On the third spectrogram, G 1205, January 21·1, Abs. II, Abs. IV, Em. II and Em. IV are concurrently present. Abs. IV is much broader than Abs. II, so D_1IV, D_2IV, and the violet end of D_2II are all blended together, forming a broad absorption band. The existence

of D_1IV is, however, easily shown by the unsymmetrical contour of this broad band and the great strength of D_2II (see fig. 4). It is difficult to measure the equivalent width in this case, so only A_e are given in Table VII. The ratio D_2/D_1 for Abs. II is apparently all right in both cases. But remembering that part of the apparent central absorption of D_2II is due to

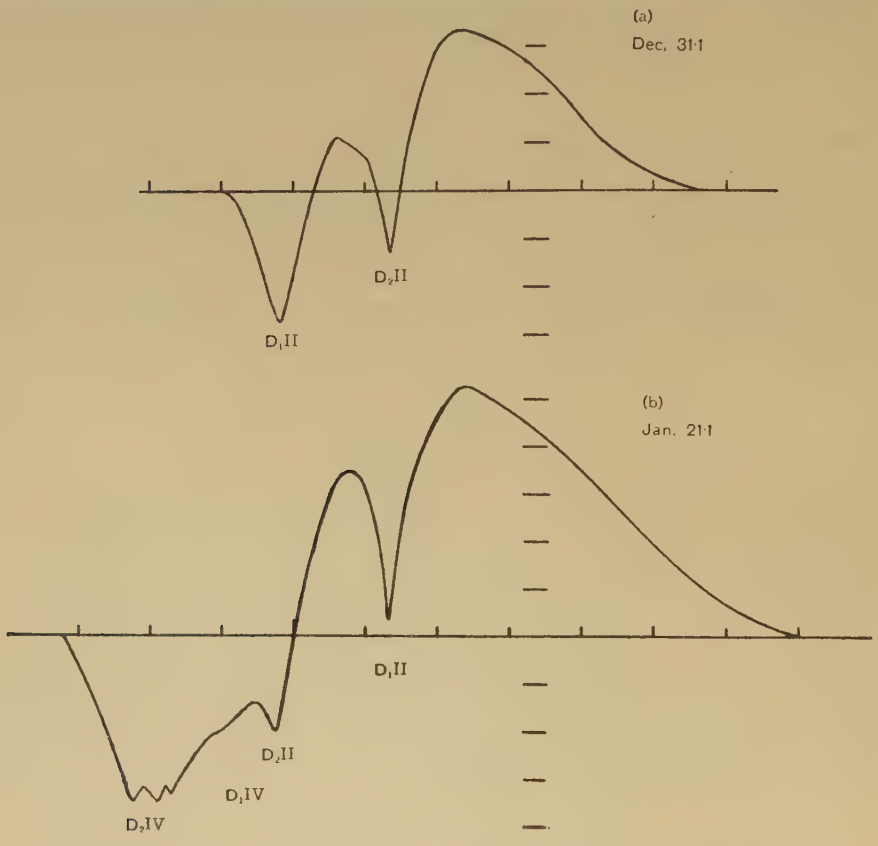

FIG. 4.—*Contour of D Lines.*

Unit of vertical scale = 20 per cent. of intensity of continuous spectrum.
Unit of horizontal scale = 20 km./sec.

D_1IV, as can be easily seen from consideration of the displacement of the components, the result is still in favour of Case 2.

Anomalous Multiplet Intensity.—The broad line absorption spectrum (blend of III and IV, simply referred to as Abs. IV in this section) consists mainly of *H*, *Ca*II, *Ti*II and *Fe*II lines. It appeared at the end of December. For *Ti*II it was not fully developed until the middle of January and disappeared in the middle of February. Only some of the *Ti*II lines have this broad component; for others Abs. IV is either absent or very faint. This anomaly can in many cases be attributed to blending, and can also be utilized for studying the relative dimensions of the shells.

Five *Ti*II multiplets are chosen and the central absorption of the lines belonging to these multiplets are measured on four Cambridge two-prism

spectrograms. On the first two Abs. IV is hardly present; whereas on the other two it is already fully developed. Assuming that line emission at the same wave-length as the absorption components is also absorbed (Case 2), the measured results are listed in Table VIII. Both Abs. II and IV of λ 3900

TABLE VIII

Central Absorption of TiII Lines

Laboratory		Nova Herculis						
Wave-length	Int.	Abs. II. Jan. 5·2	Jan. 7·2	Jan. 15·3	Jan. 26·8	Abs. IV. Jan. 15·3	Jan. 26·8	Remarks
3900·54	70	80	...	84	...	51:	...	1
3913·47	60	80	...	85	...	46	...	
4395·04	60	74	71	78	54	57	35	2
4443·81	50	82	80	79	56	66	47	
4468·50	50	77	76	73	52	66	50	3
4501·28	40	79	75	76	59	45	29	4
4549·64	60	75	72	75	62	73	60	5
4571·98	50	71	70	65	55	41	24:	6
4533·97	30	73	72	69	52	43	26	7
4563·77	30	60	59	57	48	—?	—?	8

Remarks

1. Both comp. bl em. of $H\zeta$, IV also bl II of *Fe*I, *V*II 3896.
2. Both comp. bl em. of *Fe*II 4385.
3. Abs. IV bl II of *Ti*II 4464.
4. Both bl em. of *Fe*II 4489 and 4491.
5. Partly due to *Fe*II. Both bl em. of *Fe*II 4541·52 which is very weak.
6. Bl em. of *Fe*II 4556, *Cr*II 4558 and 4555.
7. Bl em. of *Fe*II 4522·6 and 4520.
8. Both bl em. of *Fe*II 4556, *Cr*II 4558 and 4555.

are inside the red emission wing of $H\zeta$, whereas those of λ 3913 are outside it. So for each component, we can decide from the relative intensity of the two lines whether that component also absorbs from the *H* emission. If it does not, A_c obtained for λ 3900 by this method should come out smaller than that for λ 3913, and Case 1 (mere superposition) should be used instead of Case 2. The measured values of A_c show that for II the two lines have the same intensity ratio before and after the appearance of IV, therefore Abs. II of *Ti*II also absorbs from Em. IV of *H*. Unfortunately IV of 3900 is blended with II of *Fe*I, *V*II 3896, so we cannot decide from the apparent

intensity ratio of Abs. IV of the two *Ti*II lines whether Abs. IV of *Ti*II also absorbs from the *H* emission.

Both II and IV of λ 4395 are inside the emission wing of *Fe*II 4385; II is not at all weakened relative to λ 4444, whereas IV is somewhat weakened. The same discrepancy occurs in λ 4501 relative to λ 4468, and in λ 4572 relative to λ 4549. IV of 4468, is blended with *Ti*II 4464, and 4549 is partly due to *Fe*II. These blendings will explain away part of the discrepancy, but not all. For the last multiplet, both lines are blended with emission. But the combined emission of *Fe*II 4556 and *Cr*II 4558, 4555 is much stronger than that of *Fe*II 4520, 4522·6; and IV of *Ti*II 4564 is just at the position of maximum emission, whereas that of 4534 is some way from maximum emission. Hence the observed results.

The multiplet intensity of *Ti*II shows that Abs. II of *Ti*II has a much bigger effective radius than Em. IV of *Fe*II, *Cr*II and *H*; therefore the former absorbs from the latter, and our method of measuring A_c (Case 2) works. On the other hand, Abs. IV of *Ti*II has nearly the same effective radius as Em. IV of *Fe*II and *Cr*II, so it does not absorb from Em. IV, and Case 2 fails. Here Case 1 has to be assumed in order to give the right value of A_c. Owing to the crowding of lines, it is very difficult to draw the line representing the true continuous spectrum, therefore it is impossible to find out what values of A_c Case 1 would give.

Discussion.—The observational results are summarized as follows :—

1. From the intensity gradient of Balmer absorption lines we get
   P_e of Abs. IV $< P_e$ of Abs. II in March, therefore Abs. II is outside Abs. IV in March.
2. From the central absorption curves of Balmer lines, we get
   Abs. II absorbs from Em. IV, therefore Abs. II is well outside Em. IV.
3. From the central absorption of the D lines in December and January, we get
   Abs. II of D_1 absorbs from Em. II and Em. IV of D_2, so for *Na*I Abs. II is outside Em. II and Em. IV.
4. From the multiplet intensity of *Ti*II in January, we get
   Abs. II of *Ti*II well outside Em. IV of *Fe*II, *Cr*II and *H*; whereas Abs. IV of *Ti*II has more or less the same effective dimensions as Em. IV of *Fe*II and *Cr*II.

From the observational results, the following points about the nova can be deduced :—

(*a*) There is a tendency for shells of high velocity to stay inside (*i.e.* to have a smaller effective radius than) shells of lower velocity. It is at least certain that Abs. IV is most of the time inside Abs. II.

(*b*) There is a tendency for the emitting layer to be inside the absorbing layer of the same shell. This is at least true for shell II of sodium. The ejected atoms cease to emit line radiation some distance from the central star, whereas they continue to absorb until they are so far away from the

central star that they cease to be active spectroscopically. For each shell, different elements may have slightly different effective dimensions.

(*c*) The ejection of matter is probably continuous. Abs. IV emerged quite soon after the emergence of Abs. II. So if ejection is not continuous, IV would overtake II in a short time and would then be well outside II in March, contrary to what we have observed.

(*d*) Ejection is probably in patches, *i.e.* matter in each shell comes from only a number of spots (which we may call the "ejection centres") on the photospheric surface. This will explain why several shells of different velocities can exist side by side. When the distribution of the ejection centres on the photospheric surface has spherical symmetry, we get the usual line pattern for novæ—a broad emission band with centre in the undisplaced position and an absorption component displaced to the violet. When the spherical symmetry is lacking, we get the double emission maxima or even the single emission maximum. The lack of spherical symmetry may also explain the violet *H* emission in March which has no corresponding absorption component.

Summary

The central absorption of Balmer absorption components, the D lines, and a few *Ti*II lines in Nova Herculis are measured on selected spectrograms, and the relative dimensions of the shells around the nova are deduced from the measured results. Electron pressures of the *H* absorbing shells are calculated by a method described by Mohler.

It remains for me to record my grateful thanks to Professor Stratton for his interest in this investigation, for his numerous and valuable suggestions and comments, and for allowing me to consult his unpublished data on this interesting nova. I also take this opportunity to thank the directors of Mount Wilson Observatory and the Royal Observatory at Greenwich for permission to use their spectrograms.

Solar Physics Observatory,
Cambridge :
1940 *March* 4.

DISPERSION IN ESTIMATES OF SPECTRAL TYPE

H. E. Butler and A. D. Thackeray

In many investigations where stars are grouped according to spectral type it is important to realise the limitation in accuracy of the spectral classification. For instance, the observed dispersion in absolute magnitude in the main sequence must be due in part to errors in spectral types. Comparisons of some of the main classifications have been carried out by Öpik *, Hopmann †, C. Payne Gaposchkin ‡ and others, but these comparisons have usually dealt with only one pair of catalogues and it is not then possible to derive dispersions of the individual classifications without adopting some arbitrary system of weighting. A detailed comparison of the Henry Draper §, Mount Wilson || and Victoria ¶ catalogues of spectral types is carried out here, which yields the probable errors of the individual classifications in the various types from A to K. As is shown in the following analysis, this is theoretically possible only when there are at least three independent sources available. We have restricted ourselves to these three catalogues (except in the special problem of A-type stars) because they are the most complete as regards the brighter stars ; the fact that the errors of classification increase in general for fainter stars renders the extensive classifications of selected areas provided by the Potsdam, Hamburg, Upsala catalogues, etc. rather unsuitable to the present problem.

Spectral type was originally a rather loose designation of the general appearance of the spectrum. The Harvard classification, which has provided the framework of all others, depends essentially on a number of broad features visible on low-dispersion objective-prism spectra. More recent classifications, based on slit-spectra, adopt a number of fairly precise criteria, consisting usually of ratios of line-intensities ; estimates of absolute intensity are sometimes also applied. While it is undesirable to use only one pair of lines owing to possible individual irregularities, it is important that when several criteria are employed they should be given the same relative weight in each estimate, and this is undoubtedly difficult to carry out rigidly. Since line-intensities form the basis of most estimates we assume in what follows that spectral type is an index of *excitation temperature* corresponding to a standard stellar composition (*e.g.* the "Russell mixture"). The accidental errors of classification may be divided into two groups : (1) those due to observational errors such as irregular weighting of the criteria, coarseness of the grouping, preference for certain types, etc. ; and (2) those due to physical causes such as deviations from the standard

* *Tartu Publ.*, **27**, No. 1, 16, 1929.
† *Ber. Sächs. Akad. Leipzig*, **90**, 192, 1938.
‡ *Ap. J.*, **90**, 321, 1939.
§ *Harvard Annals*, **91–99**.
|| *Ap. J.*, **81**, 187, 1935.
¶ *D.A.O. Publ.*, **3**, 1, 1924.

composition, variations in width and appearance of lines resulting from Stark effect, turbulence, rotation, central reversals, etc., and in particular from differences in absolute magnitude; it is of course desirable that the line-intensities chosen as criteria should vary only with temperature and not with surface gravity; the failure of this condition will lead to inconsistent results unless the criteria adopted by the different classifications all vary with absolute magnitude in the same way. Such inconsistencies involve a correlation of accidental errors which will have an important bearing upon the following analysis.

Within a given classification systematic errors associated with apparent magnitude may appear; it is to be expected that faint stars will be subject to larger accidental errors of observation, but in the case of low-dispersion spectra systematic errors may also creep in due to attention being shifted from the lines to the continuous spectrum. Such a phenomenon has been noted by Öpik * (comparing Harvard and Mount Wilson types) and C. Payne Gaposchkin † (comparing Harvard and Potsdam types).

Analysis.—Let us suppose that T represents the "true spectral type" corresponding to a certain value of the weighted mean of the intensity ratios of certain pairs of lines in a star of standard composition at a given excitation temperature. Let t_1, t_2 . . . be a set of independent estimates of type based on criteria which are not necessarily identical with those of the "true type" but correspond approximately to the same excitation temperature. These estimates will be subject to accidental errors x_1, x_2 . . . and to systematic errors s_1, s_2 . . . and we have for each star

$$T = t_1 + s_1 + x_1 = t_2 + s_2 + x_2 = \text{etc.}$$
$$t_1 - t_2 = (s_2 - s_1) + (x_2 - x_1).$$

Suppose we have n stars common to the catalogues "1" and "2" within prescribed limits of type. Forming the sum of the differences and the sum of the squares of the differences we have

$$\sum_n (t_1 - t_2) = n(s_2 - s_1) + \Sigma(x_2 - x_1), \tag{1}$$

$$\sum_n (t_1 - t_2)^2 = n(s_2 - s_1)^2 + \Sigma x_1^2 + \Sigma x_2^2 + 2(s_2 - s_1)\Sigma(x_2 - x_1) - 2\Sigma x_1 x_2. \tag{2}$$

We write

$$s_{21} = s_2 - s_1 = \frac{1}{n}\Sigma(t_1 - t_2) - \epsilon,$$

where

$$\epsilon = \frac{1}{n}\Sigma(x_2 - x_1).$$

It is clear that ϵ tends to zero as n increases. Assuming $\epsilon = 0$, then

$$s_{21} = \frac{1}{n}\Sigma(t_1 - t_2). \tag{3}$$

* *Op. cit.*, p. 17.

† *Op. cit.*, p. 326.

If we write for the mean square deviations of the various estimates

$$\sigma_1^2 = \frac{1}{n}\Sigma x_1^2, \qquad \sigma_2^2 = \frac{1}{n}\Sigma x_2^2,$$

we can write (2) in the form

$$\frac{1}{n}\Sigma(t_1 - t_2)^2 = s_{21}^2 + \sigma_1^2 + \sigma_2^2 + 2\epsilon s_{21} - \frac{2}{n}\Sigma x_1 x_2. \tag{4}$$

Combining (3) and (4) with $\epsilon = 0$, we have

$$\frac{1}{n}\Sigma(t_1 - t_2)^2 - \frac{1}{n^2}[\Sigma(t_1 - t_2)]^2 = \sigma_1^2 + \sigma_2^2 - \frac{2}{n}\Sigma x_1 x_2. \tag{5}$$

The left-hand side of this equation, which we denote σ_{12}^2, can be calculated from the published types. Then, *provided the accidental errors* x_1, x_2 *are not correlated*, the term $\frac{2}{n}\Sigma x_1 x_2$ will tend to zero with increasing n and

$$\sigma_{12}^2 = \sigma_1^2 + \sigma_2^2. \tag{6}$$

Similarly, we can find $\sigma_2^2 + \sigma_3^2$ and $\sigma_3^2 + \sigma_1^2$ if a third catalogue is available. With three equations we can then find the individual dispersions of the three classifications. It is clear that three is the smallest number of catalogues from which such a result can be derived.

It may be pointed out that of the two assumptions

$$\epsilon = 0, \qquad \frac{2}{n}\Sigma x_1 x_2 = 0,$$

the second is far the more likely to break down. If two systems adopt the same set of criteria, while a third adopts another, it is clear that the accidental errors of the first two are likely to be positively correlated. Evidence will appear that there must be some such positive correlation between the Harvard and Victoria classifications of A-type stars. These stars have been known for a long time to present peculiar difficulties. A number of other catalogues of this type can be used to study the problem, but if the product-terms $\frac{\Sigma x_1 x_2}{n}$ do not vanish, a rigorous solution is impossible however many catalogues are available. For in the general case of n catalogues, where none of the product-terms are neglected, we shall have $\frac{1}{2}n(n-1)$ equations and $\frac{1}{2}n(n+1)$ unknowns (n dispersions and $\frac{1}{2}n(n-1)$ product-terms).

The Material.—For brevity we refer to material derived from the Mount Wilson, Harvard and Victoria catalogues as W, H and V respectively. The material has been divided into the six overlapping groups Ao to A9, A5 to F5, Fo to F9, F5 to G5, Go to G9 and G5 to K5. We have not restricted ourselves entirely to those stars common to all three catalogues. The V catalogue has been used in the first instance (as containing the fewest stars); thus all the stars common to V and W or common to V and H have been used, except that composite types or close doubles

whose spectra overlap on the Harvard plates have been rejected. Types having the peculiar characteristic "*p*" have in general been given half weight. The stars common to W and H extend to much fainter magnitudes than the V stars, and not all this material has therefore been used; but the number of stars in the W–H comparison has been increased to approximate equality with that in the V–H comparison by the inclusion of some stars not in the V catalogue.

Results.—Figs. 1–3 show histograms of the frequencies of W–H, H–V, V–W for the various groups of types, the unit being one-tenth of a spectral type.

Table I gives the systematic errors s_{HW}, s_{VH}, s_{WV}, the functions σ^2_{HW}, σ^2_{VH}, σ^2_{WV} and the individual dispersions σ^2_V, σ^2_W, σ^2_H derived by the method described assuming no correlation of accidental errors. The number of stars used in each comparison is given at the head of each column. The sum of the terms s_{HW}, s_{VH}, s_{WV} is given in the seventh row; when only stars common to the three catalogues are used this sum should be zero. The failure of this check, particularly in the group A0–A9, is a result of the smallness and inhomogeneity of the samples.

TABLE I

Type	A0–A9	A5–F5	F0–F9	F5–G5	G0–G9	G5–K5
n HW	105	177	118	181	243	471
n VH	70	210	118	201	243	468
n WV	32*	153	120	186	244	420
s_{HW}	− ·61	−·48	−·06	−·19	−·65	+·70
s_{VH}	− ·20	−·15	−·29	−·25	+·43	−·81
s_{WV}	−1·94	+·42	+·47	+·40	+·20	+·10
Sum	−2·75	−·21	+·12	−·04	−·02	−·01
σ^2_{HW}	9·04	7·97	5·65	6·34	7·96	7·90
σ^2_{VH}	4·19	4·22	4·27	4·98	7·57	6·80
σ^2_{WV}	7·32	3·23	3·03	3·72	3·70	3·54
σ^2_V	1·24	−0·26	0·82	1·18	1·66	1·22
σ^2_W	6·08	3·49	2·20	2·54	2·04	2·32
σ^2_H	2·95	4·48	3·45	3·80	5·91	5·58
σ^2_M	(1·21)	(·49)	(·57)	·71	·79	·72

* Includes 8 stars classified by W in *Ap. J.*, 56, 242, 1922, but not in the 1935 list.

It will at once be noticed that the negative value of σ^2_V in the group A5 to F5 indicates a breakdown of the method; moreover, in the group A0 to A9 σ^2_V is improbably small and σ^2_W improbably large. This must

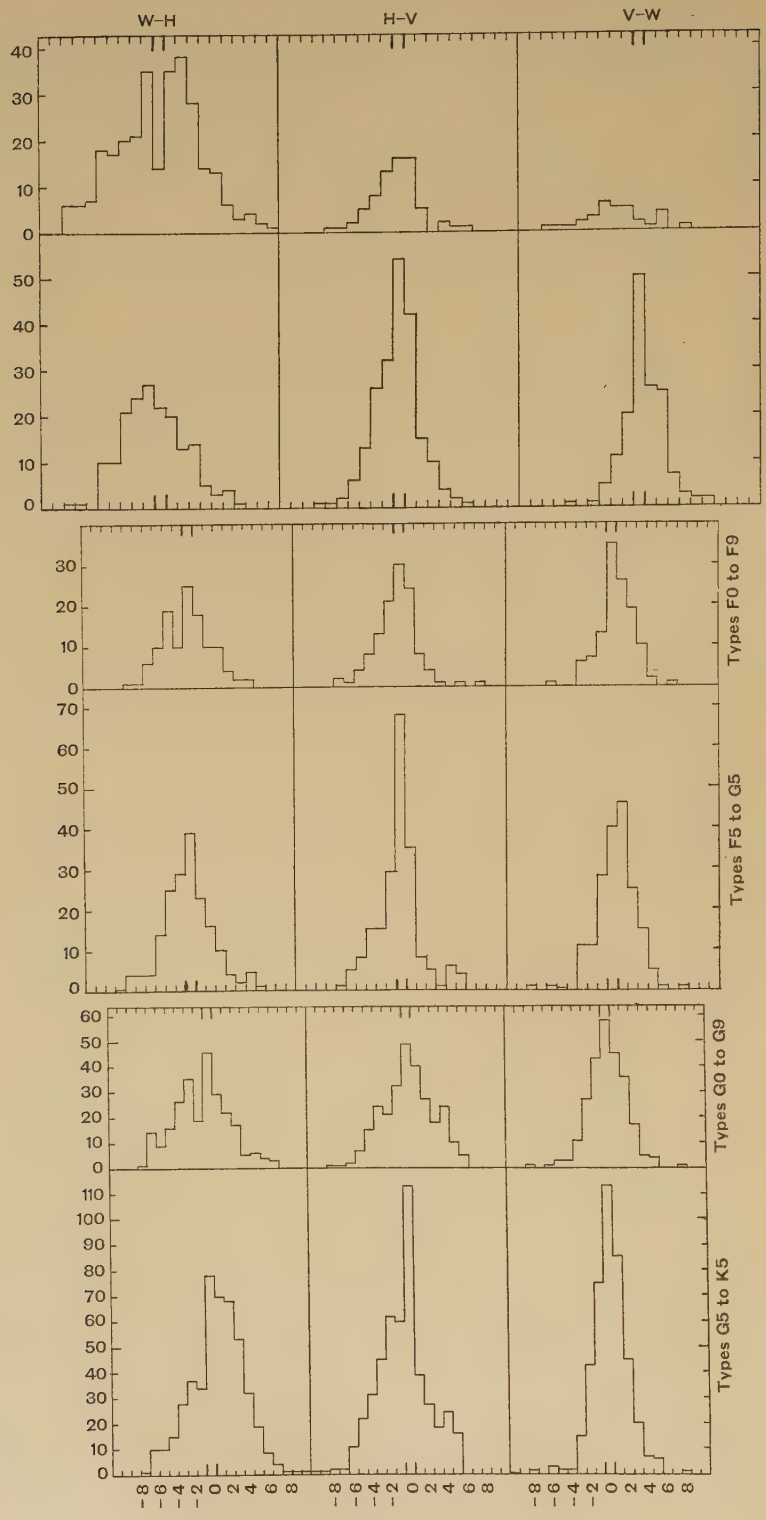
W–H
H–V
V–W
Types A0 to A9
Types A5 to F5
Types F0 to F9
Types F5 to G5
Types G0 to G9
Types G5 to K5

FIGS. 1–3.

presumably be due to a correlation of accidental errors such that $\Sigma x_W x_H$ is negative and $\Sigma x_V x_H$ positive. Examination of the criteria adopted in the three systems, which are summarised in Table II, shows that such a state of affairs is entirely possible ; for A types Victoria and Harvard both adopt the ratio K $(Ca^+)/H$, whereas Mount Wilson concentrates attention on the metallic lines. This point will be discussed further in the next section.

The fact that the correlation of accidental errors is sufficient to make σ_V^2 apparently negative in A stars may raise doubts as to the significance of the values derived for the later types. It will be noted that in every group of Table I we find $\sigma_V^2 < \sigma_W^2$ and this would follow if the V classification adopted criteria uniformly closer to the Harvard system than the W classification. However, Table II shows that the criteria in types F5 to K5 are more varied than in the A stars—there are of course more lines available—and in no other type than A do we find the position that one classification adopts a criterion quite different from the other two. It is, moreover, satisfactory that the results for the fairly wide range of types F5 to K5 agree in assigning approximately the same ratio $\frac{1}{4} : \frac{1}{3} : 1$ or $\frac{1}{4} : \frac{1}{2} : 1$ to σ_V^2, σ_W^2, σ_H^2. This suggests that an improved value of the spectral type would be obtained by weighting the types as given in the V, W and H catalogues in the ratio 4 : 3 : 1.* The last row of Table I gives the dispersion σ_M^2 of such a weighted mean. It will be seen that statistically the standard error can in this way be reduced to less than a tenth of a spectral type.

TABLE II

The Chief Criteria of Spectral Types
(See *Trans. I.A.U.*, 5, 182, 1935)

Types	Harvard	Mt. Wilson	Victoria
A0	*H, Ca⁺/H*	Metallic lines, H	*Ca⁺/H*
A2	*Ca⁺/H, Ca/Fe*	Do.	*Ca⁺/H*
A5	*Ca⁺/H, Ca⁺/H*	Do.	*Ca⁺/H*
F0	*H, Ca⁺/H*	Do.	*Ca⁺/H*
F5	*H, Fe/H*	Do.	*Ca/H, Fe/H*
G0	*H/Fe, Sr⁺/H/Ca*	*Ca*, G band	*Ca*
G5	*H/Fe,*	*Cr/Fe, H/Fe*	*Ca*
K0	*H/Fe, Ca*	*Ca, Cr*	*Ca*
K5	*Ca⁺, Ca*	*Ca, Cr*	*Ca*

The A-type Stars.—It might be thought that if we apply the system of weighting suggested by the types F5 to K5 we could take the weighted mean to be the "true type" and thus calculate accidental errors and the product-terms $\frac{\Sigma x_1 x_2}{n}$. Such a procedure was tried for the A stars and did in fact reveal an apparent positive correlation of x_V, x_H and a negative correlation of x_W, x_H. We are indebted to Sir Arthur Eddington for a rigorous

* Independent evidence of the greater weight to be assigned to V for types G5 to K5 is offered by photometric observations at Cambridge of the D lines which show slightly better correlation with V than with W.

proof that such a procedure is fallacious in that it will only lead to a linear combination of the original equations.

For a further investigation of the A-type stars we have referred to two other classifications with which comparisons are possible.* These are by A. V. Douglas † and G. Abetti ‡; we refer to them as D and A respectively. Miss Douglas followed Mount Wilson in adopting the metallic lines as criterion for spectral type, and Abetti employed both Ca^+/H and the metallic lines. Thus we can divide the five catalogues into three groups according to their criteria for spectral type :

(*a*) H, V (Ca^+/H),
(*b*) W, D (metallic lines),
(*c*) A (Ca^+/H and metallic lines).

Thus we expect positive correlation between H, V or W, D and negative correlation between any pair one of which belongs to group (*a*) and the other to group (*b*). If A shows any correlation it is likely to take opposite signs when compared with group (*a*) or (*b*). As mentioned previously, when correlation of accidental errors is present a complete solution of the problem is impossible. But it is possible to make some progress by making an assumption about the product-terms which is consistent with the system of adopted criteria. We have attempted a solution with the following assumptions, in which x_r denotes an accidental error in a catalogue belonging to group (r) :—

$$\frac{2\Sigma x_r x_s}{n} = \delta_{rs} k(\sigma_r^2 + \sigma_s^2), \tag{7}$$

where k is a constant independent of r and s, $\delta_{rs} = +1$ when r, s belong to the same group (*a*) or (*b*), $\delta_{rs} = -1$ when r, s belong to opposite groups (*a*) or (*b*). It is clear that k is closely allied to the correlation coefficient $(= \Sigma x_r x_s / n\sigma_r\sigma_s)$. In place of equation (5) we now have a set of equations of the form

$$\sigma_{12}^2 = (1 \pm k)(\sigma_1^2 + \sigma_2^2).$$

Since catalogue A is intermediate between groups (*a*) and (*b*) different treatment is required. We therefore assume

$$\frac{2\Sigma x_r x_c}{n} = \delta_r l(\sigma_r^2 + \sigma_c^2), \tag{8}$$

where $\delta_r (= \pm 1)$ takes opposite signs according as $r = a$ or b, and l is a constant independent of r.

* The classification by H. C. Woods (*M.N.*, **87**, 388, 1927) of objective prism spectra is rather unsuitable for a comparison with the material discussed here because it only deals with stars of type B9 to A5, a range which includes Harvard classes Ao, 2, 3, 5, while Harvard Fo follows immediately after A5. We cannot therefore compare material based on the group Ao to A5 with other material based on the group Ao to A9. Unfortunately, the samples are too small to analyse results for the group Ao to A5 alone.

† *Ap. J.*, **64**, 262, 1926.

‡ *Firenze Publ.*, Fasc. **42**, 11, 1925.

Results of the comparisons of the five catalogues are summarised in Table III (the comparisons HW, VH, WV already given in Table I are not reproduced here). There are too few stars common to V and D for a profitable comparison. With the assumptions (7), (8) and the data of

TABLE III

Comparison of Classifications of A-type Stars

(For WH, HV, VW see Table I)

Comparison	DH	WD	AH	AD	AW	AV
n	105	105	170	51	47	26·5
σ^2_{rs}	7·27	1·65	7·03	9·06	8·43	8·03

Tables I, III we now have nine equations and seven unknowns (five dispersions in addition to the constants k and l). If we restrict ourselves to the four catalogues D, H, V, W we have five equations and five unknowns. This gives the solution

$$\sigma^2_W = 2{\cdot}1\ (6{\cdot}0), \qquad \sigma^2_V = 3{\cdot}1\ (1{\cdot}3), \qquad \sigma^2_H = 4{\cdot}3\ (3{\cdot}0),$$
$$\sigma^2_D = 0{\cdot}8, \qquad k = 0{\cdot}43. \tag{9}$$

The figures in brackets are taken from the corresponding results in Table I and indicate the large influence of the product-terms neglected in the straightforward solution. If we now apply these results to the equations given by the comparisons AH and AD we find

$$\sigma^2_A = 5{\cdot}7, \qquad l = 0{\cdot}30. \tag{10}$$

The fact that we find $l < k$ is consistent with our assumption that A is intermediate between groups (*a*) and (*b*). The value found for l has the sense that Arcetri types have slight positive correlation with group (*b*) (W and D), indicating that the metallic lines were given rather greater weight in this classification. If the rather large value found for σ^2_A is significant it probably arises from the attempt to use both Ca^+/H and metallic lines as criteria simultaneously.

A combination of the solutions (9) and (10) enables us to compute σ^2_{AW} and σ^2_{AV}. We find

$$\sigma^2_{AW} = 10{\cdot}1, \qquad \sigma^2_{AV} = 6{\cdot}2.$$

These figures do not check very satisfactorily with those calculated directly from the data and appearing in Table III. But the samples are small for these two particular comparisons (especially AV). Moreover, it seems probable that the value for σ^2_D in (9) is too small. One circumstance which may invalidate the above analysis to some extent, even if the assumptions (7), (8) are essentially correct, is that our material consists entirely of stars common to pairs of catalogues; the stars in V, D and A form an incomplete sample of the brighter stars, and there may well be a tendency to select or avoid peculiar stars with large accidental errors which will render the material inhomogeneous.

We must conclude this section by emphasising the difficulty of finding significant values of the errors of classification of A-type stars. The correlation of accidental errors, being related as we have seen to the adopted criteria, can be attributed with some confidence to a physical cause. Part of this may be the systematic error, noted by Abrams and Öpik *, due to the disturbing influence of interstellar Ca^+ on classifications which depend on the ratio K/Hδ. But most of it appears to be associated with the *n* or *s* characteristic assigned by Mount Wilson and other classifications (corresponding to nebulous or sharp lines). As has been pointed out by Lindblad †

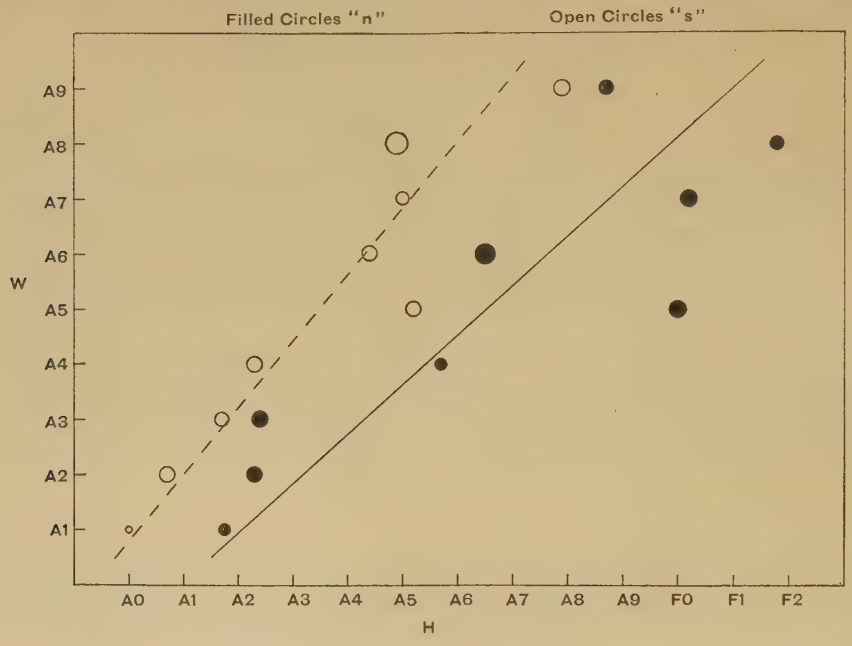

FIG. 4.—*Comparison of Harvard and Mount Wilson types A0 to A9.*

and Priscilla Fairfield ‡, *n* stars are classified late by Harvard compared with Mount Wilson, and *s* stars early. This is brought out clearly in fig. 4, where H is plotted against W, *n* and *s* stars being distinguished by closed and open circles; the size of the circles indicate the number of stars forming the mean. Unfortunately the samples are again too small for subdivision into *n* and *s* classes, quite apart from the fact that in many instances there is disagreement as to placing a star in one or other of the two classes. It may well be that the numerous lines observed in the ultra-violet by Adams and Dunham § and by Struve || will present more satisfactory criteria of spectral type than those in the blue-violet region. Two advantages of using criteria beyond the Balmer limit would be (1) avoidance of hydrogen wings which

* *Ap. J.*, **86**, 203, 1937.
† *Ap. J.*, **59**, 305, 1924.
‡ *Harv. Circ.*, **264**, 1924.
§ *Ap. J.*, **87**, 102, 1938.
|| *Ap. J.*, **90**, 699, 1939.

may affect line-intensities, (2) the region would be nearer the wave-length of maximum energy.

Late-type Giants and Dwarfs.—In the preceding analysis no distinction has been drawn between giants and dwarfs. In the F types there is the well-known gap in the giant sequence, so that our results here refer mainly to dwarfs ; but in all the later groups giants greatly outnumber the dwarfs among the brighter stars which we have used. Öpik * has already drawn attention to the fact that among K-type dwarfs the Harvard types are systematically early compared with the Mount Wilson types, and that this error increases towards fainter magnitudes ; he explains this as due to attention being shifted in the Harvard classification of faint stars from lines to the continuous spectrum ; as is well known, dwarfs are bluer than giants of the same spectral type, judged by intensities of lines, so that if the continuous spectrum is used as a criterion the stars will be classified early. Öpik's conclusion is fully verified by the results of a comparison of Mount Wilson (1935) and Harvard classifications of dwarfs. Fig. 5 shows

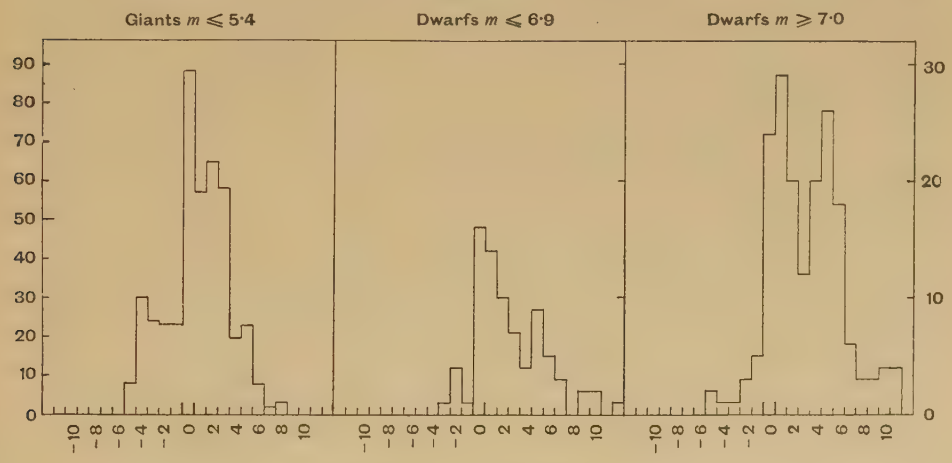

FIG. 5.—*Frequency of W–H, types G5 to K5.*

histograms of W–H for the brighter giants, and of the dwarfs divided into two groups according to apparent magnitude ($m \leqslant 6{\cdot}9$, $m \geqslant 7{\cdot}0$). The dwarf curves both show double maxima, one at about zero, the other at about +5 ; the latter maximum is particularly pronounced in the fainter stars. Thus we see that among the dwarfs of the 7th magnitude or fainter about half are classified systematically early by Harvard to the extent of four units or more, and the most natural interpretation of this is that the continuous spectrum has been used as a criterion for these stars.

Such a systematic error would have a serious effect upon the analysis given in Table I if dwarfs formed an appreciable fraction of the material used. A comparison of W, H has been carried out for the two groups G0 to G9, G5 to K5 ; in the latter group the giants were subdivided into three groups and the dwarfs into two, according to apparent magnitude.

* *Tartu Publ.*, **27**, No. 1, 16, 1929.

The results are given in Table IV, which is similar to Table I. The V material was considered to be insufficient to subdivide into groups of m. The main conclusions to be drawn from this table are :

(1) The change of systematic errors from giant to dwarf of H types increases towards fainter magnitudes.

(2) The classification of K giants by W and H appears to be free from systematic errors associated with apparent magnitude.

(3) The accuracy of W, V and H classifications of G and K stars appears to be somewhat higher for dwarfs than giants, except for the systematic error noted in (1).

(4) The individual dispersions σ^2 for giants are not greatly changed from the results of Table I, though there appears to be some negative correlation of x_W, x_V in the group Go to G9.

TABLE IV

G- and K-Type Giants and Dwarfs

	G0–G9		G5–K5				
	Giants	Dwarfs	Giants			Dwarfs	
Limits of m	...	...	$\leqslant 5{\cdot}4$	5·5–6·4	$\geqslant 6{\cdot}5$	$< 7{\cdot}0$	$\geqslant 7{\cdot}0$
n HW	160	73	432	568	370	79	181
n VH	159	72	425			43	
n WV	158	73	377			43	
s_{HW}	−0·96	+0·18	+0·79	+1·10	+0·50	+2·60	+3·16
s_{VH}	+1·15	−1·33	−0·72			−1·60	
s_{WV}	−0·18	+1·08	+0·06			+0·44	
Sum	+0·01	−0·07	+0·13			+1·44	
σ^2_{HW}	8·69	5·32	7·08	6·86	7·10	8·57	9·57
σ^2_{VH}	6·81	5·04	6·56			8·48	
σ^2_{WV}	3·80	2·68	3·62			2·72	
σ^2_V	0·96	1·20	1·55			1·32	
σ^2_W	2·84	1·48	2·07			1·40	(1·4)
σ^2_H	5·85	3·84	5·01			(7·17)	(8·2)

In conclusion, Table V gives estimates of the standard errors σ of the three classifications, based on a consideration of Table I, the special discussion of A-type stars, and the results for giants and dwarfs of Table IV. In the first three groups the results are very uncertain and are marked by

colons. In the last two groups first figures refer to giants, italicised figures refer to dwarfs. The standard errors of σ were computed for the three groups Fo to F9, Go to G9, G5 to K5 and found to be $\pm$ 0·2 to $\pm$ 0·3, $\pm$ 0·1 to $\pm$ 0·2 and $\pm$ 0·1 respectively.

TABLE V

Standard Errors of Spectral Types

(Unit = 0·1 Spectral Type)

	A0–A9	A5–F5	F0–F9	F5–G5	G0–G9	G5–K5
σ_V	1·6 :	1·5 :	1·4 :	1·2	1·2, *1·1*	1·2, *1·1*
σ_W	1·6 :	1·5 :	1·5 :	1·6	1·5, *1·2*	1·4, *1·2*
σ_H	2·1 :	2·2	1·9	1·9	2·4, *1·9*	2·3, *2·7* :

Summary

1. Individual dispersions of estimates of spectral types can only be found if there are at least three independent classifications available whose accidental errors are uncorrelated.

2. Using the Victoria, Mount Wilson and Harvard classifications and assuming their accidental errors to be uncorrelated, dispersions of the three estimates are calculated for six groups of types from A0 to K5.

3. In the types A0 to F5 Harvard and Victoria errors are positively correlated, and both are negatively correlated with Mount Wilson errors; this is attributed to the choice of criteria. In these conditions the problem becomes insoluble however many catalogues are available. Some results, however, can be obtained by using two additional classifications, by Abetti and A. V. Douglas, and by making certain assumptions about the correlation of accidental errors in the light of knowledge about the criteria used. The use of new criteria for A-type stars (*e.g.* ultra-violet lines) is recommended.

4. The Harvard classification of K dwarfs is subject to systematic errors which increase for fainter stars. The classification of K giants appears to be free from errors associated with apparent magnitude.

5. In units of tenths of a spectral type the standard errors of the Victoria, Mount Wilson and Harvard classifications of stars brighter than 6^m to 7^m vary between 1·0 and 1·6, 1·3 and 1·6, 1·9 and 2·7 respectively (Table V).

Solar Physics Observatory,
Cambridge:
1940 *March.*

A NULL TEST FOR CONCAVE MIRRORS

S. C. B. Gascoigne

Introduction.—In 1934 at the B.A. meeting in Aberdeen Dr. C. R. Burch demonstrated a null method of testing concave mirrors by aspherical compensator plates, and null methods of constructing these plates have since been developed by him in the laboratory. In this paper these methods are investigated theoretically and it is found that, applied with suitable refinements, their range of usefulness can be extended considerably beyond the limits originally envisaged by Dr. Burch. To take two well-known examples, the Radcliffe Observatory, Pretoria, mirror, an $f/5$ mirror of 190 cm. (75 inches) diameter, could be tested (using monochromatic light) to an accuracy of $\pm 2{\cdot}5 \cdot 10^{-5}$ mm., and the Common mirror, now at Cambridge, of focal ratio 3·75 and diameter 92 cm. (36 inches), to an accuracy of $\pm 5 \cdot 10^{-5}$ mm., by means of compensator plates of diameters 19 cm. and 10 cm. respectively.

The method is to interpose at a suitable position between the mirror and a star at its paraxial centre of curvature a plate figured so as to compensate the spherical aberration of the reflected beam, which then forms a stigmatic image of the star. This image can be null-tested by knife-edge or Zernike disc * in the usual manner as though the mirror were a sphere. There first arises the difficulty of figuring the compensator plate to the correct aspherical shape. When only zonal test methods can be employed this is a long and difficult operation, but when there is already in existence a surface of the required shape against which the compensator can be tested, it immediately becomes more practicable. It occurred to Dr. Burch that an approximation to such a surface could be provided by figuring the plane face of a suitably chosen plano-convex lens until a stigmatic pencil refracted by the spherical face was reflected by the figured surface back along its own path to form an image coincident with the light source. One side of a plane-parallel plate is then figured to fit the back surface of the "autostigmatic" lens. The plate will then be a compensator in the sense defined above, or more precisely an approximation to such a compensator, and it is our purpose in this paper to investigate the limits within which this approximation can be made to give results of an accuracy sufficient for astronomical purposes.

In practice the autostigmatic lens is best (null) tested with a Williams interferometer, which is a variant of the Michelson interferometer and is described in the Appendix. The compensator is then tested against the lens by normal incidence interference, so that it is tested by reflection but used by transmission. Hence, when the light passes through it twice, errors on its surface appear halved on the surface of the mirror, while if the compensator is designed for single transmission (as may be done by decentring the star and knife-edge), errors can be tolerated in the figuring of the compensator

* F. Zernike, *M.N.*, 94, 377, 1934 ; C. R. Burch, *M.N.*, 94, 384, 1934.

four times as great as those permissible on the final surface of the mirror. The same compensator may be used to test different mirrors by suitably varying its distance from each, and even mirrors of different types, such as, for example, the type used in the Ritchey-Chrétien telescope. Finally, the compensator need be only a tenth of the diameter of the mirror, which may represent a considerable saving over testing by autocollimation.

The discussion necessarily involves a good deal of algebraic analysis, and the reader who is interested primarily in results is advised to turn at once to page 483, where he will find all necessary working instructions. Of the preceding part, section 2 is concerned with the derivation of formulæ which describe the refraction of spherically aberrant pencils by aspherical surfaces. These results are applied in section 3 to determine the shape of the back surface of the autostigmatic lens, and in sections 4 and 5 to find the equation of the mirror for which a test would be null when we use as compensator a plate figured to fit the back surface of the autostigmatic lens. In section 6 we work out in some detail how closely such a "null" mirror may be made to approximate to a paraboloid, and indicate the extension of the analysis to

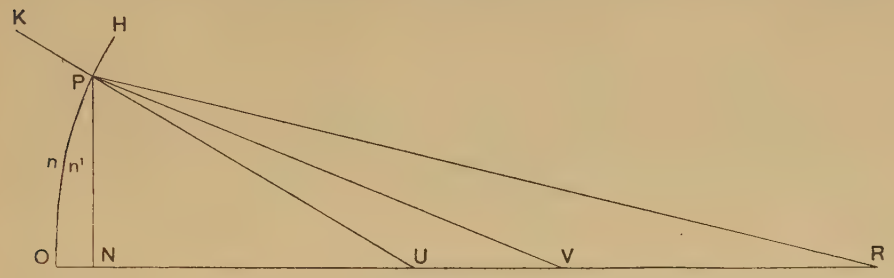

FIG. 1.

other types of concave mirror. In section 7 a discussion is given of the tolerances and of the maximum separation of star and knife-edge permissible on account of astigmatism.

I wish to thank Dr. Linfoot for much assistance with the preparation of this paper, and Dr. Burch for valuable discussions in connection with it.

2. *Formulæ for the Longitudinal Spherical Aberration Produced by Refraction at Aspherical Surfaces.*—We first extend well-known results (see Whittaker, "Theory of Optical Instruments", section 21) on the behaviour of a pencil possessing spherical aberration which falls symmetrically on a pseudo-plane refracting surface, *i.e.* a nearly plane surface of revolution whose paraxial radius of curvature is infinite, and whose equation may therefore be in the form (2.3), where B, C . . . are small and become zero if the surface is a true plane.

Fig. 1 shows a section of the system by a plane through its axis of symmetry OR. Let OH be the curve in which the surface is cut by this plane. KP is a ray of the incident pencil in medium of refractive index n which meets the surface at a point P a (small) distance h from the axis. PV is the

refracted ray in medium of refractive index n', cutting the axis in V. PR is the normal to the surface at P. If the paraxial parts of incident and refracted pencils converge to paraxial foci distant s, s' from O, we may express OU, OV by series of the form (2.1), (2.2), where the coefficients A, A' are a measure of the longitudinal spherical aberration, or L.S.A. :

$$\mathrm{OU} = s + A_2h^2 + A_4h^4 + \ldots \tag{2.1}$$

$$\mathrm{OV} = s' + A_2'h^2 + A_4'h^4 + \ldots \tag{2.2}$$

$$\mathrm{ON} = \frac{Bh^4}{4} + \frac{Ch^6}{6} + \ldots \tag{2.3}$$

We have assumed h small. Neglecting powers higher than the fifth, we have

$$\tan \mathrm{O\hat{U}P} = \frac{\mathrm{PN}}{\mathrm{UN}} = \frac{h}{s + A_2h^2 + (A_4 - B/4)h^4 + \ldots}$$

$$= \frac{h}{s} - \frac{A_2h^3}{s^2} + \left(\frac{A_2^2}{s^3} - \frac{A_4}{s^2} + \frac{B}{4s^2}\right)h^5 + \ldots$$

$$\sin \mathrm{O\hat{U}P} = \frac{h}{s} - \left(\frac{A_2}{s^2} + \frac{1}{2s^3}\right)h^3 + \left(\frac{3}{8s^5} + \frac{3A_2}{2s^4} + \frac{A_2^2}{s^3} - \frac{A_4}{s^2} + \frac{B}{4s^2}\right)h^5 + \ldots$$

$$\cos \mathrm{O\hat{U}P} = 1 - \frac{h^2}{2s} + \left(\frac{A_2}{s^3} + \frac{3}{8s^4}\right)h^4 + \ldots$$

$$\tan \mathrm{O\hat{R}P} = \frac{d\mathrm{ON}}{dh} = Bh^3 + Ch^5 + \ldots$$

$$\sin \mathrm{O\hat{R}P} = Bh^3 + Ch^5 + \ldots$$

$$\cos \mathrm{O\hat{R}P} = 1 + \ldots$$

The expressions for sin O$\hat{\mathrm{V}}$P, cos O$\hat{\mathrm{V}}$P are similar with s' and A' in place of s and A.

By Snell's law,

$$n \sin (\mathrm{O\hat{U}P} - \mathrm{O\hat{R}P}) = n' \sin (\mathrm{O\hat{V}P} - \mathrm{O\hat{R}P}).$$

Substituting for the appropriate trigonometric functions from the above,

$$\frac{nh}{s} - n\left(\frac{A_2}{s^2} + \frac{1}{2s^3}\right)h^3 + n\left(\frac{3}{8s^5} + \frac{3A_2}{2s^4} + \frac{A_2^2}{s^3} - \frac{A_4}{s^2} + \frac{B}{4s^2}\right)h^5$$
$$- n(Bh^3 + Ch^5)\left(1 - \frac{h^2}{2s^2}\right) + \ldots$$

$$= \frac{n'h'}{s'} - n'\left(\frac{A_2'}{s'^2} + \frac{1}{2s'^3}\right)h^3 + n'\left(\frac{3}{8s'^5} + \frac{3A'^2}{2s'^4} + \frac{A_2'^2}{s'^3} - \frac{A_4'}{s'^2} + \frac{B}{4s'^2}\right)h^5$$
$$- n'(Bh^3 + Ch^5)\left(1 - \frac{h^2}{2s'^2}\right) + \ldots$$

Equating coefficients of powers of h,

$$\frac{n}{s}=\frac{n'}{s'}, \tag{2.4}$$

$$nB+\frac{nA_2}{s^2}+\frac{n}{2s^3}=n'B+\frac{n'A_2'}{s'^2}+\frac{n'}{2s'^3}; \tag{2.5}$$

$$nC-\frac{3nB}{4s^2}-\frac{3n}{8s^5}-\frac{3nA_2}{2s^4}-\frac{nA_2^2}{s^3}+\frac{nA_4}{s^2}$$
$$=n'C-\frac{3n'B}{4s'^2}-\frac{3n'}{8s'^5}-\frac{3n'A_2'}{2s'^4}-\frac{n'A_2'^2}{s'^3}+\frac{n'A_4'}{s'^2}. \tag{2.6}$$

We will now generalise these equations to the case when the refracting surface is not a pseudo-plane but what we may call a pseudo-sphere. Then its form may be conveniently described by the equation

$$\mathrm{ON}=\frac{h^2}{2r}+\left(\frac{1}{8r^3}+\frac{B}{4}\right)h^4+\left(\frac{1}{16r^5}+\frac{C}{6}\right)h^6+\ \ldots \tag{2.7}$$

where B, C are coefficients expressing the amount by which the surface departs from a sphere of radius r, and are zero when the surface coincides with this sphere. (2.7) thus includes (2.3) as the particular case when $1/r=0$, or the paraxial radius of curvature is infinite. By working precisely similar to the above we deduce the following equations, generalisations of (2.4), (2.5), (2.6) respectively :—

$$n\left(\frac{1}{r}-\frac{1}{s}\right)=n'\left(\frac{1}{r}-\frac{1}{s'}\right), \tag{2.8}$$

$$nB+\frac{nA_2}{s^2}+\frac{n}{2s}\left(\frac{1}{r}-\frac{1}{s}\right)^2=n'B+\frac{n'A_2'}{s'^2}+\frac{n'}{2s'}\left(\frac{1}{r}-\frac{1}{s'}\right)^2, \tag{2.9}$$

$$n\left[B\left(\frac{3}{2r^2}-\frac{1}{rs}+\frac{3}{4s^2}\right)-C-\frac{3}{8s^2}\left(\frac{1}{r}-\frac{1}{s}\right)^3-\frac{1}{8sr^2}\left(\frac{1}{r}-\frac{1}{s}\right)^2\right.$$
$$\left.+\frac{A_2}{2s^2}\left(\frac{1}{r}-\frac{1}{s}\right)\left(\frac{1}{r}-\frac{3}{s}\right)+\frac{A_2^2}{s^3}-\frac{A_4}{s^2}\right] \tag{2.10}$$
$$=\text{a similar expression with } n',\ s',\ A' \text{ for } n,\ s,\ A.$$

These equations connect B and V, the coefficients of fourth and sixth powers in the asphericity of the refracting surface with r, its paraxial radius of curvature, s and s', the object and image distances, and A, A' the coefficients which describe up to the fifth power the L.S.A. of incident and refracted pencils.

They can be used in various ways. For example, if we know the L.S.A. of an incident pencil we can find the equation of that surface which makes the refracted pencil stigmatic; or we can find the L.S.A. introduced by a given surface into any pencil incident upon it. But it is first necessary to express the L.S.A. of a particular ray (with respect to the paraxial ray) in terms of the axial distance at which it meets the refracting surface.

3. *The Autostigmatic Lens.*—We wish first to find the equation of the reflecting back-surface of the autostigmatic lens. Fig. 2 is an axial section of such a lens. QR is the spherical refracting surface of centre C and radius ρ, and bounds a medium of refractive index n. OP is the aspherical reflecting surface. If the star is placed at an axial point U distant u from R, the nearest point of the sphere, then OP is such that any ray from U refracted at Q is reflected by it back along its own path. Suppose that its equation referred to O as origin is

$$x=\frac{h^2}{2r}+\left(\frac{1}{8r^3}+\frac{B}{4}\right)h^4+\left(\frac{1}{16r^5}+\frac{C}{6}\right)h^6+\ \ldots \qquad (3.1)$$

where $x=\mathrm{OM}$ and h is the axial distance of P. As in (2.7), B and C represent the departure from spherical form. The sign convention is chosen so that all curvatures are positive as shown in the figure; thus when r, the paraxial

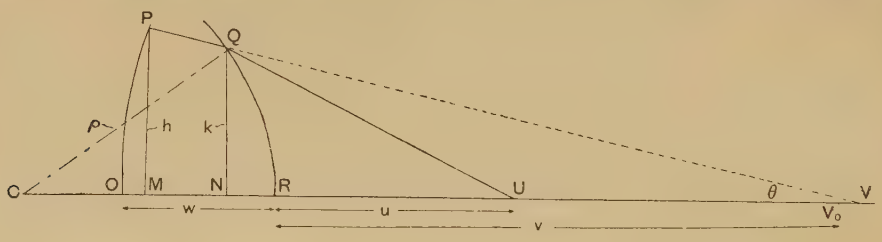

Fig. 2.

radius of curvature of OP, is positive, that surface is concave to U. It will be noticed that r and ρ, though of opposite curvature physically, have the same sign. As will appear in the course of the section, practical convenience justifies this departure from the usual rule.

Our problem is to find expressions for the coefficients B, C of (3.1) in terms of u, ρ, n and w, the axial thickness of the lens. This can be done by observing that if the (spherically aberrant) image of U is formed at V, then the surface OP must reflect this image into itself. As mentioned at the end of section 2, we must describe the L.S.A. of an image-forming ray in terms of the height h at which it is incident upon the aspherical surface. This gives us expressions for the coefficients A, A' of section 2; we substitute these in the appropriate equations and so find B and C. But the expression for C is so complicated that it is almost useless, and we are forced to approximate to it by using the fact that in practice U is always near focus.

Let the paraxial image of U be formed at V_0, where $\mathrm{RV}_0=v$. Then

$$\frac{n-1}{\rho}=\frac{1}{u}-\frac{n}{v}. \qquad (3.2)$$

If U is inside focus by a small distance ν (so that v is large), we have of course that

$$u+\nu=\frac{\rho}{n-1},$$

which with (3.2) gives

$$\frac{(n-1)^2\nu}{\rho^2}=\frac{n}{v}+O\left(\frac{1}{v^2}\right). \tag{3.3}$$

In general U forms a spherically aberrant virtual image, so that if $QN=k$, the ray QP meets the axis not in V_0 but in V, where

$$RV=v+\Delta_2k^2+\Delta_4k^4+\ldots \tag{3.4}$$

The aberration coefficients Δ_2, Δ_4 correspond to A_2, A_4 of section 2. We evaluate them as particular cases of (2.9) and (2.10) by observing, in the notation of section 2, first, that QR is a sphere of radius $-\rho$ so that $B=C=0$; secondly, that the incident pencil is stigmatic so that $A_2=A_4=0$. Then if in (2.9), (2.10) we set $A_2=A_4=B=C=0$, $A_2'=\Delta_2$, $A_4'=\Delta_4$, $s=u$, $s'=v$, $r=-\rho$, $n=1$ and $n'=-n$, these equations become respectively

$$\frac{n\Delta_2}{v^2}+\frac{1}{2v}\left(\frac{1}{\rho}+\frac{1}{v}\right)^2=\frac{1}{2u}\left(\frac{1}{\rho}+\frac{1}{u}\right)^2, \tag{3.5}$$

$$\frac{3n}{8v^2}\left(\frac{1}{\rho}+\frac{1}{v}\right)^3-\frac{n}{8v\rho^2}\left(\frac{1}{\rho}+\frac{1}{v}\right)^2+\frac{n\Delta_2}{2v^2}\left(\frac{1}{\rho}+\frac{1}{v}\right)\left(\frac{1}{\rho}+\frac{3}{v}\right)+\frac{n\Delta_2^2}{v^3}-\frac{n\Delta_4}{v^2}$$
$$=\frac{3}{8u^2}\left(\frac{1}{\rho}+\frac{1}{u}\right)^3-\frac{1}{8u\rho^2}\left(\frac{1}{\rho}+\frac{1}{u}\right)^2. \tag{3.6}$$

We next express (3.4) in terms of h, the height at which it is incident on the surface OP, rather than k. As both h and k are small, we have from fig. 2,

$$\frac{k}{h}=\frac{NV}{MV}=\frac{v+\left(\Delta_2+\frac{1}{2\rho}\right)k^2+\ldots}{v+w+\Delta_2k^2-h^2/2r+\ldots}$$
$$=\frac{v}{v+w}+\left(\frac{v}{v+w}\right)\left[\frac{v}{2\rho(v+w)^2}+\frac{1}{2r(v+w)}-\frac{\Delta_2vw}{(v+w)^3}\right]h^2+O(h^4). \tag{3.7}$$

Substituting from (3.7) in (3.4), we have

$$OV=v+w+\Delta_2\left(\frac{v}{v+w}\right)^2h^2+O(h^4), \tag{3.8}$$

which expresses the L.S.A. in the required form.

Consider now OP as an aspherical mirror reflecting the aberrant object V back into itself. We have to determine the form of a reflecting surface knowing the L.S.A. of incident and reflected beams, both of which are given by (3.8). As the paraxial object and image must both be at the paraxial centre of curvature of OP, we have in the notation of section 2, $n'=-n$, $r=s=s'$, $A_2=A_2'$, $A_4=A_4'$. Equations (2.9), (2.10) then take the following simple forms :—

$$B+\frac{A_2}{s^2}=0. \tag{3.9}$$

$$C-\frac{5B}{4s^2}-\frac{A_2^2}{s^3}+\frac{A_4}{s^2}=0. \tag{3.10}$$

In our particular case we have from (3.7) that

$$\left.\begin{aligned} r = s = s' &= v + w, \\ A_2 &= \left(\frac{v}{v+w}\right)^2 \Delta_2, \end{aligned}\right\} \tag{3.11}$$

where Δ_2 is given by (3.5). (3.9) then becomes

$$B = -\frac{n(n-1)}{2}\left(\frac{v}{v+w}\right)^4\left(\frac{1}{\rho}+\frac{1}{v}\right)^2\left(\frac{1}{\rho}+\frac{n+1}{nv}\right). \tag{3.12}$$

This is an exact expression for B. When v is large enough for $1/v^2$ to be neglected, w always being assumed much smaller than v, (3.12) becomes

$$B = -\frac{n(n-1)}{2\rho^3}\left[1 - \frac{4w}{v} + \frac{(3n+1)\rho}{nv}\right]. \tag{3.13}$$

The expression for C corresponding to (3.12) for B is extremely complicated. As will appear from section 4, we need only know C to within a few per cent. Now it can be seen from (3.13) that the value of B when U is at focus, *i.e.* when $1/v = 0$, differs from that when U is near focus only by some multiple of the small quantity $1/v$. This is true also for C. In the case of C, therefore, we will neglect $1/v$ and assume that its value is that which it has when U is exactly at focus. The condition for this is that $(n-1)u = \rho$, or that $1/v = 0$. When this is satisfied, equations (3.5) and (3.6) become

$$\frac{\Delta_2}{v^2} = \frac{n(n-1)}{2\rho^3}. \tag{3.14}$$

$$\frac{{\Delta_2}^2}{v^3} - \frac{\Delta_4}{v^2} = \frac{3n}{8\rho^5}(n-1)(n^2-n+1). \tag{3.15}$$

It will be noted that as $v \to \infty$, Δ_2 and Δ_4 also $\to \infty$ in such a manner that $\lim \frac{\Delta_2}{v^2}$, $\lim \left(\frac{{\Delta_2}^2}{v^3} - \frac{\Delta_4}{v^2}\right)$ remain finite.

To determine C, we first note that when $v \to \infty$, $r \to \infty$, (3.1) becomes

$$x = \frac{Bh^4}{4} + \frac{Ch^6}{6} + \ldots \tag{3.16}$$

so that the surface OP is now a pseudo-flat. If $N\hat{V}Q$ be denoted by θ, the angle being positive as shown in fig. 2, then from (3.16),

$$\tan\theta = Bh^3 + Ch^5 + \ldots \tag{3.17}$$

From (3.7),

$$\frac{k}{h} = 1 - \frac{\Delta_2 w h^2}{v^2} + \ldots$$

whence (3.17) becomes

$$\tan\theta = Bk^3 + \left(C - \frac{3\Delta_2 wB}{v^2}\right)k^5 + \ldots \tag{3.18}$$

This gives an expression for θ in terms of k. We shall proceed to find another and then, by equating coefficients, determine B and C. Now from (3.4) and fig. 2,

$$\tan\theta=\frac{NQ}{NV}=\frac{k}{v+\left(\Delta_2+\frac{1}{2\rho}\right)k^2+\left(\Delta_4+\frac{1}{8\rho^3}\right)k^4+\ \ldots},$$

and when $v\to\infty$, this may be expanded in the form

$$\tan\theta=-\frac{\Delta_2k^3}{v^2}+\left(\frac{\Delta_2{}^2}{v^3}-\frac{\Delta_4}{v^2}\right)k^5+\ \ldots \tag{3.19}$$

Then substituting for Δ_2, Δ_4 from (3.14), (3.15), and equating coefficients between (3.18) and (3.19),

$$\left.\begin{aligned} B&=-\frac{n(n-1)}{2\rho^3},\\ C&=-\frac{3n(n-1)(1+n-n^2)}{8\rho^5}-3wB^2.\end{aligned}\right\} \tag{3.20}$$

(3.20) follows immediately from (3.13). A more convenient expression for C is KB^2, where

$$K=-3\left[\frac{(1+n-n^2)\rho}{2n(n-1)}-w\right]. \tag{3.21}$$

We note that K is very sensitive to small changes in n, and that when $n=1{\cdot}6181$ the term in ρ vanishes.

So far, then, we have found expressions for B and C, the coefficients of fourth and sixth powers in the asphericity of the autostigmatic lens, in terms of its refractive index n, thickness w and radius ρ. The expression for C is approximate, being strictly true only when the star is at focus, but that for B is exact. The latter, however, involves the virtual image-distance v, a difficult quantity to measure accurately, and we therefore give an alternative form for B which facilitates its practical determination.

When QR is convex to U, ρ is positive and B and C are both negative, so that the asphericity is also convex to U. In practice r is always positive, *i.e.* the paraxial part of OP is concave to U. Hence there is on this surface a "flat" ring, where it is met by a tangent plane perpendicular to the axis. The radius b of this ring is much more convenient to measure than v, and we shall therefore express (3.12) in terms of b rather than of $1/v$. Now b is the non-zero value of h, which makes $\frac{dx}{dh}=0$.

Setting in (3.1) $v+w=r$ and differentiating,

$$\frac{1}{v+w}+Bb^2+Cb^4=O\left(\frac{1}{v^5}\right), \tag{3.22}$$

because $b=O\left(\frac{1}{v}\right)$. We notice from (3.3) and (3.22) that to produce on the

surface a ring of radius b the star must be set inside focus by a distance ν given to the first order by

$$b^2 = \frac{2(n-1)\rho\nu}{n^2}. \tag{3.23}$$

Inserting in (3.13) the value of $1/v$ given by (3.22), we have the following approximation to B:—

$$B = -\frac{n(n-1)}{2\rho^3}\left[1 + \frac{(3n+1)(n-1)b^2}{2\rho^2} - \frac{2n(n-1)wb^2}{\rho^3}\right], \tag{3.24}$$

which for most purposes will be sufficient. To improve upon it we may proceed as follows. Having determined w, b, n and ρ, we calculate B from (3.24) and C from (3.21). We substitute these values of B and C in (3.22) to obtain a value of v, substitute this in (3.12) to compute a more accurate value of B, use this in turn to improve the approximation for v, and so proceed by successive approximation.

Finally, we obtain by computation an estimate of the error caused by neglecting eighth-power and higher terms. Referring again to fig. 1, we compute by the usual methods the paths of a series of rays which make successively greater angles $\mathrm{R\hat{U}Q}$ with the optical axis. Our knowledge of the equation of the aspherical surface up to the sixth-power terms enables us to find with sufficient accuracy the points P where each ray cuts the surface, and we can then compare $\tan\theta$, as found by the ray-trace, with the gradient of the normal at P, computed from the known terms in the equation of the surface. If the difference is substantially due to the neglected eighth-power term it will increase as the seventh power of h. This is found to be the case, and from the computation of a number of special cases, of which the example below is one, we can assert with some confidence that for values of n not too far from 1·52, the coefficient of h^8 in equation (3.1) ranges within about 50 per cent. on either side of the value $\frac{0{\cdot}13}{8\rho^7}$.

Example.—We choose a glass for which $n = 1{\cdot}515$ and suppose that w is 2 cm. and that the radius ρ is 33 cm. exactly. For simplicity, and to make (3.21) the exact value of the sixth-power coefficient, we place the star exactly at focus. Then the equation of the aspherical surface is found to be

$$\mathrm{ON} = -\frac{0{\cdot}1085546}{4}\left(\frac{h}{10}\right)^4 - \frac{0{\cdot}0023202}{6}\left(\frac{h}{10}\right)^6 + \frac{G}{8}\left(\frac{h}{10}\right)^8 + \ldots$$

where G is to be determined. It follows that

$$\frac{d\mathrm{ON}}{dh} = -0{\cdot}01085546\left(\frac{h}{10}\right)^3 - 0{\cdot}00023202\left(\frac{h}{10}\right)^5 + \frac{G}{10}\left(\frac{h}{10}\right)^7 + \ldots$$

In the table below Δ is $\left(\tan\theta - \frac{d\mathrm{ON}}{dh}\right)$, and if we find $\Delta\Big/\left(\frac{h}{10}\right)^7$ to be fairly constant, we can assume it equal to $G/10$. Seven-figure tables have been

used, so that we must expect an uncertainty of a few units in the last significant figure in Δ.

QÛR	4°	6°	7°	8°
tan θ	−0·0009939	−0·0034531	−0·0055913	−0·0085422
h	4·500643	6·805010	7·982483	9·182854
$\left(\frac{d\mathrm{OM}}{dh}\right)_{\mathrm{P}}$	−0·0009939	−0·0034548	−0·0055968	−0·0085574
$10^7\,\Delta$	0	17	55	152
$10^{13}\,\Delta/h^7$	...	25	26·7	22·7

whence we can take G to be $25\,.\,10^{-5}$; the coefficient of h^8 is then $0{\cdot}11/8\rho^7$.

We can summarise this section as follows. Given the radius ρ, thickness w and refractive index n of an autostigmatic lens, together with the radius b of the flat ring on its aspherical surface, we can give an accurate expression by (3.24) for the coefficients in the equation of that surface of the second and fourth powers, a close approximation to the coefficient of the sixth power (3.21) and a numerical estimate of the coefficient of the eighth power.

4. *The Double Transmission Compensator.*—We shall now consider a plate originally plane parallel, one surface of which has been figured to fit the back surface of an autostigmatic lens. Suppose this plate to be interposed between a concave aspherical mirror and an artificial star placed near its paraxial centre of curvature. The final image of the star, formed by a pencil refracted by the plate and then reflected by the mirror back through the plate, will in general suffer from spherical aberration. There will, however, be a particular mirror—let us call it the null mirror—which causes the incident pencil to return along its own path to a stigmatic image, and our object in this section is to determine the shape of this mirror in terms of its distances from plate and star and of the equation of the plate. We can then decide where the plate and star must be placed for the null mirror to have as nearly as possible the same shape as the mirror we wish to test, which in the only case we shall discuss in detail will be a paraboloid.

The general plan of this section is similar to that of section 3. We first find an expression for the L.S.A. of the virtual image formed by an originally stigmatic pencil after it has traversed the plate, this expression being in terms of the axial distance at which an image-forming ray meets the mirror. We then find what must be the equation of the mirror which reflects this aberrant image back into itself.

Fig. 3 (p. 472) shows a section of the system through its axis of symmetry OU. HKQR represents the figured plate of paraxial thickness HK = e. If the figured face HQ has been made to fit the back of an autostigmatic lens of constants n, ρ, w, b defined as in section 3, then its equation referred to H as origin is

$$x=\frac{h^2}{2r}+\left(\frac{1}{8r^3}+\frac{B}{4}\right)h^4+\left(\frac{1}{16r^5}+\frac{C}{6}\right)h^6+\ \ldots \qquad (4.1)$$

where x is the abscissa corresponding to h as ordinary, and r, B, C are identical with the r, B, C of section 3, except of course that they have the

opposite sign. OP is a section of the mirror. If its focal length is f and its paraxial centre of curvature F, then $OF = 2f = g$ say, and we can write its equation as

$$ON = \frac{y^2}{2g} + \left(\frac{1}{8g^3} + \frac{D}{4}\right)y^4 + \left(\frac{1}{16g^5} + \frac{E}{6}\right)y^6 + \ldots \qquad (4.2)$$

where y is the axial distance of P, any point on the mirror, and D and E are the coefficients we have to determine, describing the asphericity of the mirror. U is the artificial star distant $FU = u$ from F, and $FH = d$. URQP is a ray from the star U which is refracted by the surfaces RK and QH in turn so that it lies successively along QR and PQ. QR and PQ meet the

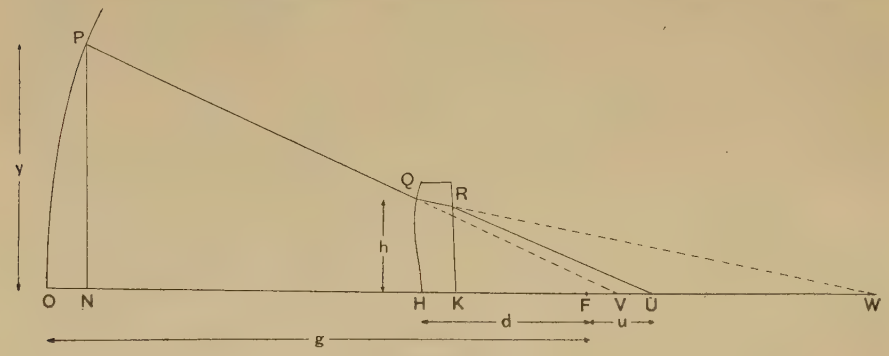

FIG. 3.

axes in W and V respectively, which are therefore points in the intermediate and final images of U.

The refraction at the flat surface gives a pencil whose aberration we now determine. From Snell's law

$$\sin K\hat{U}R = n \sin K\hat{W}R$$

we have

$$n^2\{k^2 + (d+u-e)^2\} = n^2\{k^2 + KW^2\},$$

whence

$$KW = n(d+u-e) + \frac{(n^2-1)k^2}{2n(d+u-e)} - \frac{(n^2-1)^2k^4}{8n^3(d+u-e)^3} + \ldots \qquad (4.3)$$

where k is the axial distance at which the ray from U meets RK. Our first object is to find the L.S.A. of the image at W in terms of h. We have from the figure, (4.1) and (4.3),

$$\frac{k}{h} = \frac{KW}{KW + e - x} = \frac{n(d+u-e) + \frac{(n^2-1)k^2}{2n(d+u-e)} + \ldots}{n\left(d+u-\frac{n-1}{n}e\right) + \frac{(n^2-1)k^2}{2n(d+u-e)} - \frac{h^2}{2rn} + \ldots}$$

$$= \frac{d+u-e}{d+u-\frac{n-1}{n}e} + \frac{(n^2-1)(d+u-e)eh^2}{2n^3\left(d+u-\frac{n-1}{n}e\right)^4} + \frac{(d+u-e)h^2}{2nr\left(d+u-\frac{n-1}{n}e\right)^2} + O(h^4). \qquad (4.4)$$

We obtain the desired expression by substituting in (4.3) the value of k given by (4.4) and by observing that $\mathrm{HW} = \mathrm{KW} + e$.

It is clear that such an expression will be very complicated, and at this stage it is convenient for subsequent approximation to work out an equation for the null mirror in the case where we can neglect u, e and $\frac{1}{r}$; that is, where we assume the star to be exactly at the paraxial centre of curvature of the mirror, the thickness of the plate to be negligible and its aspherical surface to be a pseudo-plane, so that its equation is given by

$$x = \frac{Bh^4}{4} + \frac{Ch^6}{6} + \ldots \tag{4.5}$$

instead of by (4.1). As h is now equal to k and HW to KW, (4.3) becomes

$$\mathrm{HW} = nd + \frac{(n^2-1)h^2}{2nd} - \frac{(n^2-1)^2h^4}{8n^3d^3} + \ldots \tag{4.6}$$

(4·6) describes the L.S.A. of the pencil incident on the aspherical surface (4.5). We can now apply (2.5), (2.6) to find the L.S.A. of the refracted pencil. If this is given by

$$\mathrm{HV} = s' + \Delta_2 h^2 + \Delta_4 h^4 + \ldots \tag{4.7}$$

then in the notation of section 2 we must have

$$\left.\begin{array}{ll} n = n, \quad n' = 1; & s = nd, \quad s' = d; \\ A_2 = \dfrac{n^2-1}{2nd}, & A_4 = -\dfrac{(n^2-1)^2}{8n^3d^3}, \\ A_2' = \Delta_2, & A_4' = \Delta_4. \end{array}\right\} \tag{4.8}$$

When we substitute from (4.8) in (2.5) and (2.6) they become respectively

$$\Delta_2 = (n-1)Bd^2, \tag{4.9}$$

$$\Delta_4 = (n-1)Cd^2 + \frac{3(2n+1)(n-1)B}{4n} + (n-1)^2B^2d^3, \tag{4.10}$$

and with these values of Δ_2, Δ_4 we can write

$$\mathrm{OV} = g + \Delta_2 h^2 + \Delta_4 h^4 + \ldots \tag{4.11}$$

To express this in terms of y, we see from

$$\frac{h}{y} = \frac{\mathrm{HV}}{\mathrm{NV}} = \frac{d + \Delta_2 h^2 + \ldots}{g + \Delta_2 h^2 - \dfrac{y^2}{2g} + \ldots} = \frac{d}{g} + \left(1 - \frac{d}{g}\right)\frac{d^2\Delta_2 y^2}{g^3} + \frac{dy^2}{2g^3} + O(y^4) \tag{4.12}$$

that

$$\mathrm{OV} = g + \Delta_2 d^2\left(\frac{y}{g}\right)^2 + \left[2\Delta_2^2 d^3\left(1 - \frac{d}{g}\right) + \Delta_2 d^2 + \Delta_4 d^4\right]\left(\frac{y}{g}\right)^4 + \ldots \tag{4.13}$$

The surface OP is to be such that it reflects the virtual aberrant image at V

into itself. To find its equation we can therefore use (3.9), (3.10), in which we must set

$$g=s, \qquad A_2=\frac{\Delta_2 d^2}{g^2}, \qquad A_4=\left[2\Delta_2{}^2d^3\left(1-\frac{d}{g}\right)+\Delta_2 d^2+\Delta_4 d^4\right]\Big/g^4,$$

and, from (4.2), $B=D$ and $C=E$. Then we find that

$$Dg^4+\Delta_2 d^2=0, \tag{4.14}$$

$$Eg^6=-9\Delta_2 d^2/4-\Delta_4 d^4-2\Delta_2{}^2d^3+3\Delta_2{}^2d^4/g, \tag{4.15}$$

and (4.2) becomes

$$\mathrm{ON}=\frac{y^2}{2g}+(g/2-\Delta_2 d^2)\frac{y^4}{4g^4}+\left(\frac{3g}{8}+\frac{3\Delta_2{}^2d^4}{g}-\frac{9\Delta_2 d^2}{4}-2\Delta_2{}^2d^3-\Delta_4 d^4\right)\frac{y^6}{6g^6}+\ldots \tag{4.16}$$

This, then, is the equation, up to sixth powers, of the mirror for which in our simplified conditions a test would be null. Now suppose that we wish to make this mirror as nearly as possible a paraboloid. We choose d so that the coefficient of y^4 is zero, whence from (4.9)

$$g=2(n-1)Bd^4. \tag{4.17}$$

Then the coefficient of the sixth power can be verified to be approximately $g\left(\frac{1}{6}+\frac{S}{8}\right)$, where S is the diameter-ratio of mirror to plate, so that if (4.17) is satisfied, (4.16) becomes approximately

$$\mathrm{ON}=\frac{y^2}{2g}-g\left(\frac{1}{6}+\frac{S}{8}\right)\left(\frac{y}{g}\right)^6+\ldots \tag{4.18}$$

Hence the null mirror is low with respect to a paraboloid of focal length $g/2$ or f by a term $2f\left(\frac{1}{6}+\frac{S}{8}\right)\left(\frac{y}{2f}\right)^6$, which attains its maximum value of $2f\left(\frac{1}{6}+\frac{S}{8}\right)\left(\frac{1}{4F}\right)^6$ at the edge, where $\frac{y}{2f}=\frac{1}{4F}$, F being the focal ratio of the mirror. For ordinary values of S, *i.e.* those in the neighbourhood of 10, this maximum will not be far from $3f/(4F)^6$. Thus a 40-cm. (16-in.) mirror of focal ratio 5, figured true to test with a plate placed according to (4.17), would be turned down at the edge with respect to a true paraboloid by about 10^{-5} cm. or $\lambda/5$. In the form just described, the method of testing with compensator plates is therefore limited to mirrors on which a figuring error of $2f/(4F)^6$ is negligible—that is, roughly speaking, to mirrors of focal ratio greater than 5. In section 6 we will show how its range can be considerably extended.

We must now take into account the quantities u, e and $1/r$. We assume that they are so small that the squares of u/d, e/d and d/r may be neglected. The practical justification for this procedure is, first, that the greatest of these

ratios is in practice never more than about 1/50; secondly, that the errors arising are errors only in correction terms which are themselves small; thirdly, that in the few cases actually calculated the difference between exact and approximate theory has been quite negligible. We will also suppose that the value of E in (4.15) is near enough to the true value for our purposes; the difference is certainly not greater than a few per cent. It would in fact be superfluous to make a more accurate calculation of E because of the approximation errors in the eighth-power terms.

With the above assumptions, equation (4.4) becomes

$$\frac{k}{h} = 1 - \frac{e}{nd} + \frac{(n^2-1)eh^2}{2n^3d^2} + \frac{h^2}{2nrd} + O(h^4),$$

whence the expression for the L.S.A. of the image at W is given by

$$\mathrm{HW} = n\left(d + u - \frac{n-1}{n}e\right) + \frac{n^2-1}{2nd}\left(1 - \frac{u}{d} - \frac{(2-n)e}{nd}\right)h^2 + \frac{(n^2-1)h^4}{2n^2rd^2} - \frac{(n^2-1)^2}{8n^3d^3}\left(1 - \frac{3u}{d} + \frac{3e}{d}\right)h^4 + \ldots \quad (4.19)$$

This refers to the incident pencil. The equation of the surface HQ is now

$$x = \frac{h^2}{2r} + \frac{Bh^4}{4} + \frac{Ch^6}{6} + \ldots \quad (4.20)$$

because the $1/r^3$ and $1/r^5$ terms may be neglected. As this is the equation of a pseudo-sphere we must use (2.8) and (2.9) in place of (2.5) and (2.6) to find the L.S.A. of the refracted pencil. We do not require (2.10) because of our assumption that the value already calculated for the sixth-power coefficient E is good enough. As in (4.7), let

$$\mathrm{HV} = s' + \Delta_2 h^2 + \Delta_4 h^4 + \ldots \quad (4.21)$$

In this equation s' and Δ_2 have slightly different values from the corresponding quantities in (4.7). To find them we must make the following substitutions from (4.19), (4.20) in (2.8) and (2.9):—

$$n = n, \qquad n' = 1; \qquad s = n\left(d + u - \frac{n-1}{n}e\right);$$

$$A_2 = \left(1 - \frac{u}{d} - \frac{(2-n)e}{nd}\right)\frac{n^2-1}{2nd}, \qquad A_2' = \Delta_2. \quad (4.22)$$

Then

$$s' = d + u - \frac{n-1}{n}e + \frac{(n-1)d^2}{r} = d + \epsilon, \quad \text{say} \quad (4.23)$$

$$\Delta_2 = (n-1)B(d+\epsilon)^2 - \frac{(n^2-1)e}{2n^3d^2} + \frac{(3n+2)(n-1)}{2nr}, \quad (4.24)$$

which readily reduces to (4·9) following the earlier approximation. As

before, we wish to express $OV = HV + u - d$ in terms of h rather than y. It is easy to show from

$$\frac{h}{y} = \frac{d + \epsilon - \frac{h^2}{2r} + \ldots}{g + \epsilon - \frac{y^2}{2r} + \ldots} = \frac{d+\epsilon}{g} - \frac{d\epsilon}{g^2} + O(y^2)$$

that

$$OV = g + \epsilon + \Delta_2 d^2 \left(1 + \frac{2\epsilon}{d} - \frac{2\epsilon}{g}\right)\left(\frac{y}{g}\right)^2 + \left[\Delta_2 d^2 + 2\Delta_2^2 d^3 \left(1 - \frac{d}{g}\right) + \Delta_4 d^4\right]\left(\frac{y}{g}\right)^4 + \ldots \quad (4.25)$$

the exact analogy of (4.13), Δ_2 being defined by (4.24) and Δ_4 by (4.10). The rest of the calculation proceeds exactly as before. In (3.9) we set

$$B = D, \qquad A_2 = \frac{\Delta_2 d^2}{g^2}\left(1 + \frac{2\epsilon}{d} - \frac{2\epsilon}{g}\right) \quad \text{and} \quad s = g + \epsilon.$$

Then

$$D + \left(1 + \frac{2\epsilon}{d} - \frac{4\epsilon}{g}\right)\frac{\Delta_2 d^2}{g^4} = 0,$$

and from this and (4.16) the equation of the null mirror is

$$ON = \frac{y^2}{2(g+\epsilon)} + \left\{\frac{g}{2} - \frac{3\epsilon}{2} - \Delta_2 d^2\left(1 + \frac{2\epsilon}{d} - \frac{4\epsilon}{g}\right)\right\}\frac{y^4}{4g^4} + \left\{\frac{3g}{8} + \frac{3\Delta_2^2 d^4}{g} - \frac{9\Delta_2 d^2}{4} - 2\Delta_2^2 d^3 - \Delta_4 d^4\right\}\frac{y^6}{6g^6} + \ldots \quad (4.26)$$

This equation contains (4.16) as the special case $\epsilon \equiv 0$. It describes the mirror for which the test would be null in terms of g, its paraxial radius of curvature, d the distance at which the compensator plate is placed from the paraxial centre of curvature, ϵ the small correction term arising from the thickness of the plate, etc., and Δ_2, Δ_4, quantities which are connected by (4.24), (4.10) with the constants of the aspherical lens against which the plate was tested. The equation will be discussed further in section 6.

We note here two formulæ useful in computing tolerances. These enable us to find the change in shape of the null mirror produced by small variations in d and u, and are respectively

$$\left(\frac{\partial ON}{\partial d}\right)_{\epsilon \equiv 0} = -\frac{g}{2d}\left(\frac{y}{g}\right)^4 + O(y^6); \quad (4.27)$$

$$\left(\frac{\partial ON}{\partial u}\right)_{\epsilon \equiv 0} = -\frac{y^2}{2g^2} + \left(\frac{1}{8} - \frac{g}{2d}\right)\left(\frac{y}{g}\right)^4 + O(y^6). \quad (4.28)$$

They follow by simple differentiation from (4.26), using (4.17), (4.23) and (4.24).

It remains to find an estimate for the neglected terms in (4.26), *i.e.* those

higher than the sixth power, and to do this we use a numerical method identical in principle with that described at the end of section 3. We take a compensator plate of known equation, and having selected suitable values of d, g, u and e, calculate from them the equation of the null mirror up to sixth-power terms. We compute the paths of a series of rays originating at U, and in particular determine the angles $O\hat{V}P$ which the final rays make with the optical axis and the points P where they meet the mirror. These rays should be normals to the mirror, so that the gradients of the normals at P as found from the formula should be identical with the tangents of the angles $O\hat{V}P$ as computed by the ray-trace, and if the discrepancy between them is substantially proportional to the seventh power of the axial distance y, we can infer that this discrepancy is due almost entirely to an eighth-power term whose coefficient we can determine, and that the contributions to it from higher powers may be neglected.

We adopt as aspherical surface that considered at the end of section 3. Its equation in the notation of (4.1) is

$$x = -\frac{0{\cdot}1085546}{4}\left(\frac{h}{10}\right)^4 - \frac{0{\cdot}0023202}{6}\left(\frac{h}{10}\right)^6 + \frac{0{\cdot}00025}{8}\left(\frac{h}{10}\right)^8 + \ldots$$

Set $d = 100{\cdot}00$ cm., $n = 1{\cdot}515$, $e = 3$ cm., $u = 1{\cdot}020$ cm. and $g = 1175{\cdot}525$ cm. With this choice the null mirror is as close an approximation as possible to a paraboloid, as will be shown in section 6. (From the point of view of the present problem, however, this is quite irrelevant.) The equation of the mirror is then

$$\mathrm{ON} = \frac{y^2}{2g} + \frac{2{\cdot}9265}{4}\left(\frac{y}{g}\right)^4 - \frac{1170{\cdot}60}{6}\left(\frac{y}{g}\right)^6 - \frac{Gg}{8}\left(\frac{y}{g}\right)^8,$$

where G is to be determined. Also

$$\frac{d\mathrm{ON}}{dy} = \frac{y}{g} + 0{\cdot}0024895\left(\frac{y}{g}\right)^3 - 0{\cdot}99581\left(\frac{y}{g}\right)^5 - G\left(\frac{y}{g}\right)^7. \qquad (4.29)$$

In the table Δ is $\left(\frac{d\mathrm{ON}}{dy} - \tan O\hat{V}P\right)$. Reference to fig. 3 should explain the other entries. The last figure in each entry is uncertain by a few units.

$O\hat{U}R$	2° 30′	3°	3° 30′	4°	5°
h	4·366016	5·240628	6·115982	6·992263	8·747571
FV	1·0847	1·5753	2·1662	2·8642	4·5997
$O\hat{V}P$	2° 28′·3912	2° 57′·2119	3° 25′·5565	3° 52′·3403	4° 46′·8718
tan $O\hat{V}P$	0·0431921	0·0515946	0·0598653	0·0679804	0·0836419
y	50·77286	60·65121	70·37678	79·92269	98·36392
$\left(\frac{d\mathrm{ON}}{dy}\right)_P$	0·0431922	0·0515948	0·0598661	0·0679823	0·0836503
$10^7\,\Delta$	1	2	8	19	84
$\frac{\Delta g^7}{100y^7}$	(3)	(2)	2·9	2·83	2·92

From (4.29) we see that $G=\Delta\left(\frac{g}{y}\right)^7$, $=290$ say, and can make the general deduction that in any null mirror the coefficient of $\left(\frac{y}{g}\right)^8$, $-\frac{Gg}{8}$, is not far from $-36g$. The numerical factor depends, of course, on the refractive index, the relative values of d and g and so on, but, if the behaviour of the sixth-power coefficient is any criterion, its variation is quite small even for considerable changes in these quantities.

In this section, then, we have, in (4.26), found explicitly the equation of the null mirror up to the sixth power, expressed in terms of its distance from star and compensator plate, and of the thickness and paraxial curvature of the plate; and we have given a numerical estimate of the eighth-power term which should suffice for nearly all practical applications, and have shown that powers higher than the eighth are negligible.

5. *The Figured Plate as a Single Transmission Compensator.*—In section 4 we have found the shape of the null mirror when the star and plate are so disposed that the light passes through the latter twice. In this section we suppose the star and knife-edge to be decentred sufficiently to allow the light to traverse the plate once only. This arrangement has certain advantages, notably that figuring errors on the plate appear on the mirror divided by four. We will suppose also that the image is formed at the same distance from the mirror as the star; the more general case when these distances are different is formally very complicated and yields nothing new for the practical problem.

The working in this section is then almost identical with that in section 4. We have to determine the equation of the mirror by which an incident aberrant pencil is reflected not into itself, as in section 4, but into a stigmatic pencil, the paraxial foci of incident and reflected pencils being equidistant from the mirror. With the notation of section 4 and with the assumptions there adopted, that u/d, e/d and d/r are so small that we may neglect their squares generally and their first powers in coefficients of y^6, the L.S.A. of the incident pencil is given by (4.25). Then the paraxial radius of curvature of the null mirror is clearly $g+\epsilon$, and its equation may be written

$$\mathrm{ON}=\frac{y^2}{2(g+\epsilon)}+\left(\frac{1}{8g^3}-\frac{3\epsilon}{8g^4}+\frac{D'}{4}\right)y^4+\left(\frac{1}{16g^5}+\frac{E'}{6}\right)y^6+\ldots \qquad (5.1)$$

D' and E' are found as before from (2.9) and (2.10). For these equations to be applicable we must set in them, from (4.25) and (5.1),

$$n'=-n, \qquad s=s'=r=g+\epsilon;$$

$$A_2=\left(1+\frac{2\epsilon}{d}-\frac{2\epsilon}{g}\right)\frac{\Delta_2 d^2}{g^2},$$

$$A_4=\left\{\Delta_2 d^2+\Delta_4 d^4+2\Delta_2{}^2 d^3\left(1-\frac{d}{g}\right)\right\}\Big/g^4,$$

Δ_2, Δ_4 being defined by (4.24), (4.10) respectively. Then (2.9) and (2.10) become

$$2D'g^4+\left(1+\frac{2\epsilon}{d}-\frac{4\epsilon}{v}\right)\Delta_2d^2=0,$$

$$2E'g^6=3\Delta_2{}^2d^4/g-9\Delta_2d^2/4-\Delta_4d^4-2\Delta_2{}^2d^3,$$

so that the coefficients D', E' are just half of the D, E of section 4. Substituting these values for them in (5.1), the equation of the null mirror now becomes

$$\mathrm{ON}=\frac{y^2}{2(g+\epsilon)}+\left\{g-3\epsilon-\Delta_2d^2\left(1+\frac{2\epsilon}{d}-\frac{4\epsilon}{g}\right)\right\}\frac{y^4}{8g^4}$$
$$+\left\{\frac{3g}{4}+\frac{3\Delta_2{}^2d^4}{g}-\frac{9\Delta_2d^2}{4}-2\Delta_2{}^2d^3-\Delta_4d^4\right\}\frac{y^6}{12g^6}+\ \ldots \qquad (5.2)$$

Consider the simplified case of section 4. Neglect u, e and $1/r$ throughout and choose d so that the coefficient of y^4 is zero. Then d is given by

$$\Delta_2d^2=g, \qquad (5.3)$$

and (5.2) reduces to

$$\mathrm{ON}=\frac{y^2}{2g}-\frac{gS}{3}\left(\frac{y}{g}\right)^6+\ \ldots \qquad (5.4)$$

the analogue of (4.18), the sixth-power coefficient being approximate only. Thus as we would expect, the null mirror is again low with respect to a paraboloid, the maximum deficit for a size ratio S being $gS/3(4F)^6$. Comparing this result with the corresponding one deduced from (4.18), we see that when a given plate is used as a single transmission compensator the error is about twice that when the plate is used by double transmission.

Finally, when as in section 4 we work out formulæ for $\left(\frac{\partial \mathrm{ON}}{\partial d}\right)_{\epsilon\equiv 0}$ and $\left(\frac{\partial \mathrm{ON}}{\partial u}\right)_{\epsilon\equiv 0}$ by differentiating (5.2) and using (4.23), (4.24) and (5.3), we find they are identical with (4.27) and (4.28).

6. *The Null Method as an Approximation to a Paraboloid.*—In sections 4 and 5 we found the equation of the mirror which would give a null test when we used as compensator a plate figured to fit the back of a given spherical lens, and we have seen that the plate can be placed so that the greatest deviation between such a mirror and a paraboloid of similar dimensions, of focal length f and focal ratio F say, is that the former is turned down with respect to the latter by a negative sixth-power term with a maximum value (at the edge) of roughly $3f/(4F)^6$. As noted in section 4, the use of such plates is thus effectively limited to plates of $F > 5$. By choosing a slightly different position of the plate it is possible, however, to introduce into the equation of the null mirror a positive ("turn-up") fourth-power term, the effect of which can be made largely to offset that of the sixth-power term, and indeed by extending this process to vary also the second-power term, we can reduce the original sixth-power error above by a factor of about 20. The eighth-power error then becomes appreciable, and for $F < 5$ has to be taken into account, which, however, can be done simply enough. In this section we

explain the method and condense it into working equations suitable to the requirements of the practical optician.

It is easily shown that for $0 \leqslant x \leqslant 1$ the numerical value of the expression

$$x^6 - \tfrac{3}{2}x^4 + \tfrac{1}{2}x^2 \tag{6.1}$$

nowhere exceeds 0·04811. This value is attained as a maximum at $x = 0{\cdot}4597$ and as a minimum at $x = 0{\cdot}8881$. We shall need this result in what follows.

Consider first the particular case of section 4 in which $u = e = 1/r = 0$, when by (4.9) and (4.16) the equation of the null mirror is

$$\mathrm{ON} = \frac{y^2}{2g} + \left\{\frac{g}{2} - (n-1)Bd^4\right\}\frac{y^4}{4g^4} + \left(\frac{3g}{8} + Eg^6\right)\frac{y^6}{6g^6} + O(y^8);$$

or, writing $z = 4Fy/g$,

$$\mathrm{ON} = \frac{y^2}{2g} + \left\{\frac{g}{2} - (n-1)Bd^4\right\}\frac{z^4}{4(4F)^4} + \frac{Mz^6}{(4F)^6} + O(y^8). \tag{6.2}$$

In this equation the only quantity at our disposal is d, and this we wish to choose so that (6.2) may represent as nearly as possible a paraboloid. We know from (4.17) that a close approximation to d is given by the d_0 which satisfies

$$g = 2(n-1)Bd_0^4. \tag{6.3}$$

Let us then set $d = (1-R)^{\frac{1}{4}}d_0$, so that we may write

$$\frac{g}{2} - (n-1)Bd^4 = \frac{Rg}{2}. \tag{6.4}$$

Suppose also that $g = g_0 + \nu$, and assume ν small enough for ν^2/g^2 to be neglected. (We have as yet placed no restriction on R.) Then with these substitutions (6.2) becomes

$$\mathrm{ON} = \frac{y^2}{2g_0} - \left\{\frac{\nu z^2}{2(4F)^2} - \frac{Rgz^4}{8(4F)^4} + \frac{Mz^6}{(4F)^6}\right\} + O(y^8). \tag{6.5}$$

We wish to choose ν, R so that the combined effect of the terms in the square brackets will be as small as possible. By comparing them with (6.1) and remembering that the maximum value of z is 1, we see that if

$$\left.\begin{aligned} \frac{Rg}{8} &= \frac{3M}{2(4F)^2}, \\ \frac{\nu}{2} &= \frac{M}{2(4F)^4}, \end{aligned}\right\} \tag{6.6}$$

the numerical value of the square bracket will not be greater than $0{\cdot}04811\ M/(4F)^6$. With the rough value $3g/2$ of M deduced from (4.18), we have as approximations to ν and R,

$$R \simeq \frac{18}{(4F)^2}; \qquad \nu \simeq \frac{3g}{2(4F)^4}, \tag{6.7}$$

so that our assumption as to the smallness of ν is justified.

In practice, a more accurate value than $3g/2$ is needed for M. But the calculation of M involves d and therefore R. For $F > 3$, that is for nearly every case which will arise in practice, R will be $< 1/8$, and small enough for powers higher than the square to be neglected, and we shall here assume this to be so. Otherwise it would be necessary to find R by successive approximation, starting with the value given by (6.7). From (4.26),

$$\frac{6M}{g} = \frac{9\Delta_2 d^2}{4g} + \frac{2\Delta_2{}^2 d^3}{g} + \frac{\Delta_4 d^4}{g} - \frac{3\Delta_2{}^2 d^4}{g^2} - \frac{3}{8}, \tag{6.8}$$

and from (4.9), (6.4),

$$\Delta_2 d^2 = (1-R)g/2.$$

By (4.10), (6.4),

$$\Delta_4 d^4 = \frac{(1-R)^2 g^2}{4d} + \frac{3(2n+1)(1-R)g}{8n} + \frac{(1-R)^2 g^2 K}{4(n-1)d^2},$$

where, by (3.21),

$$K = C/B^2 \simeq d/6.$$

Using these two equations, we can after some reduction write for (6.7),

$$\frac{6M}{g} = \frac{3(2n+1)}{8} + \frac{3g}{4d_0} + \frac{gK}{4(n-1)d_0{}^2} - \left\{\frac{3(n+1)}{8n} + \frac{21g}{16d_0} + \frac{3gK}{8(n-1)d_0{}^2}\right\}R + \left\{\frac{g}{2d_0} + \frac{3gK}{32(n-1)d_0{}^2} - \frac{3}{4}\right\}R^2 + O(R^3). \tag{6.9}$$

With (6.6) this gives a quadratic for R.

We may summarise the preceding discussion as follows. If a mirror of paraxial focal length $g/2$ and focal ratio F is tested with a star at its paraxial centre of curvature and a compensator plate at a distance d inside this, then d and ν can be chosen so that the shape of the mirror nowhere differs from that of a paraboloid of focal length $\frac{1}{2}(g-\nu)$ by more than $3g/40(4F)^6$. This statement has been made without consideration of eighth-power terms or of the small quantities u/d, e/d and d/r. The discussion is extended to include the latter as follows. When u/d, e/d, d/r are small enough for their squares to be neglected, we have from (4.24) and (4.26) that the equation of the null mirror may be written

$$\mathrm{ON} = \frac{y^2}{2(g+\epsilon)} + \left\{\frac{g}{2} - \frac{3\epsilon}{2} - (n-1)Bd^4 + \frac{(n^2-1)e}{2n^3} - \frac{(3n+2)(n-1)d^2}{2nr} - 4(n-1)Bd^4\left(\frac{1}{d} - \frac{1}{e}\right)\epsilon\right\}\frac{z^4}{4(4F)^4} - \frac{Mz^6}{(4F)^6} + O(y^8). \tag{6.10}$$

Here $z = \dfrac{4Fy}{g}$ and M is identical with the M of (6.8). We have at our disposal d and u, the latter occurring in ϵ. For simplicity we will choose u so that $\epsilon = 0$. Then from (4.23),

$$u = \frac{(n-1)e}{n} - \frac{(n-1)d^2}{r}, \tag{6.11}$$

or, without approximation,

$$u\left\{1+\frac{(n-1)d}{r}\right\}=\frac{(n-1)e}{n}-\frac{(n-1)d^2}{r}. \tag{6.12}$$

Set as before, $d=(1-R)^{\frac{1}{2}}d_0$, $g=g_0+\nu$, ν small. Then (6.10) becomes

$$\mathrm{ON}=\frac{y^2}{2g_0}-\left[\frac{\nu z^2}{(4F)^2}-\left\{\frac{Rg}{2}+\frac{(n^2-1)e}{2n^3}-\frac{(3n+2)(n-1)(1-R)^{\frac{1}{2}}d_0^2}{2nr}\right\}\frac{z^4}{4(4F)^4}+\frac{Mz^6}{(4F)^6}\right]+O(y^8). \tag{6.13}$$

To minimise the term in square brackets in the range, we have from (6.1) the following equations for ν and R :—

$$\frac{Rg}{2}+\frac{(n-1)e}{2n^3}-\frac{(3n+2)(n-1)(1-R)^{\frac{1}{2}}d_0^2}{2nr}=\frac{6M}{(4F)^2}, \tag{6.14}$$

$$\frac{\nu}{2}=\frac{M}{2(4F)^4}. \tag{6.15}$$

Again neglecting higher powers of R than the square, (6.14) and (6.9) give a quadratic for R which is, however, too complicated to be written out at length.

When the term in y^6 is annulled so far as possible by the use of (6.1), the null mirror considered as a paraboloid is free from error at the edge. The effect of the eighth power is to turn it down at the edge by $36g/(4F)^8$, which even for $F=5{\cdot}5$ is comparable with the $3g/40(4F)^6$ remaining after the compensation of the original sixth-power discrepancy. It is clear that we may without appreciable error consider this as due to a sixth-power term with a maximum value of $36g/(4F)^8$, so that, to compensate for eighth- as well as for sixth-power terms, we must add to the M of (6.9) a term $36g/(4F)^2$.

The case when the compensator is used by single transmission is precisely similar. If d_0, R are defined by

$$g=(n-1)Bd_0^4, \qquad d=(1-R)^{\frac{1}{2}}d_0$$

respectively, and if u satisfies (6.12) so that $\epsilon=0$, the equation (5.2) for the null mirror becomes

$$\mathrm{ON}=\frac{y^2}{2g}+\left\{Rg+\frac{(n^2-1)e}{2n^3d^2}-\frac{(3n+2)(n-1)d^2}{2nr}\right\}\frac{z^4}{4(4F)^4}-\frac{Mz^6}{(4F)^6}, \tag{6.16}$$

where $z=4Fy/g$ and M is given by

$$\frac{12M}{g}=\left(\frac{3}{4n}+\frac{3g}{d_0}+\frac{gK}{(n-1)d_0^2}\right)-\left(\frac{21g}{4d_0}+\frac{3gK}{2(n-1)d_0^2}-\frac{3(3n-1)}{4n}\right)R+\left(\frac{2g}{d_0}+\frac{3gK}{8(n-1)d_0^2}-3\right)R^2+O(R^3). \tag{6.17}$$

We calculate R by setting

$$Rg+\frac{(n^2-1)e}{2n^3d^2}-\frac{(3n+2)(n-1)(1-R)^{\frac{1}{2}}d_0^2}{2nr}=\frac{6M}{(4F)^2}+\frac{432g}{(4F)^4}, \qquad (6.18)$$

where the second term on the right-hand side takes eighth-power terms into account.

Thus we have shown that a null mirror figured from a compensator made by the null method here investigated differs from a paraboloid by an amount which is everywhere less than $f/5(4F)^6$, $\simeq f/21{,}000F^6$, where f is the focal length in use and F the focal ratio in use.

Working instructions can now be laid down as follows. Take an autostigmatic lens of radius ρ, refractive index n and thickness w, with a flat ring of radius b on its figured face. Calculate $\frac{1}{r}$, B and K in terms of these four dimensions by the appropriate formulæ (3.22), (3.24) and (3.21) respectively. Suppose that the thickness of the compensator plate made to fit the back surface of the lens is e, and that it is to be used by double transmission to test a mirror of focal length f, or $g/2$, and focal ratio F. Then defining d_0 by (6.19) and M by (6.9), the distance d at which the further surface of the plate is to be placed from the paraxial centre of curvature of the mirror is given by

$$d^4=(1-R)d_0{}^4=\frac{(1-R)f}{(n-1)B}, \qquad (6.19)$$

where the small correction term R is found from

$$\frac{Rg}{2}+\frac{(n^2-1)e}{2n^3}-\frac{(3n+2)(n-1)d_0{}^2}{2nr}+\frac{(3n+2)(n-1)d_0{}^2R}{4nr}+\frac{(3n+2)(n-1)d_0{}^2R^2}{8nr}$$
$$=\frac{6M}{(4F)^2}+\frac{216g}{(4F)^4}. \qquad (6.20)$$

This can be solved directly or by successive approximation. d having been found, u, the distance by which the star must be set back from the paraxial centre of curvature, is given by (6·12).

If the compensator is to be used by single transmission, d is given by

$$d^4=(1-R)d_0{}^4=\frac{(1-R)2f}{(n-1)B},$$

R being found from (6.17) and (6.18). u is again given by (6.12).

As an example, we will find the d and u for the case considered in section 4. Here we are using the compensator of section 3 to test by double transmission an $F/5$ paraboloid of focal length 587·76 cm., *i.e.* of 117·5 cm. (46 in.) aperture. For the autostigmatic lens of section 3 we had $\rho=33$ cm., $n=1{\cdot}515$, $w=2$ cm. and $b=0$, and had found that $\frac{1}{r}=0$, $B=1{\cdot}085546\,.\,10^{-5}$ and $k=19{\cdot}6892$. Now suppose that the compensator is 2 cm. thick (it will be about 11 cm. in diameter) and that it is made of glass of refractive

index 1·515. If we set $g = 1175{\cdot}525$ cm., then from (6.19) $d_0^4 = 1{\cdot}0513478 \,.\, 10^8$, whence $d_0 = 101{\cdot}2597$ cm. With this d_0 we find from (6.9),

$$6M/g = 10{\cdot}80005 - 17{\cdot}5030R + 5{\cdot}465R^2.$$

In this particular case we are not correcting for the eighth power. Also we have that $\frac{1}{r} = 0$, so that equation (6.20) for R becomes

$$587{\cdot}7625R + 0{\cdot}55873 = 31{\cdot}73932 - 51{\cdot}4381R + 16{\cdot}06R^2,$$

whence $R = 0{\cdot}04878658$, and

$$d = (1 - R)^{\frac{1}{4}} d_0 = 100{\cdot}0014 \text{ cm.}$$

Then from (6.12) $u = 1{\cdot}0198$. As will be shown in section 7, it is sufficiently accurate to specify $d = 100{\cdot}00$ cm., $u = 1{\cdot}02$ cm. With this R, the value of M is 1951·0, and the equation of the null mirror

$$\text{ON} = \frac{y^2}{2g} + \frac{29{\cdot}265}{4}\left(\frac{y}{g}\right)^4 - \frac{11706{\cdot}0}{6}\left(\frac{y}{g}\right)^6 - \ldots$$

This nowhere differs from a paraboloid by more than

$$\frac{0{\cdot}048M}{(4F)^6} = 1{\cdot}64 \,.\, 10^{-6} \text{ cm.} \simeq \frac{\lambda}{30}, \quad \text{where} \quad \lambda = 5 \,.\, 10^{-5} \text{ cm.}$$

Similarly, the Pretoria 75-inch mirror, for which $g = 1900$ cm., could be tested with a 17-cm. compensator to a tenth of a reflection fringe.

It will now be clear how the null mirror can be made to approximate to any required concave form. Consider, for instance, the concave mirror of the Ritchey-Chrétien combination * in the example given by Chrétien. If g is the paraxial radius of curvature of this mirror, its equation is

$$\frac{x}{g} = \frac{1}{2}\left(\frac{y}{g}\right)^2 - 0{\cdot}0183\left(\frac{y}{g}\right)^4 - 0{\cdot}0074760\left(\frac{y}{g}\right)^6 - \ldots \qquad (6.21)$$

Choose d_0 so that the fourth-power terms of (6.21) and the null mirror (4.16) agree exactly (we neglect e, u, $\frac{1}{r}$ for the moment). Then we have

$$d_0^4 = \frac{0{\cdot}573g}{(n-1)B}.$$

Now define d and R by

$$d^4 = (1 - R)d_0^4 = \frac{(1 - R)0{\cdot}573g}{(n-1)B},$$

and if M is the coefficient of $\left(\frac{y}{g}\right)^6$ in the equation of the null mirror we find precisely as before that

* Chrétien, *Rev. d'Opt.*, 1, 1922.

$$6M = -0{\cdot}076113 + \left(2+\frac{1}{n}\right)0{\cdot}43000 + 0{\cdot}98613\frac{2}{d_0} + \frac{0{\cdot}32871Kg}{(n-1)d_0^2}$$
$$-\left\{0{\cdot}43000\left(2+\frac{1}{n}\right) - 0{\cdot}68227 + 1{\cdot}72573\frac{2}{d_0} + \frac{0{\cdot}49307Kg}{(n-1)d_0^2}\right\}R + O(R^2),$$

the analogue of (6.9) except for a factor g. We can now write the equation of the null mirror as follows :—

$$\frac{x}{g} = \frac{1}{2}\left(\frac{y}{g}\right)^2 - 0{\cdot}0183\left(\frac{y}{g}\right)^4 - 0{\cdot}0074760\left(\frac{y}{g}\right)^6$$
$$+\left[\left\{0{\cdot}143R + \frac{(n^2-1)e}{8n^3g} - \frac{(3n+2)(n-1)d^2}{8nrg}\right\}\left(\frac{y}{g}\right)^4\right.$$
$$\left. -(M - 0{\cdot}0074760)\left(\frac{y}{g}\right)^6\right] + \ldots$$

where we now include e and $\frac{1}{r}$. To minimise the term in square brackets we must determine R from

$$0{\cdot}143R + \frac{(n^2-1)e}{8n^3g} - \frac{(3n+2)(n-1)d^2}{8nrg} = \frac{1{\cdot}5}{(4F)^2}(M - 0{\cdot}0074760),$$

then the "irreducible" error is as before $\frac{0{\cdot}048Mg}{(4F)^6}$. For $2/d_0 = 10$, $M \simeq 1{\cdot}9$, and this error is about $2/10(4F)^6$. Eighth-power terms can be taken into account as in the case of the paraboloid.

7. *Tolerances and Astigmatism.*—Suppose that the apparatus has been set up in perfect adjustment so that the null mirror is sensibly a paraboloid. Give small increments δd, δu to d and u, the distance of the plate and star from the paraxial centre of curvature. By (4.27) and (4.28) the null mirror now differs from a paraboloid by

$$-S(\delta d + \delta u)\frac{y^4}{2g^4} + \frac{\delta u y^4}{8g^4}, \tag{7.1}$$

where S is the diameter-ratio of mirror to plate. This expression holds for both single and double transmission. If $u = 0$, the variation δd will introduce on the mirror an error whose maximum value is $S\delta d/2(4F)^4$, from which we can find the tolerance in d. Those in related quantities can be readily calculated. Thus if $\delta\rho$ is the small variation in ρ equivalent to a variation δd in d, it follows from (3.20) and (4.17) that

$$\frac{3\delta\rho}{\rho} = \frac{4\delta d}{d}, \tag{7.2}$$

whence an error $\delta\rho$ in the measurement of ρ will produce on the mirror an error of $3Sd\delta\rho/8\rho(4F)^4$, or approximately $S\delta\rho/(4F)^4$. Returning to (7.1), suppose now that the compensator and star are rigidly attached so that $(u+d)$ is constant and hence $(\delta u + \delta d)$ is zero. Then if this rigid frame is moved with respect to the paraxial centre of curvature by δd, the new null

mirror will differ from a paraboloid at most by $\delta d/8(4F)^4$, an error only $1/4S$ times as great as that which would result from an identical movement of either of the two constituents with respect to each other.

The discussion may be summarised as follows. An error $\delta\rho$ in the determination of ρ, the radius of the convex face of the lens, must be small enough for $S\delta\rho/(4F)^4$ to be negligible ; and an error $\delta(u+d)$ in the distance between the plate and star must be small enough for $\frac{S\delta(u+d)}{2(4F)^4}$ to be negligible. These dimensions are the two which require the highest accuracy. In the case of the 117-cm. mirror previously considered, an error of a fortieth of a reflection fringe would be produced by an error in ρ of 0·01 cm. or in $(u+d)$ of 0·02 cm. The former corresponds to an error in the convexity of the lens of four Newton rings, which can be detected without difficulty, given a

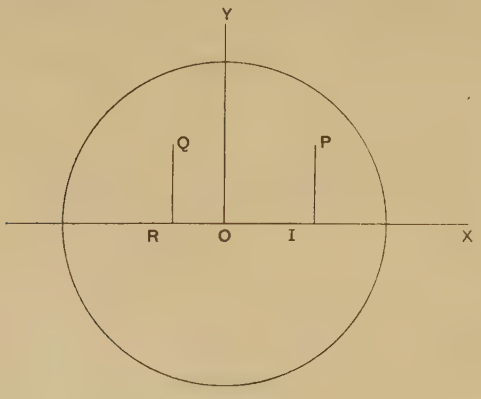

Fig. 4.

concave test sphere of a slightly greater radius which has itself been determined with the required precision.

It remains to investigate the astigmatism. In the following discussion the thickness of the plate and its paraxial curvature will be neglected, because it can readily be shown that the contributions from these two quantities are small in comparison with that arising from reflection at the paraboloid and from the asphericity of the compensator.

In the single transmission case the plate is adjusted in a position slightly inclined to the paraboloid, so that the incident pencil passes symmetrically through it. The astigmatism is therefore all due to reflection in the mirror, and if the axial displacement of the star is δ_0, its longitudinal astigmatism (L.A.) (= distance between the focal lines) is δ_0^2/f, f being the focal length of the mirror. When objectionable, this astigmatism can be annulled by a device such as an astigmatic lens.

In the double transmission case the principal effect is due to the fourth-power asphericity term. We will consider this by the methods of Martin's *Applied Optics*, 1, p. 135. Fig. 4 is a section of the plate by a plane perpendicular to its axis. O is the centre and OX, OY perpendicular axes, OX being parallel to the axial displacement of the star. Let the principal

ray meet the plate in a point I before reflection and in R after reflection, and let $OI = -OR = \delta$. This ray meets the paraboloid in its pole. Let the ray which meets the paraboloid at a point specified by co-ordinates $2fx/d$, $2fy/d$, with respect to axes through its pole parallel to OX and OY, meet the compensator in P before and in Q after reflection. Then

$$OP^2 = (x+\delta)^2 + y^2, \qquad OQ^2 = (x-\delta)^2 + y^2, \tag{7.3}$$

and the optical path difference between the rays IR and PQ is, neglecting that part of it arising from reflection in the paraboloid,

$$\frac{(n-1)B}{4}(OP^4 - OI^4 + OQ^4 - OR^4).$$

Using (7.3) this becomes

$$\{(x^2+y^2)^2 + 2\delta^2(3x^2+y^2)\}\frac{f}{2d^4}.$$

The astigmatism term is $(3x^2+y^2)f\delta^2/d^4$, and it follows from Martin (*loc. cit.*) that the separation of the focal lines is

$$\frac{4f\delta^2}{d^2} = \frac{S^2\delta^2}{f},$$

which is the same as that due to an off-axis distance of $S\delta$. Now the error in the mirror caused by an off-axis distance $S\delta$ is $S^2\delta^2/4f(4F)^2$. Thus, postulating that not more than a twentieth of a fringe should be so caused, we require that

$$\delta < \frac{F\sqrt{f}\text{ cm.}}{80S},$$

a condition which can be satisfied without serious difficulty.

Summary

Methods are described for null-testing concave mirrors at centre of curvature by interposing figured plates between the star and mirror to compensate their spherical aberration. The plates are themselves null-tested by normal incidence interference against the figured back of a pseudo-plano convex lens which is in turn null-tested autostigmatically. The method admits of wide application ; for example, a 190-cm. $f/5$ paraboloid tested in this manner with a 19-cm. diameter plate would not be in error by more than $\pm 2{\cdot}5 \cdot 10^{-5}$ mm.

H. H. Wills Physical Laboratory,
University of Bristol.

[*Appendix* on the following page.

Appendix

THE WILLIAMS INTERFEROMETER

C. R. Burch, B.A., Ph.D.

In the well-known Twyman-Green method of testing an objective, one places a convex spherical mirror behind the objective, with its centre at focus, so that parallel light travelling towards the objective is returned along its tracks: the combination objective-plus-mirror is thus behaving like a

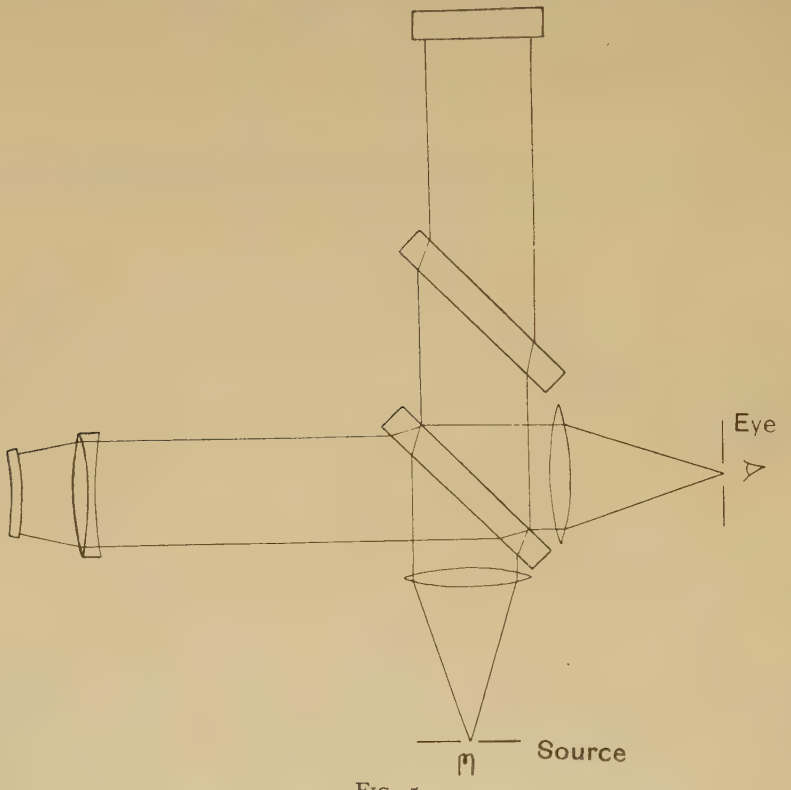

FIG. 5.

flat, and may be made to give interference fringes against the image of a flat in a Michelson interferometer. This method, shown in fig. 5, has the disadvantage that a pair of plane-parallel plates is required $\sqrt{2}$ times bigger than the objective to be tested.

Dr. W. Ewart Williams seems to have been the first to realise that since the combination lens-plus-flat, used in autocollimation tests of objectives, returns light from the focus along its own tracks back to the focus—behaving like a spherical mirror—it may be made to give interference fringes against the image of a spherical mirror in a Michelson interferometer. The necessary pair of plane-parallel plates may thus be quite small, no matter how big the

objective under test may be (see fig. 6). Nor is it even necessary that the plates should be particularly accurately parallel or of equal thickness. For example, Mr. Gascoigne has calculated that in testing an $F/10$ objective in this way, using dividing plates 5 mm. thick, 25 mm. diameter, 10 mm. apart (see fig. 6), if either plate is wedge-shaped to the extent of 100 fringes (0·001 inch) in 25 mm. diameter, or if the separating-piece against which they are supported is wedge-shaped to 500 fringes in 25 mm., or if the thickness of the plates differs by 0·07 mm., the resulting error on the fringe system seen on the lens will be only 0·1 fringe in each case. These tolerances depend on the square of the focal ratio.

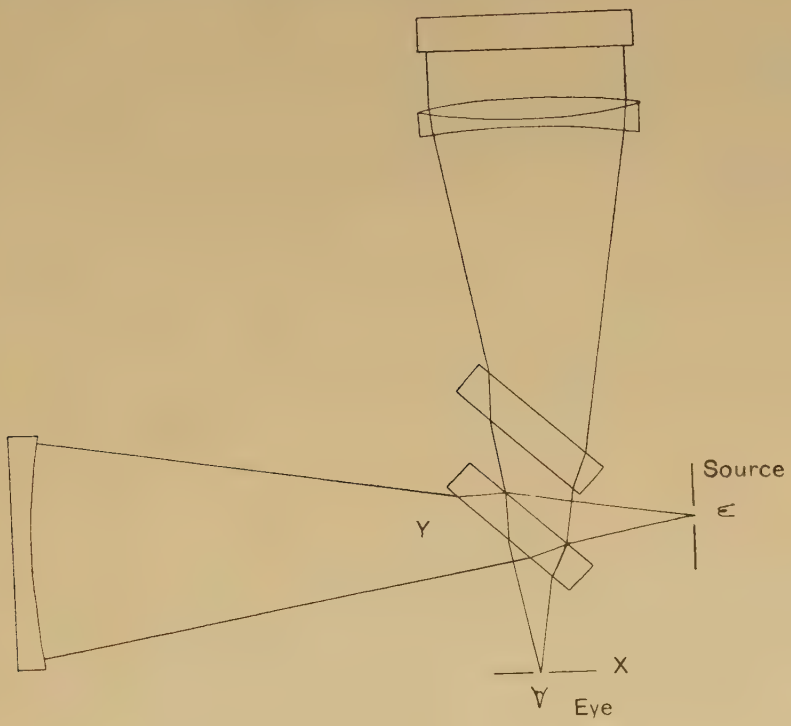

Fig. 6.

Further, it is not necessary to half-silver the dividing surface, for the unwanted reflections from the other surfaces of the plates form images separated by several millimetres from the "wanted" image of the source; the unwanted reflections are thus entirely eliminated by the 5-mm. aperture diaphragm at X (fig. 6). Half-silvering gives the advantage of more light, but a source $\frac{1}{2}$ mm. diameter (or even more) is permissible (depending on the off-axis properties of the system under test), and this gives enough light, using a vacuum mercury arc, even with unsilvered plates, an unsilvered flat behind the lens and an unsilvered mirror in the comparison arm. Such a mercury arc gives sufficiently homogeneous spectral lines to permit a path-difference between the two interference arms of an inch, with good fringe visibility.

The procedure for finding the fringes is as follows :—

(1) Adjust the spherical mirror so that the light returns along its tracks (producing only one shadow of a pin held in the cone near Y). The right-hand image is the "wanted" one ; the left-hand image is produced by an unwanted reflection.
(2) Adjust the autocollimating arm so that the "wanted" *left-hand* image produced by it coincides with the "wanted" right-hand image produced by the spherical mirror.
(3) Place the diaphragm as shown to eliminate the unwanted reflections ; then look through it at the lens.

It seems surprising that an instrument so simple to construct and to use should have escaped the notice of opticians for twenty years after the invention of the Twyman-Green interferometer, and that four years should have elapsed since Dr. Williams first drew attention to it in lectures, without any description having found its way into print. The world, as Sherlock Holmes has pointed out, is full of obvious things, which nobody by any chance ever observes.

ON A CHANGE IN THE PERIOD OF RW SAGITTARII

P. M. Ryves

In a previous communication to the Society * it was shown that RW Sagittarii was a variable star of long-period type and small amplitude, the extreme range being $2^{m}\cdot1$ and the period 188 days. This result was based on observations made at Zaragoza, Spain, in the years 1910–14 and on a short series in 1922–23, the latter being used to check the period.

Since the last-mentioned year RW Sagittarii has been observed regularly and the accumulated material is now sufficient for a more complete investigation. Unfortunately, on account of world affairs, the major portion of the original observations is, for the time being, inaccessible so that the investigation must be postponed. Meantime, a discussion of some provisional data which are available has revealed certain points of interest which it has been considered best to publish without further delay.

A re-examination of the earlier work in conjunction with some of the later observations has confirmed the general results already obtained. The period of 188 days, previously deduced, is found to satisfy the observations up to 1926 or 1927. As the minima are generally better defined than the maxima, minimum phase has been used in the re-determination of the period. The result differs by only a few hours from the value already found from the maxima, and the revised elements,

$$\text{Min.} = \text{J.D. } 2418825 + 188n,$$

are similar to the old, except that they refer to the minimum phase instead of to the maximum. From a comparison of epochs it seems that the rise occupies approximately 84 days and the fall 104 days, but these quantities cannot be fixed precisely, on account of the variability of the light-curve, a usual characteristic of stars of long period and small amplitude. So far, then, in spite of a rather long break in the series of observations (1915–1921 inclusive), it appears to be well established that from 1910 to 1926 the period of RW Sagittarii was sensibly constant at 188 days, within a small fraction of a day.

After 1926, however, the observed dates of minima commenced to lag behind the calculated dates by increasing quantities. Various attempts were made to reconcile the new with the old observations by adopting a longer period with or without a discontinuity, until finally it became evident that the discrepancies could be explained only by supposing a change of period to have taken place. A period of 191 days conforms well with the later observations, and, in view of the circumstances to which reference was made at the commencement of this note, greater precision will not be attempted, neither will the light-curve be fully described until all the

* *M.N.*, 84, 34, 1923.

observations can be utilized. The change of period appears to have been effected quite abruptly about cycle 30 or 31 (1925–26). The following are provisional elements for use from the new epoch onwards :—

$$\text{Min.} = \text{J.D. } 2424462 + 191n.$$

Table I contains the observed dates (provisional) of minima, as far as these are available, and the differences, O – C, from the dates given by the

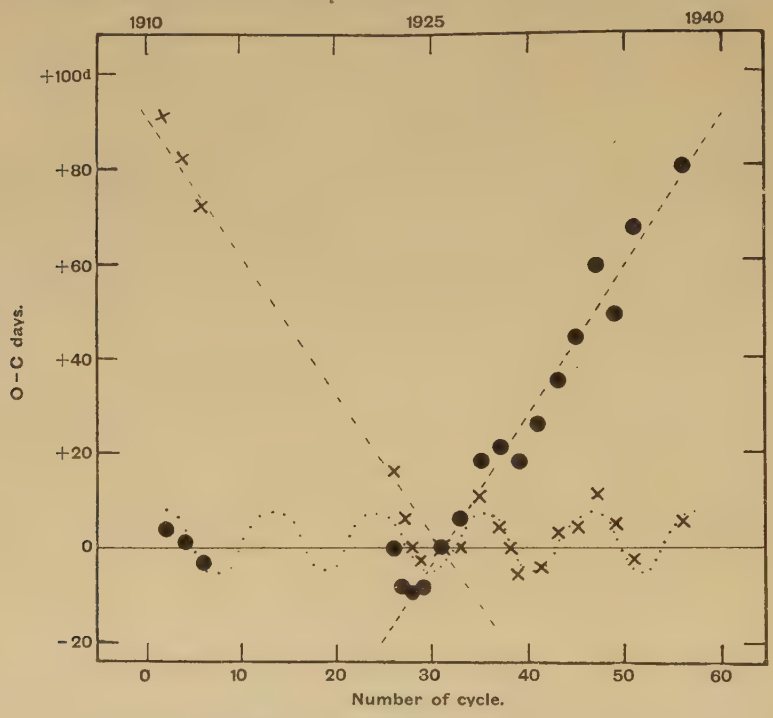

FIG. 1.—*The period of RW Sagittarii : Black dots represent O – C differences from a period of* 188 *days; crosses, differences from a period of* 191 *days.*

two sets of elements respectively. It will be noticed that positive and negative residuals alternate in a systematic manner and the cyclic character of these departures is shown more clearly in the accompanying diagram. The observed date of minimum appears to oscillate around the mean date in a period equivalent to about eleven cycles of the star's period. A sine term included in the elements would have improved the agreement but improvements effected in this way are usually not permanent. Fig. 1 also indicates, by the way in which the residuals depart from the zero line when the wrong period is used, that any solution on the basis of one unvarying period throughout the whole series of cycles would be quite out of the question.

The minimum observed in 1926, about the time that the change of period is assumed to have taken place and where the two sets of elements coincide, was well defined and symmetrical, but during the preceding cycles, where the phase difference amounts to several days, there are considerable irregularities

in the light-curve. It seems probable that some connection may exist between the change of period and the unusually irregular character of the light changes at this time, but it would be difficult to establish a certain relation of cause and effect. The change of period or the simultaneous co-existence of two different periodic tendencies, may conceivably have been the cause of perturbations in the light variation; on the other hand, some readjustment of equilibrium, of which the irregular light variation was the visible sign, may have necessitated a change of period.

TABLE I

Observed Dates of Minima

Year	J.D.	Cycle	$O-C_1$	$O-C_2$	
1910	241 8825	0	(Epoch, not fully observed)		
11	9205	2	+ 4	+91	
12	9578	4	+ 1	+82	
13	9950	6	− 3	+72	
1923	242 3714	26	0	+16	
24	3893	27	− 8	+ 6	
25	4080	28	− 9	0	
25	4268	29	− 9	− 3	
26	4653	31	0	0	New Ep.
27	5035	33	+ 6	0	
28	5423	35	+18	+10	
29	5803	37	+21	+ 4	
30	6175	39	+18	− 6	
31	6559	41	+26	− 4	
32	6948	43	+35	0	
33	7331	45	+44	+ 4	
34	7720	47	+59	+11	
35	8086	49	+49	+ 5	
37	8470	51	+57	− 3	
1939	9433	56	+80	+ 5	

A peculiar inflection or hump on the ascending branch of the curve which occurs in three successive cycles is a special feature not observed at other times, and a possible relation between this inflection and the sine term oscillation mentioned above is suggested. Eleven cycles of the 188-day period = 2068 days, whilst twelve cycles of 172 days (the approximate interval between successive humps) = 2064 days. The date oscillation, which in so many variable stars has originated the adoption of a sine term, appears in this case to be actually visible as an inflexion or secondary minimum on the light-curve.

After the change of period the variation of RW Sagittarii became more regular, but the curve for 1927 shows indications of a short-term variation, of very small amplitude, superimposed on the principal light-curve. Commencing at about J.D. 2424950, this secondary wave, with a period of approximately 22 days, can be traced through nearly the whole of the star's annual season of visibility (see fig. 2). The amplitude is exceedingly small, less than $0^m.2$, and the mean departure from a smooth curve is of the order of $0^m.05$,

but the distribution of these departures is such that it would be difficult to account for it on any theory of random distribution.

There is no certain indication of this secondary wave in the following cycles after 1927, but the material available is insufficient to decide whether

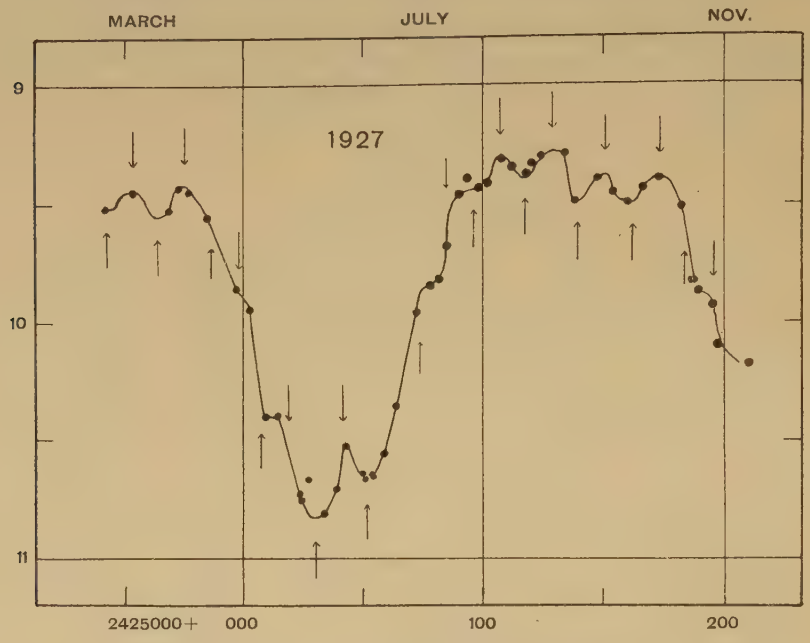

FIG. 2.—*RW Sagittarii: Light-curve, 1927, showing superimposed secondary variation. Arrows at intervals of 22 days.*

or no it is a permanent feature. An alternative suggestion which may be put forward is that the secondary oscillations are a result of the upheaval or adjustment of equilibrium which RW Sagittarii had recently undergone, and are analogous to the semi-periodic fluctuation which is observed in the light of many novæ on the decline shortly after principal maximum.

Summary

Further observations of RW Sagittarii confirm the results previously obtained, viz. that the variation is of long-period type and small amplitude with the irregularities which frequently accompany these characters.

A period of 188 days satisfies the observations up to 1926, when a change took place to 191 days.

About the time of this change of period the light-curve shows peculiar irregularities, including indications of a second wave or inflection with a period of about 172 days, and a superimposed short-term variation, period 22 days.

1940 *April* 3.

MEAN AREAS AND HELIOGRAPHIC LATITUDES OF SUNSPOTS IN THE YEAR 1937

Royal Observatory, Greenwich

(Communicated by the Astronomer Royal)

The following results are in continuation of those given in *M.N.*, **98**, 425, 1938, and are derived from the measurement at Greenwich of photographs taken at the Royal Observatories of Greenwich and the Cape and at the Kodaikanal Observatory, India. In addition, a negative on glass for November 3 was kindly supplied by the Director of the Mount Wilson Observatory.

Table I gives the mean daily areas of umbræ, whole spots and faculæ for each synodic rotation of the Sun included in the year 1937; the means for the year as a whole are included in Table II, which summarizes the yearly values from 1933–37.

TABLE I

No. of Rotation	Rotation Commenced U.T.	Days Photographed	Mean Daily Areas: Projected *			Mean Daily Areas: Corrected for Foreshortening †		
			Umbræ	Whole Spots	Faculæ	Umbræ	Whole Spots	Faculæ
1114	1936 Dec. 22·30	28	382	1926	3044	286	1476	3692
1115	1937 Jan. 18·63	27	700	3901	3319	500	2817	4073
1116	Feb. 14·97	28	455	2490	3026	347	1930	3690
1117	Mar. 14·30	27	286	1557	2150	210	1147	2658
1118	Apr. 10·60	27	550	3086	2370	404	2309	2961
1119	May 7·85	27	599	3341	2644	462	2583	3261
1120	June 4·06	27	729	3766	2810	535	2768	3491
1121	July 1·26	28	761	4306	3331	565	3209	4164
1122	28·46	27	682	3724	3525	513	2805	4347
1123	Aug. 24·69	27	452	2343	3054	338	1793	3764
1124	Sept. 20·95	27	636	3672	2935	446	2562	3571
1125	Oct. 18·24	28	315	1674	2760	219	1146	3348
1126	Nov. 14·54	27	138	657	2628	114	539	3170

TABLE II

Year	No. of Days: Photographed	No. of Days: Without Spots	Mean Daily Areas: Projected *			Mean Daily Areas: Corrected for Foreshortening †		
			Umbræ	Whole Spots	Faculæ	Umbræ	Whole Spots	Faculæ
1933	365	234	24	120	225	18	88	267
1934	365	145	27	142	297	22	119	354
1935	365	21	152	810	910	117	624	1100
1936	366	0	288	1529	2106	217	1141	2545
1937	365	0	509	2795	2856	375	2074	3505

* Expressed in millionths of the Sun's disc.

† Expressed in millionths of the Sun's hemisphere.

Table III gives for each rotation in the year 1937 the mean daily area of the whole spots (corrected for foreshortening) and the mean heliographic latitude of the spotted areas for both northern and southern hemispheres.

TABLE III

No. of Rotation	Rotation Commenced U.T.	Spots North of the Equator		Spots South of the Equator		Mean Latitude of entire Spotted Area	Mean Distance from Equator of all Spots
		Mean Daily Area	Mean Heliographic Latitude	Mean Daily Area	Mean Heliographic Latitude		
			°		°	°	°
1114	1936 Dec. 22·30	713	19·10	764	18·15	− 0·17	18·61
1115	1937 Jan. 18·63	1030	18·88	1787	14·58	− 2·35	16·16
1116	Feb. 14·97	1598	15·69	332	18·73	+ 9·77	16·21
1117	Mar. 14·30	840	11·17	307	18·04	+ 3·36	13·00
1118	Apr. 10·60	1547	19·51	761	16·18	+ 7·74	18·41
1119	May 7·85	1658	15·49	925	17·06	+ 3·83	16·05
1120	June 4·06	1483	17·26	1285	14·48	+ 2·52	15·97
1121	July 1·26	2147	20·12	1062	14·52	+ 8·65	18·27
1122	28·46	1875	26·01	929	16·33	+11·98	22·80
1123	Aug. 24·69	1571	18·55	222	14·33	+14·48	18·03
1124	Sept. 20·95	2111	11·98	451	16·72	+ 6·93	12·82
1125	Oct. 18·24	540	11·73	607	16·90	− 3·42	14·47
1126	Nov. 14·54	165	15·38	374	17·39	− 7·37	16·78

The mean heliographic latitude of the entire spotted area and the mean distance from the equator of all spots are also tabulated. The mean values for the year 1937 are included in Table IV.

TABLE IV

Year	Days Photographed	Spots North of the Equator		Spots South of the Equator		Mean Latitude of entire Spotted Area	Mean Distance from Equator of all Spots
		Mean Daily Area	Mean Heliographic Latitude	Mean Daily Area	Mean Heliographic Latitude		
			°		°	°	
1933	365	86	10·60	2	8·35	+10·23	10·56
1934	365	44	16·45	74	28·09	−11·49	23·75
1934	Old Cycle	19	4·10	1	4·37	+ 3·79	4·11
	New Cycle	26	25·44	74	28·31	−14·46	27·57
1935	365	205	22·42	419	23·72	− 8·57	23·30
1936	366	463	19·36	678	21·02	− 4·63	20·35
1937	365	1317	17·63	757	15·96	+ 5·36	17·02

Tables II and IV are in continuation of similar tables given in *Monthly Notices*: for the years 1874 to 1888—**49**, 381–382; 1889 to 1902—**63**, 465–466;

1901 to 1914—**76**, 402–403; 1913 to 1924—**85**, 1007–1008; 1923 to 1933—**94**, 870–871.

The rotations in Tables I and III are numbered in continuation of Carrington's series.

The chief features of the record of sunspots and faculæ for the year 1937 are as follows :—

1. A continued large increase in the mean daily area of sunspots and of faculæ. The ratio of daily areas, corrected for foreshortening, for the years 1936 and 1937 is 1 : 1·8 for sunspots and 1 : 1·3 for faculæ. The mean daily area of 2074 units is the highest value yet recorded for any year in the Greenwich records (*i.e.* since 1874). The second highest is 1537 units in 1917. The mean daily area of faculæ of 3505 units is also the highest yet measured, the year 1892 yielding a mean area of 3270 units.

2. On no day in the year were sunspots and faculæ absent from the Sun's disc.

3. For the first three years of the present cycle, the southern hemisphere was markedly the more active. During 1937, the northern hemisphere was predominant, the ratio of the mean daily area of sunspots, north and south of the equator, being 1·7 : 1.

4. The number of spot groups lasting for two days or longer was 496, of which 267 were in the northern and 229 in the southern hemisphere. In addition, there were 173 one-day groups which were mostly very small; of these, 93 were north and 80 south of the Sun's equator. During the year there were 31 large groups, each exceeding 500 millionths of the Sun's hemisphere in mean area. (The corresponding number in 1936 was 14.) Seven of these groups exceeded 1000 millionths, and two of these just exceeded 2500 millionths. These two great groups with respective central meridian passage on July 28 (lat. 31° N.) and on October 4 (lat. 9° N.) are the 2nd and 3rd largest groups (according to mean area) and the 3rd and 5th (according to maximum area) recorded in the Greenwich series of sunspot measures.

5. The mean latitude of all spots, weighted according to area, is 17°·02, *i.e.* 3°·3 nearer the Sun's equator than in 1936. In the three years, 1934–37, the mean latitude has decreased 10½°, taking the mean latitude of the *new* cycle spots as datum in 1934. The number of spots in 1937 nearer the equator than ± 10° was 17 per cent. of the total number of all groups seen during the year, as compared with 4 per cent. in 1936. Sunspot activity reached a high maximum in 1937 ; the mean latitude (17°) of sunspots during the year is, however, somewhat high compared with that of about 14° given by the mean of the five previous maxima.

Royal Observatory, Greenwich :
1940 *March* 19.